ISSN 1023-9855

Thoracic Medicine

Volume 39 • Number 1 • March 2024

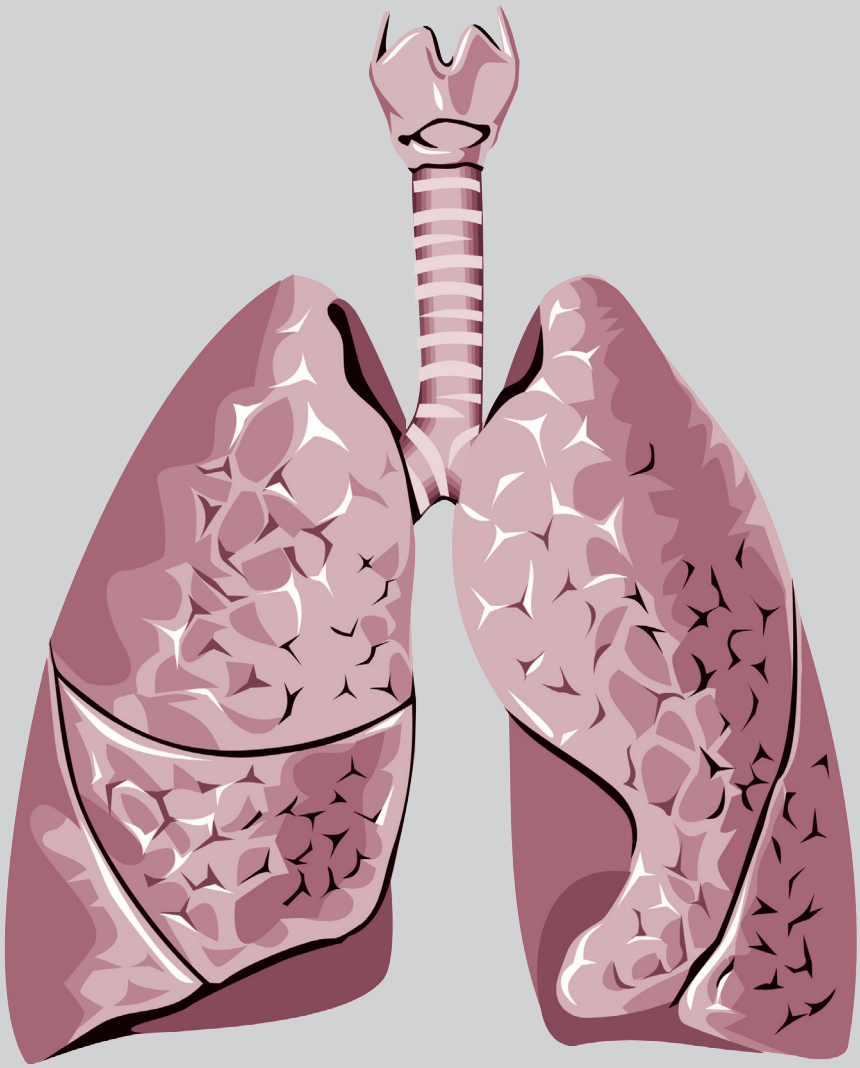

The Official Journal of

Taiwan Society of Pulmonary and Critical Care Medicine

Taiwan Society of Sleep Medicine

Taiwan Society for Respiratory Therapy

Taiwan Society of Tuberculosis and Lung Diseases

Thoracic Medicine

The Official Journal of
Taiwan Society of Pulmonary and Critical Care Medicine
Taiwan Society for Respiratory Therapy
Taiwan Society of Sleep Medicine
Taiwan Society of Tuberculosis and Lung Diseases

Publisher

Yuh-Min Chen, M.D., Ph.D., President
Taiwan Society of Pulmonary and Critical Care Medicine

Chia-Chen Chu, Ph.D., RRT, FAARC President
Taiwan Society for Respiratory Therapy

Jann-Yuan Wang M.D., Ph.D., President
Taiwan Society of Tuberculosis and Lung Diseases

Kun-Ta Chou, M.D., President
Taiwan Society of Sleep Medicine

Editor-in-Chief

Kang-Yun Lee, M.D., Ph.D., Professor
Taipei Medical University-Shuang Ho Hospital, Taiwan

Deputy Editors-in-Chief

Po-Chun Lo, M.D.,
Department of Internal Medicine, Taoyuan General Hospital, Ministry of Health and Welfare, Taoyuan, Taiwan

Editorial Board

Section of Pulmonary and Critical Care Medicine

Jin-Yuan Shih, M.D., Professor
National Taiwan University Hospital, Taiwan
Gee-Chen Chang, M.D., Professor
Chung Shan Medical University Hospital, Taiwan
Jann-Yuan Wang M.D., Ph.D., Professor
National Taiwan University Hospital, Taiwan
Kuang-Yao Yang, M.D., Ph.D., Professor
Taipei Veterans General Hospital, Taiwan
Chi-Li Chung, M.D., Ph.D., Associate Professor
Taipei Medical University Hospital, Taiwan
Chien-Chung Lin, M.D., Ph.D., Professor
Department of Internal Medicine, College of medicine, National Cheng Kung University,Taiwan

Section of Respiratory Therapy

Hui-Ling Lin, Ph.D. RRT, RN, FAARC, Professor
Chang Gung University, Taiwan
I- Chun Chuang, Ph.D., Associate Professor
Kaohsiung Medical University College of Medicine, Taiwan
Chun-Chun Hsu, Ph.D, Associate Professor
Taipei Medical University
Shih-Hsing Yang, Ph.D., Associate Professor
Fu Jen Catholic University, Taiwan
Chin-Jung Liu, Ph.D., Associate Professor
China Medical University Hospital, Taichung, Taiwan

Section of Tuberculosis and Lung Diseases

Jann-Yuan Wang, M.D., Professor
National Taiwan University Hospital, Taiwan
Chen-Yuan Chiang, M.D., Associate Professor
Taipei Municipal Wanfang Hospital, Taiwan
Ming-Chi Yu, M.D., Professor
Taipei Municipal Wanfang Hospital, Taiwan
Yi-Wen Huang, M.D., Professor
Changhua Hospital, Ministry of Health & Welfare, Taiwan
Wei-Juin Su, M.D., Professor
Taipei Veterans General Hospital, Taiwan

Section of Sleep Medicine

Li- Ang Lee, M.D., Associate Professor
Linkou Chang Gung Memorial Hospital, Taiwan
Pei-Lin Lee, M.D., Assistant Professor
National Taiwan University Hospital, Taiwan
Hsin-Chien Lee, M.D., Associate Professor
Taipei Medical University-Shuang-Ho Hospital, Taiwan
Kun-Ta Chou, M.D., Associate Professor
Taipei Veterans General Hospital, Taiwan
Li-Pang Chuang, M.D., Assistant Professor
Linkou Chang Gung Memorial Hospital, Taiwan

International Editorial Board

Charles L. Daley, M.D., Professor
National Jewish Health Center, Colorado, USA
Chi-Chiu Leung, MBBS, FFPH, FCCP, Professor
Stanley Ho Centre for Emerging Infectious Diseases, Hong Kong, China

Daniel D. Rowley, MSc, RRT-ACCS, RRT-NPS, RPFT, FAARC
University of Virginia Medical Center, Charlottesville, Virginia, U.S.A.
Fang Han, M.D., Professor
Peking University People's Hospital Beijing, China
Liang Xu, MD.
Director of Wuhan Wuchang Hospital Professor of Wuhan University of Science and Technology Wuhan, China
J. Brady Scott, Ph.D., RRT-ACCS, AE-C, FAARC, FCCP, Professor
Rush University, Chicago, Illinois, USA
Kazuhiro Ito, Ph.D., DVM, Honorary Professor
Imperial College London, UK
Kazuo Chin (HWA BOO JIN), M.D., Professor
Graduate School of Medicine, Kyoto University
Masaki Nakane, M.D., Ph.D., Professor
Yamagata University Hospital, Japan
Naricha Chirakalwasan, M.D., FAASM, FAPSR, Associate Professor
Faculty of Medicine, Chulalongkorn University, Thailand
Petros C. Karakousis, M.D., Professor
The Johns Hopkins University School of Medicine, USA

Thoracic Medicine

The Official Journal of
Taiwan Society of Pulmonary and Critical Care Medicine
Taiwan Society for Respiratory Therapy
Taiwan Society of Sleep Medicine
Taiwan Society of Tuberculosis and Lung Diseases

Volume 39
Number 1
March 2024

CONTENTS

勘誤聲明

出版信息	2024 年第 39 卷第 1 期，頁碼為第 36-42 頁
論文標題	Multifocal Mass-like Pulmonary Consolidation in a Patient with Community-Acquired Pneumonia Caused by Pseudomonas Aeruginosa
作者	Chang-Ching Lee, Sheng-Wei Pan
勘誤內容	**舊版：** 頁碼為第 39 頁 Fig.4. CXR on day 21 (before discharge) showed improvement of the bilateral consolidation. 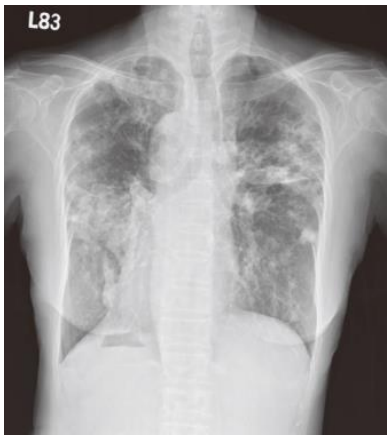 Fig. 5. CXR on day 44 showed marked regression of the bilateral mass-like lesions and chronic change of the cystic bronchiectasis at the right upper lobe and left lingula. 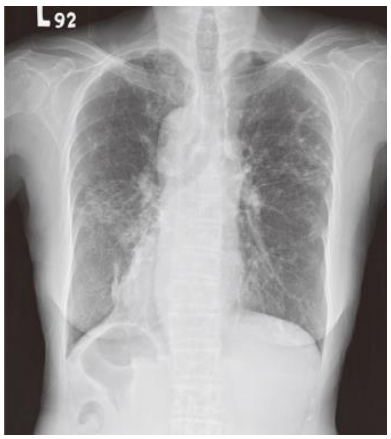

更正版：

頁碼為第 39 頁 Fig.4. CXR on day 21 (before discharge) showed improvement of the bilateral consolidation.

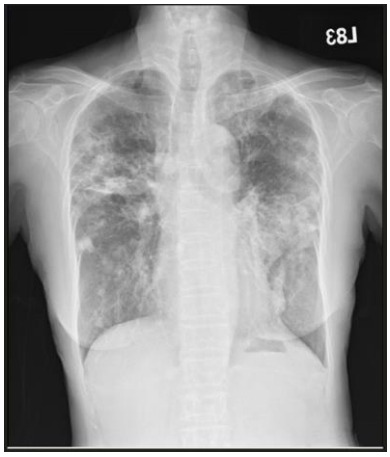

Fig. 5. CXR on day 44 showed marked regression of the bilateral mass-like lesions and chronic change of the cystic bronchiectasis at the right upper lobe and left lingula.

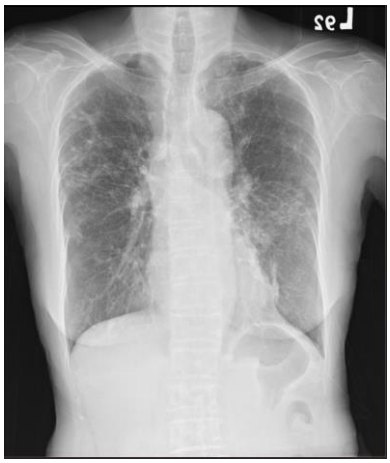

Pre-Extubation Cuff Leak Test and Extubation Outcome in Critically Ill COVID-19 and Non-COVID-19 Pneumonitis Patients with Acute Respiratory Failure

Mei-Chun Lin[1], Hsun-Yun Chang[1], Ching-Tzu Huang[1], Hsiu-Feng Hsiao[1,2], Han-Chung Hu[1,2,3], Chung-Chi Huang[1,2,3], Meng-Jer Hsieh[1,2,3]

Background: The cuff leak test (CLT) is recommended to predict post-extubation stridor (PES) in high-risk patients. The impact of the CLT, and extubation outcomes in severe COVID-19 patients were analyzed.

Methods: The CLT was performed in severe COVID-19 patients with endotracheal intubation. The results of the CLT were compared with that in patients with severe non-COVID community-acquired pneumonia (CAP). The CLT results were also compared in COVID-19 patients with or without pre-extubation corticosteroid therapy.

Results: This study includes 34 severe COVID-19 and 42 severe non-COVID CAP patients. Twenty-one of the 34 COVID-19 patients had the CLT before extubation. The positive CLT percentages were similar in the COVID-19 and non-COVID CAP patients (9.5% vs. 14.3%, *P*=0.593). The cuff leak volumes (307.80±118.58 ml vs. 272.30±148.98 ml, *P*=0.346) and cuff leak percentages (50.49±17.24% vs. 45.94±22.02%, *P*=0.412) were not significantly different between the 2 groups. All of the COVID-19 patients were extubated successfully without PES, irrespective of the CLT results. Only 1 in 6 CLT-positive non-COVID CAP patients had PES, but this was managed well without re-intubation. Multivariate analysis revealed female gender and the duration of endotracheal intubation were positively correlated with a positive CLT.

Conclusion: The positive CLT rate in severe COVID-19 patients was no higher than that in severe non-COVID CAP patients. The CLT results and extubation outcomes in COVID-19 patients were similar to those in non-COVID CAP patients. Similar to other patients with endotracheal intubation, severe COVID-19 patients with a higher risk of PES would undergo a CLT, especially female patients and those with a longer duration of endotracheal intubation. ***(Thorac Med 2024; 39: 1-12)***

Key words: Cuff leak test, post-extubation stridor, COVID-19, acute respiratory failure, corticosteroids

[1]Department of Respiratory Therapy, Linkou Chang-Gung Memorial Hospital, Chang-Gung Medical Foundation, Taoyuan, Taiwan, [2]Department of Respiratory Therapy, School of Medicine, Chang-Gung University, Taoyuan, Taiwan, [3]Department of Pulmonary and Critical Care Medicine, Linkou Chang-Gung Memorial Hospital, Chang-Gung Medical Foundation, Taoyuan, Taiwan

Address reprint requests to: Dr. Meng-Jer Hsieh, Department of Pulmonary and Critical Care Medicine, Linkou Chang Gung Memorial Hospital, Chang Gung Medical Foundation, No. 5, Fu-Xing St. Kwei-Shan Dist. Taoyuan City, 33333 Taiwan.

Introduction

Upper airway obstruction caused by laryngeal edema following extubation is a serious cause of extubation failure. Post-extubation laryngeal edema and stridor have been reported to have incidences of 2-26%, and commonly result in extubation failure and subsequent reintubation [1]. Reintubation after extubation failure is associated with higher morbidity, longer duration of mechanical ventilation (MV), and intensive care unit (ICU) stay [2-3]. Evaluating the risk of post-extubation stridor (PES) before scheduled extubation is important for patients at higher risk of post-extubation laryngeal edema.

In cases of COVID-19, caused by novel coronavirus (SARS-CoV-2) infection, patients may progress to severe pneumonitis, and even acute respiratory distress syndrome (ARDS) requiring MV. Re-intubation of COVID-19 patients after extubation failure is associated not only with the risk of a poorer outcome for the patients, but also an increased risk of virus-containing aerosol generation and disease transmission. Therefore, we should be more cautious in the pre-extubation assessment and post-extubation management of patients with severe COVID-19. However, in patients with severe COVID-19, health care professionals might perform pre-extubation evaluations such as auscultation or a cuff leak test (CLT) less frequently, because of infection control considerations. An insufficient pre-extubation evaluation could increase the risk of PES and associated extubation failure.

PES can be detected clinically, and is considered a clinical factor of post-extubation laryngeal edema. The CLT is the most frequently used method to predict the presence of laryngeal edema and PES [4]. A failed CLT indicates little or no air leakage around the tube when the cuff is deflated, suggesting possible upper airway obstruction caused by laryngeal edema [5]. Using a CLT before extubation could be a feasible way to assess the presence or absence of obstruction of the upper airway in patients with COVID-19.

There are 2 types of CLT: a qualitative CLT and a quantitative CLT [6]. The qualitative CLT examines the presence or absence of audible expired air around an endotracheal tube, and the quantitative CLT measures the difference in expired volumes between an inflated cuff and after cuff deflation. In 1996, Miller and Cole, et al., used a CLT to evaluate airway patency in 100 MV patients. With a cut-off value of < 110 mL, the positive predictive value for PES was 0.80. The positive predictive value for the absence of PES with a volume of 110 mL was 0.98. The specificity and sensitivity of the test were 0.99 and 0.6, respectively [7]. Besides measuring the volume change, the difference in expired volumes between an inflated and a deflated cuff presented as a percentage of expired volume with the cuff inflated can be used as a cut-off value in the CLT. CLT failure is indicated when the change is less than 10% or 15.5% [8-9]. Jaber *et al*. modified the measurement method of Miller *et al*. to obtain a cut-off value of 12% [5]. The practice guidelines published by the American Thoracic Society (ATS) and the American College of Chest Physicians (ACCP) recommend using a CLT to evaluate MV adults who are at high risk of PES [10].

Because of the lack of pre-extubation CLT data in severe COVID-19 patients in the literature, this study aimed to investigate the feasibility of using a pre-extubation CLT, and its relation to extubation outcomes in critically ill

COVID-19 patients with acute respiratory failure. The results of using the CLT in COVID-19 patients will be compared with those in severe non-COVID CAP patients. For severe COVID-19, the use of dexamethasone has proven to improve patient survival [11], and systemic corticosteroids are therefore recommended for hospitalized patients in the treatment guidelines [12-13]. We also analyzed the effect of pre-extubation systemic corticosteroids on the CLT results in these patients.

Materials and Methods

Patients

Adult patients aged more than 20 years old, who fulfilled the following criteria and were admitted to the ICU of Linkou Chang-Gung Memorial Hospital from January 2020 to September 2021, were eligible for this study: (1) laboratory-confirmed COVID-19 infection with acute respiratory failure requiring endotracheal intubation and MV, (2) severe community-acquired pneumonia (CAP) not caused by SARS-CoV-2 infection (severe non-COVID CAP) with acute respiratory failure requiring endotracheal intubation and MV. Patient data, including demographic data, disease severity as represented by the APACHE II scores, use of corticosteroids, weaning parameters, days of endotracheal intubation, and CLT results represented as cuff leak volumes and cuff leak percentages, were retrieved by retrospective review of electronic medical records. Extubation success was defined as no re-intubation within 48 hours after extubation. The extubation outcome, cuff leak volumes, and cuff leak percentages between severe COVID-19 patients and severe non-COVID CAP patients, and in severe COVID-19 patients with and without pre-extubation systemic corticosteroids before extubation, were compared.

Cuff leak test (CLT)

Careful endotracheal and oral suction was performed before performing the CLT. The test follows the methods described by Miller and Cole [7]. Briefly, the respiratory therapist places the ventilator in the assist-control mode, with tidal volume (Vt) set to 10 ml/kg. The initial measurement of expiratory Vt is performed when the cuff is inflated. The cuff then deflates, and after removing the artifacts caused by coughing, 4 to 6 consecutive breath cycles are used to calculate the average of exhaled Vt. Leak volume and leak percentage are calculated as the difference between exhalatory Vt with the cuff inflated and after cuff deflation. A positive CLT was defined as a cuff leak volume below the cut-off value of 110 ml, according to the previous studies [7].

Statistical analysis

The clinical characteristics, underlying medical diseases, days of endotracheal intubation, and weaning profiles, as well as cuff leak volumes and cuff leak percentages, were compared using the chi-square test for categorical variables and the independent sample t-test or Mann–Whitney U test for numerical variables. Differences were considered to be statistically significant at $p < 0.05$. Data were entered and analyzed using the IBM SPSS Statistics for Windows (Version 24.0. Armonk, NY: IBM Corp.).

Results

During the study period, 50 severe COVID-19 patients with respiratory failure and en-

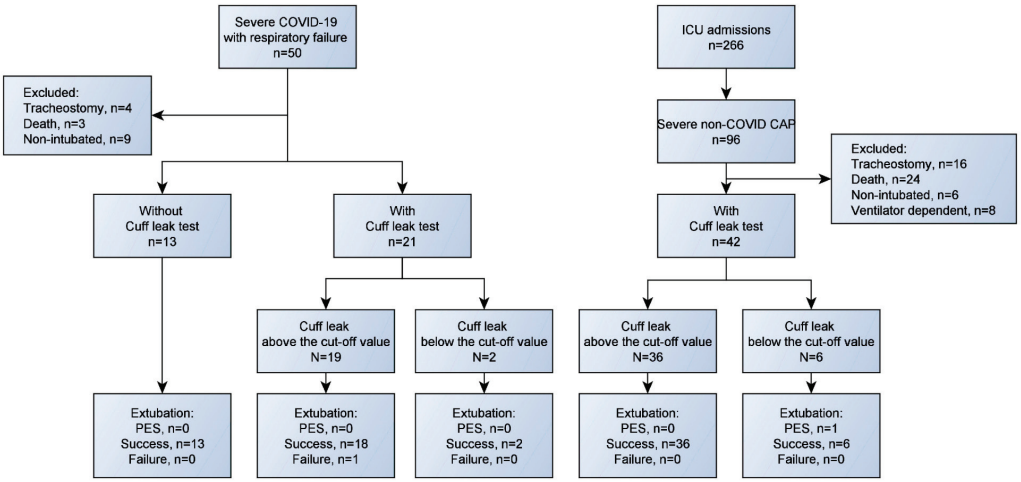

Fig. 1. Patient distribution, cuff leak test and extubation outcome of severe COVID-19 and severe non-COVID CAP patients

dotracheal intubation were admitted to our ICU. Among them, 34 had improved conditions and were extubated under supervision, including 21 who had the CLT and 13 who did not have the CLT before extubation. During the same period, 96 severe non-COVID CAP patients were admitted, and 42 had the CLT before extubation. The patients' distribution is shown in Figure 1.

(1) *Severe COVID-19 patients with or without CLT*

Among the severe COVID-19 patients, no CLT was performed with 13 patients, and all of them were successfully extubated without PES or re-intubation. COVID-19 patients with or without the CLT had no significant difference in age, gender, BMI, duration of endotracheal intubation before extubation, and disease severity as represented by the APACHE II scores. There was also no between-group difference in weaning parameters including RR, Vt, Ve, and RSBI (Table 1). The mean leak volume and percentage of cuff leak in COVID-19 patients were 307.80±118.58 ml and 50.49%±17.24%, respectively. Two of the 21 (9.5%) COVID-19 patients that had a CLT had a positive result, and both were successfully extubated without PES or re-intubation. The other 19 (90.5%) patients had a cuff leak volume greater than 110 ml, and 1 of them (with a cuff leak volume of 230 ml) had been re-intubated but had no PES clinically.

(2) *Comparison of CLT between severe COVID-19 and severe non-COVID CAP patients*

There was no significant difference in age, gender, or severity as represented by the APACHE II score between patients with severe COVID-19 and those with severe non-COVID CAP. The duration of endotracheal intubation before extubation was numerically longer in severe COVID-19 patients, but the difference did not reach statistical significance. The average BMI of the severe COVID-19 patients was significantly higher than that of the severe non-COVID CAP patients. When comparing the associated co-morbidities in both groups, severe non-COVID CAP patients had a higher percentage of malignant diseases than severe

Table 1. Characteristics of Severe COVID-19 Patients and Severe non-COVID CAP Patients

Patients Variables	(1)Severe COVID-19 Without CLT n=13	(2)Severe COVID-19 With CLT n=21	(3)Severe Non-COVID CAP With CLT n=42	P value (1)VS. (2)	P value (2)VS. (3)
Age, years, mean±SD	68.00±10.97	66.29±11.26	71.90±11.67	0.666	0.073
Female gender, n (%)	5 (38.5)	5 (23.8%)	14 (33.3%)	0.362	0.437
BMI, kg/m^2, mean±SD	23.97±3.38	26.17±4.02	23.57±5.10*	0.111	0.047*
APACHE II score, mean±SD	19.31±2.84	17.05±6.58	18.79±5.59	0.252	0.278
Days of endotracheal intubation, median (range, IQR)	10 (5-22, 6)	13 (7-55, 12)	9 (1-42, 6)	0.132	0.066
Hospital days, median (range, IQR)	32 (12-120, 25)	29 (14-120, 41)	41.5 (13-123,37)	0.661	0.993
Comorbidities, n (%)					
Diabetes	2 (15.4%)	7 (33.3%)	9 (21.4%)	0.427	0.306
Hypertension	5 (38.5%)	12 (57.1%)	21 (50.0%)	0.290	0.593
Cardiovascular disease	5 (38.5%)	4 (19.0%)	4 (9.5%)	0.211	0.285
Lung cancer	1 (7.7%)	1 (4.8%)	6 (14.3%)	1.000	0.257
Other malignancy	0	0	9 (21.4%)		0.022*
COPD	0	1 (4.8%)	4 (9.5%)	1.000	0.510
Chronic kidney disease	1 (7.7%)	3 (14.3%)	7 (16.7%)	1.000	0.807
Cerebrovascular disease	0	1 (4.8%)	6 (14.3%)	1.000	0.257
Cuff leak test					
Cuff leak volume (ml), mean±SD		307.80±118.58	272.30±148.98		0.346
Cuff leak percentage (%), mean±SD		50.49±17.24	45.94±22.02		0.412
Cuff leak volume < 110 ml, n (%)		2 (9.5%)	6 (14.3%)		0.593
Cuff leak percentage < 12%, n (%)		1 (4.8%)	5 (11.9%)		0.654
Cuff leak percentage < 20%, n (%)		2 (9.5%)	6 (14.3%)		0.593
Post-extubation stridor	0	0	1 (2.4%)		-
Re-intubation	0	1 (4.8%)	0		-
Weaning parameters, mean±SD					
RR	20.90±4.15	21.29±4.56	22.86±5.69	0.823	0.275
Vt (ml)	486.00±156.16	436.43±93.41	411.59±158.69	0.277	0.511
Ve (L)	9.78±2.35	9.21±2.44	9.10±3.24	0.545	0.888
RSBI	48.2±21.91	52.05±22.17	65.31±38.69	0.654	0.152

BMI: body mass index, APACHE: Acute Physiology and Chronic Health Evaluation; MV: mechanical ventilation, COPD: chronic obstructive pulmonary disease, RR: respiratory rate, Vt: tidal volume, Ve: minute ventilation, RSBI: rapid shallow breathing index.

* P<0.05

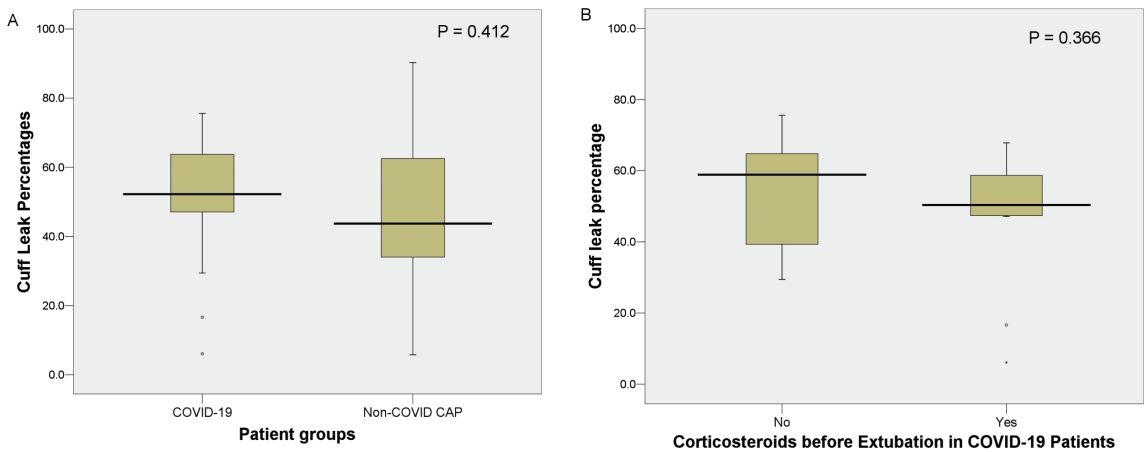

Fig. 2. Cuff leak percentages in A. Severe COVID-19 and severe non-COVID CAP patients, B. Severe COVID-19 patients with or without systemic corticosteroid before extubation

COVID-19 patients. Weaning parameters, including RR, Vt, Ve, and RSBI, showed no significant between-group difference. The cuff leak volumes and cuff leak percentages were not significantly different between patients with severe COVID-19 and those with severe non-COVID CAP (Table 1 and Figure 2A). However, 2 (9.5%) and 6 (14.3%) patients in the severe COVID-19 and severe non-COVID CAP groups, respectively, had a positive CLT. The percentages of patients with a positive CLT were not significantly different between the 2 groups. In the severe non-COVID CAP group, only 1 in 6 CLT-positive patients developed PES, and another 5 were extubated successfully without PES. We administered hydrocortisone (100 mg) intravenously 1 hour before extubation for all patients with a positive CLT, followed by post-extubation systemic corticosteroids with dexamethasone 5 mg intravenously every 12 hours. The patients who developed PES and another 3 CLT-positive non-COVID CAP patients received post-extubation biphasic positive airway pressure ventilation (BiPAP) temporarily, without subsequent re-intubation.

(3) *Comparison of CLT between severe COVID-19 patients with and without systemic corticosteroid before extubation*

There was no significant difference in age, gender, or APACHE II score among the severe COVID-19 patients with and without systemic corticosteroids before extubation. The duration of endotracheal intubation before extubation was longer in severe COVID-19 patients without pre-extubation corticosteroid, but the difference did not reach statistical significance. The BMI of severe COVID-19 patients without pre-extubation corticosteroids was significantly lower than that of those with pre-extubation corticosteroids. Weaning parameters, including RR, Vt, Ve, and RSBI, had no significant between-group difference. The cuff leak volumes and cuff leak percentages were not significantly different between severe COVID-19 patients with and without pre-extubation systemic corticosteroids (Table 2 and Figure 2B).

(4) *Risk factors for a positive CLT*

Univariate analysis revealed that female gender is the only risk factor with a higher risk

Table 2. Characteristics of the COVID-19 Patients with or Without Concurrent Corticosteroid Before Extubation

Variables	With corticosteroid (N=11)	With corticosteroid (N=11)	*P* value
Age, years, mean±SD	65.36±11.08	67.30±11.97	0.705
Female gender, n (%)	4 (36.4%)	1 (10%)	0.311
BMI, kg/m2, mean±SD	28.37±3.91	23.74±2.51	0.005*
APACHE II score, mean±SD	18.36±6.20	15.60±7.01	0.350
Days on endotracheal intubation, median (range, IQR)	10 (7-55, 8)	15.5 (7-50, 16)	0.692
Hospital days, median (range, IQR)	22 (14-111, 33)	32 (14-120, 59)	0.397
Re-intubation, n	1	0	-
Cuff leak test			
Cuff leak volume < 110 ml, n (%)	2 (18.2%)	0	0.476
Cuff leak volume (ml), mean±SD	283.18±125.65	334.80±110.25	0.332
Cuff leak percentage (%), mean±SD	47.15±19.17	54.14±14.98	0.366

BMI: body mass index, APACHE: Acute Physiology and Chronic Health Evaluation, MV: mechanical ventilation. IRQ, interquartile range.
* $P<0.05$

of a positive CLT. COVID-19 patients had no more of an increased risk of a positive CLT than non-COVID CAP patients. Multivariate analysis showed that female gender and duration of endotracheal intubation were positively correlated with an increased risk of a positive CLT.

Discussion

The CLT is commonly used for pre-extubation evaluation of the risk of PES in patients with respiratory failure and endotracheal intubation. Due to a consideration of aerosol generation and associated virus transmission, CTL is less frequently performed in severe COVID-19 patients. Up to this point, there is no published literature that presents data on CLT in COVID-19 patients. We performed CLT in patients with severe COVID-19 and respiratory failure receiving endotracheal intubation, and compared the results to those of severe non-COVID CAP patients.

Our study reveals an extremely low rate of extubation failure in patients with severe COVID-19. Only 1 in 21 COVID-19 patients was re-intubated, but there was no obvious PES clinically. Another 13 patients without a pre-extubation CLT were extubated successfully without recurrent respiratory failure. Meanwhile, only 1 of 42 severe non-COVID CAP patients had PES, and no re-intubation was performed in any of the 42 patients. The percentages of a positive CLT were comparable in COVID-19 and non-COVID CAP patients (9.5% vs. 14.3%, P=0.593). The cuff leak volumes and cuff leak percentages showed no significant difference between severe COVID-19 patients and severe non-COVID CAP patients. There

Table 3. Logistic Regression analysis of Risk Factors for a Positive CLT

	Univariate logistic regression			Multivariate logistic regression		
Risk factors	OR	95% C.I.	*P* value	OR	95% C.I.	*P* value
Age	1.026	0.960-1.096	0.444			
Gender (female vs. male)	25.083	2.805-224.309	0.004	124.073	2.888-5330.330	0.012
Duration of endotracheal intubation, days	1.042	0.984-1-102	0.159	1.118	1.010-1.238	0.031
BMI	1.032	0.889-1.198	0.678			
COVID vs. non-COVID	1.583	0.291-8.616	0.595			

OR: odds ratio, 95% C.I.: 95% confidence interval, APACHE II score: the Acute Physiology and Chronic Health Evaluation II score.
* $P<0.05$* $P<0.05$

was no significant difference in CLT results between COVID-19 patients with and without pre-extubation corticosteroids. Multivariate analysis revealed female gender and duration of endotracheal intubation were predictive factors for a positive CLT.

Endotracheal intubation for MV might result in injury to the larynx, the vocal cords, and upper trachea. A study that included 100 patients undergoing endoscopy after extubation found that 57% of the patients had signs of laryngeal injury with mucosal ulcers or granulation tissue [14]. Four types of laryngeal anomalies, including edema, ulceration, granulation, and abnormal vocal cord mobility, have been identified in patients with PES and re-intubation [15]. A meta-analysis in 2020 reported the incidence of post-extubation airway obstruction ranged from 4% to 37%, with a pooled estimate of 9% [16]. In another systematic review article, up to 30% of patients receiving a pre-extubation CLT had positive results [17]. Our study found a 9.5% positive CLT result in severe COVID-19 patients, which was slightly higher than that (14.3%) in severe non-COVID CAP patients. Unlike a previous study with a 20% PES incidence in COVID-19 pneumonia patients [18], the incidence of PES in this study was very low, with only 1 (1.3%) of 76 patients developing PES, and was managed well with systemic corticosteroids and temporary BiPAP use without re-intubation. None (0/34) of our COVID-19 patients had PES.

Corticosteroids are strong anti-inflammatory medications and could help to decrease the risk of post-extubation laryngeal edema. A single dose of 100 mg hydrocortisone administered systemically 1 hour before extubation had no beneficial effects on preventing PES [19]. Nevertheless, prospective randomized-controlled studies have shown corticosteroids significantly decreased the risk of PES and re-intubation, especially for patients with lower cuff leak volumes [20]. The 2017 ATS/ACCP practice guideline suggests administering systemic corticosteroids at least 4 hours before extubation for adults who have failed a CLT. For severe COVID-19 patients, the administration of systemic dexamethasone effectively reduced 28-day mortality by 17%, and reduced the mortality rate for MV patients by 36% [11]. It is recommended for all COVID-19 patients with

severe pneumonia at a dose of 6 mg daily for up to 10 days, or until the day of discharge [12].

We followed the recommendation for the use of corticosteroids in severe COVID-19 patients by providing 10 days' dexamethasone treatment. Those who were extubated within less than 10 days after intubation were all under dexamethasone therapy before extubation. Our data show that COVID-19 patients without corticosteroid therapy before extubation had a lower BMI than those with corticosteroids, which might indicate the possible association between poorer nutritional status and longer duration of MV. Other parameters including age, APACHE II scores, and days of intubation had no significant between-group difference. The percentage of patients with positive CLT, the cuff leak volumes, and cuff leak percentages were similar without statistical difference between those with and without pre-extubation corticosteroids. Meanwhile, none of our 34 COVID-19 patients had PES. Preventive pre-extubation corticosteroids might not be necessary for all patients with endotracheal intubation, but should be considered in selected patients who have a higher risk of PES.

Risk factors for stridor and laryngeal edema after extubation include advanced age, female gender, higher BMI, larger endotracheal tube diameter, longer intubation duration, trauma of the upper airway after unintended extubation, and emergency intubation [15, 21]. Univariate analysis for the risk of a positive CLT in our study revealed female gender is the only factor to predict a positive CLT. Other factors, including age, BMI, duration of intubation, or patient group (COVID-19 vs. non-COVID CAP), had no significant impact on the occurrence of a positive CLT using univariate analysis. Nevertheless, multivariate analysis found that female gender and duration of intubation were both significant predictors for a positive CLT. Seven of 8 positive CLT patients in this study were female, and female gender had a high odds ratio for a positive CLT, compared to male gender. Our data are comparable to that of previous studies, which concluded that female gender and prolonged intubation are risk factors for stridor and laryngeal edema in patients with COVID-19 [22-23]. The CLT is suggested in these groups of high-risk patients.

The CLT procedure is potentially associated with an increased risk of aerosol generation, but a previous review article on high-risk aerosol-generating procedures (AGPs) did not mention CLT [24]. When the cuff is deflated during the CLT, the air passing outside the endotracheal tube could generate a certain amount of virus-containing particles in COVID-19 patients. CLT has the potential to create aerosols with high viral loads, which may lead to a higher risk of infection by SARS-CoV-2 for health care workers. The CDC recommends that AGPs that could generate infectious aerosols should be performed cautiously and avoided if appropriate alternatives exist [25]. AGPs such as the CLT should take place in an airborne infection isolation room if possible. The number of health care professionals present during the procedure of CLT should be limited to only those essential for respiratory care and procedure support. With these precautions, CLT could be performed safely in selected patients with a higher PES risk.

There are several limitations to this study. First, the patient numbers in this study are relatively small because the CLT has not been performed routinely in patients with severe COVID-19. Second, the baseline characteristics of patients with severe COVID-19 and severe

non-COVID CAP were not matched properly because of the limited patient numbers. Third, the definition of PES was subjective, and relied on clinical audible stridor, but not a visualization of laryngeal edema or direct measurement of the upper airway narrowing. Fourth, the calibers of the endotracheal tube could influence the leak volumes in CLT -- a larger endotracheal tube would result in a lower leak volume. Most of our patients used a 7.5 mm endotracheal tube, and no larger tube was used in this study. The negative effects of larger endotracheal tubes on leak volumes could be neglected in this study. The final limitation of this study is that pre-extubation corticosteroids were not randomly assigned to the patients. Therefore, the non-randomized study design would decrease the power of this study.

Conclusion

Our study showed that less than 10% of severe COVID-19 patients had a positive CLT. The percentages of patients with a positive CLT, and the cuff leak volumes and cuff leak percentages of the severe COVID-19 patients were comparable to those of the patients with severe COVID-19 CAP. The incidence of PES in this study was extremely low, and possibly because of this, pre-extubation corticosteroid therapy did not have a significant impact on extubation outcomes. As in previous studies, female gender and the duration of intubation before extubation were associated with higher risks for positive CLT in our patients. The high positive predicted values and specificity suggest that clinicians should consider intervening in patients with a positive test, but the low sensitivity suggests that patients still need to be closely monitored post-extubation. We should take adequate action to prevent PES before extubation in those with a cuff leak volume less than the cut-off value. For those with a negative CLT, extubation should not be delayed when the patients fulfill the criteria for discontinuation of MV and extubation. For severe COVID-19 patients with endotracheal intubation, it is reasonable to follow the clinical practice guideline for pre-extubation evaluation with a CLT in selected patients with a higher risk of PES, especially female patients and patients with an increased duration of endotracheal intubation.

Declarations

1. *Ethics approval and consent to participate*: This study was approved by the Institutional Review Board of Chang-Gung Medical Foundation. (IRB No.: 202102012B0, Protocol Title: To investigate cuff leak test to predict extubation success for COVID-19 patients with mechanical ventilation, Dec 16, 2021). Anonymized clinical data were deemed low risk and informed consent was waived by the IRB of Chang-Gung Medical Foundation. The procedures followed were in accordance with the ethical standards of the responsible committee on human experimentation and with the Helsinki Declaration of 1975. All methods were carried out in accordance with relevant guidelines and regulations.
2. *Consent for publication*: Not applicable
3. *Availability of data and materials*: The datasets used and/or analyzed during the current study are available from the corresponding author on reasonable request.
4. *Competing interests*: The authors declare that they have no competing interests.
5. *Funding*: None.

6. *Authors' contributions*: MCL, HYC, CTH, HFH, HCH, CCH, and MJH have made substantial contributions to the conception and design of the work. MCL and HYC have made substantial contributions to the acquisition, analysis, and interpretation of data. MCL has drafted the work. MJH has substantively analyzed, reviewed, and revised the work. All authors have approved the submitted version and have agreed both to be personally accountable for the author's own contributions and [[to ensure that questions related to the accuracy or integrity of any part of the work…are addressed???, are answered???... this is incomplete, we need to know what will be done with any questions.
7. *Acknowledgements*: Not applicable
8. *Authors' information*: Not applicable

References

1. Pluijms WA, van Mook WN, Wittekamp BH, *et al*. Postextubation laryngeal edema and stridor resulting in respiratory failure in critically ill adult patients: updated review. Crit Care 2015; 19(1): 295.
2. Thille AW, Harrois A, Schortgen F, *et al*. Outcomes of extubation failure in medical intensive care unit patients. Crit Care Med 2011; 39(12): 2612-2618.
3. Frutos-Vivar F, Esteban A, Apezteguia C, *et al*. Outcome of reintubated patients after scheduled extubation. J Crit Care 2011; 26(5): 502-509.
4. Potgieter PD, Hammond JM. "Cuff" test for safe extubation following laryngeal edema. Crit Care Med 1988; 16(8): 818.
5. Jaber S, Chanques G, Matecki S, *et al*. Post-extubation stridor in intensive care unit patients. Risk factors evaluation and importance of the cuff-leak test. Intensive Care Med 2003; 29(1): 69-74.
6. Wittekamp BH, van Mook WN, Tjan DH, *et al*. Clinical review: post-extubation laryngeal edema and extubation failure in critically ill adult patients. Crit Care 2009; 13(6): 233.
7. Miller RL, Cole RP. Association between reduced cuff leak volume and postextubation stridor. Chest 1996; 110(4): 1035-1040.
8. De Bast Y, De Backer D, Moraine JJ, *et al*. The cuff leak test to predict failure of tracheal extubation for laryngeal edema. Intensive Care Med 2002; 28(9): 1267-1272.
9. Sandhu RS, Pasquale MD, Miller K, *et al*. Measurement of endotracheal tube cuff leak to predict postextubation stridor and need for reintubation. J Am Coll Surg 2000; 190(6): 682-687.
10. Girard TD, Alhazzani W, Kress JP, *et al*. An Official American Thoracic Society/American College of Chest Physicians Clinical Practice Guideline: Liberation from Mechanical Ventilation in Critically Ill Adults. Rehabilitation Protocols, Ventilator Liberation Protocols, and Cuff Leak Tests. Am J Respir Crit Care Med 2017; 195(1): 120-133.
11. The RECOVERY Collaborative Group. Dexamethasone in hospitalized patients with Covid-19. N Engl J Med 2020; 384(8): 693-704.
12. National Institutes of Health. Coronavirus Disease 2019 (COVID-19) Treatment Guidelines.
13. World Health Organization. Therapeutics and COVID-19: living guideline.
14. Gros A, Holzapfel L, Marqué S, *et al*. Intra-individual variation of the cuff-leak test as a predictor of post-extubation stridor. Respir Care 2012; 57(12): 2026-2031.
15. Tadié JM, Behm E, Lecuyer L, *et al*. Post-intubation laryngeal injuries and extubation failure: a fiberoptic endoscopic study. Intensive Care Med 2010; 36(6): 991-998.
16. Kuriyama A, Jackson JL, Kamei J. Performance of the cuff leak test in adults in predicting post-extubation airway complications: a systematic review and meta-analysis. Crit Care 2020; 24(1): 640.
17. Zhou T, Zhang HP, Chen WW, *et al*. Cuff-leak test for predicting postextubation airway complications: a systematic review. J Evid Based Med 2011; 4(4): 242-254.
18. Pangilinan LP, Burns GD, Kallet R. Increased risk of post extubation stridor with COVID-19 pneumonia. Respir Care 2021; 66(Suppl 10): 3611470.
19. Ho LI, Harn HJ, Lien TC, *et al*. Postextubation laryngeal

edema in adults. Risk factor evaluation and prevention by hydrocortisone. Intensive Care Med 1996; 22(9): 933-936.

20. Jaber S, Jung B, Chanques G, *et al*. Effects of steroids on reintubation and post-extubation stridor in adults: meta-analysis of randomised controlled trials. Crit Care 2009; 13(2): R49.
21. Erginel S, Ucgun I, Yildirim H, *et al*. High body mass index and long duration of intubation increase post-extubation stridor in patients with mechanical ventilation. Tohoku J Exp Med 2005; 207(2): 125-132.
22. Moran JV, Godil SA, Goldner B, *et al*. Post-extubation stridor complicating COVID-19-associated acute respiratory distress syndrome: a case series. Cureus 2020; 12(9): e10492.
23. McGrath BA, Wallace S, Goswamy J. Laryngeal oedema associated with COVID-19 complicating airway management. Anaesthesia 2020; 75(7): 972.
24. Howard BE. High-risk aerosol-generating procedures in COVID-19: respiratory protective equipment considerations. Otolaryngol Head Neck Surg 2020; 163(1): 98-103.
25. Centers for Disease Control and Prevention. Interim Infection Prevention and Control Recommendations for Healthcare Personnel During the Coronavirus Disease 2019 (COVID-19) Pandemic.

Collateral Circulation of Phrenic Venous Pathway in Lung Cancer-Associated Superior Vena Cava Syndrome: A Case Report

Tse-Hsien Lo[1], Jia-Jun Wu[1,2,3], Gee-Chen Chang[1,2,3,4]

Superior vena cava (SVC) syndrome is a common complication of lung cancer, including both non-small cell and small cell lung cancers. The formation of collateral circulation can reduce clinical symptoms, such as shortness of breath, a puffy face, and neck and arm swelling. Here, we report a case of SVC syndrome in a 70-year-old woman, a never-smoker, who presented with right neck and right arm numbness for 1 month. Right upper lobe lung cancer with partial compression of the SVC was diagnosed. Chest computed tomography revealed a rare collateral circulation pathway, i.e., the phrenic venous pathway. Collateral circulation was observed during the follow-up period. ***(Thorac Med 2024; 39: 24-30)***

Key words: Collateral circulation, lung cancer, phrenic collateral circulation, superior vena cava (SVC) syndrome.

Introduction

The superior vena cava (SVC) serves as the major central venous drainage vessel of the head, neck, and upper extremities [1]. Its venous returns are formed from the bilateral brachiocephalic and azygos veins. External compression or thrombosis of the SVC results in SVC syndrome, which leads to congestion of the venous drainage system of the upper trunk [2-3]. The etiologies of SVC compression include benign or malignant conditions, such as tumors of the lung or mediastinum, an aortic aneurysm, a mediastinal hematoma, or infectious processes (tuberculoma or mediastinitis). Idiopathic SVC thrombosis, intravascular catheters, or pacemaker devices can cause intraluminal stenosis of the SVC [2,4]. Approximately 65% of SVC syndrome cases result from malignancies. Among them, lung cancer is the most common cause, accounting for approximately 75% of malignant cases [2].

Clinical presentations of SVC syndrome include facial congestion, neck and arm swell-

[1]Division of Pulmonary Medicine, Department of Internal Medicine, Chung Shan Medical University Hospital, Taichung, Taiwan, [2]School of Medicine, Chung Shan Medical University, Taichung, Taiwan, [3]Institute of Medicine, Chung Shan Medical University, Taichung, Taiwan, [4]Institute of Biomedical Sciences, National Chung Hsing University, Taichung, Taiwan
Address reprint requests to: Dr. Gee-Chen Chang, Division of Pulmonary Medicine, Department of Internal Medicine, Chung Shan Medical University Hospital, Taichung, Taiwan (No. 110, Sect. 1, Jianguo N. Road, Taichung, 402, Taiwan).

ings, and shortness of breath [3,5]. Occasionally, collateral circulations form another route of venous drainage during SVC impairment. The number of collateral pathways depends on the severity of obstruction [3]. Herein, we present a rare case of lung cancer-associated SVC syndrome with collateral circulation of the phrenic venous pathway.

Case description

A 70-year-old female never-smoker presented at the chest medicine outpatient department with numbness of the right neck and right arm for more than 1 month. She complained of other associated symptoms, including loss of appetite, occasional blood-streaked sputum expectoration, and body weight loss (5 kilograms within the last 3 months). She did not complain of dyspnea on exertion, fever, chills, or hoarseness of her voice. Physical examination revealed the general appearance of chronic illness, and a clear consciousness. The conjunctiva was pink in color. Redness of the face, facial or arm swelling, or stridor was not found. The veins in the bilateral neck area were not distended, and the superficial veins in the chest wall were not engorged. The initial complete blood count revealed no leukocytosis, anemia, or thrombocytopenia. Renal and liver functions were within normal ranges. Marked elevations of carcinoembryonic antigen, at 6,164.1 (reference range: 0~5) ng/mL, and carbohydrate antigen-125, at 106.6 (reference range: 0~35) U/mL, were noted. Contrast-enhanced chest computed tomography (CT) revealed a lung tumor at the right upper lobe, and left supraclavicular lymph node metastasis. Furthermore, the SVC was partially compressed by the tumor, which was located at the azygos level (Figure 1). The histological diagnosis was adenocarcinoma, which was confirmed based on excisional biopsy findings of the left supraclavicular lymph node. The epidermal growth factor receptor (EGFR) mutation test showed an exon 21 mutation (L858R).

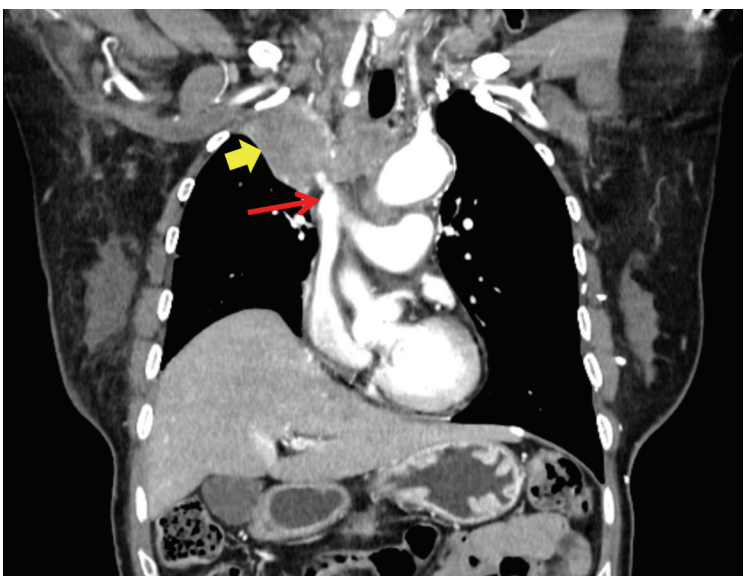

Fig. 1. Coronal view of the chest CT image showed a right upper lobe lung tumor (yellow arrow) compressing the superior vena cava (red arrow).

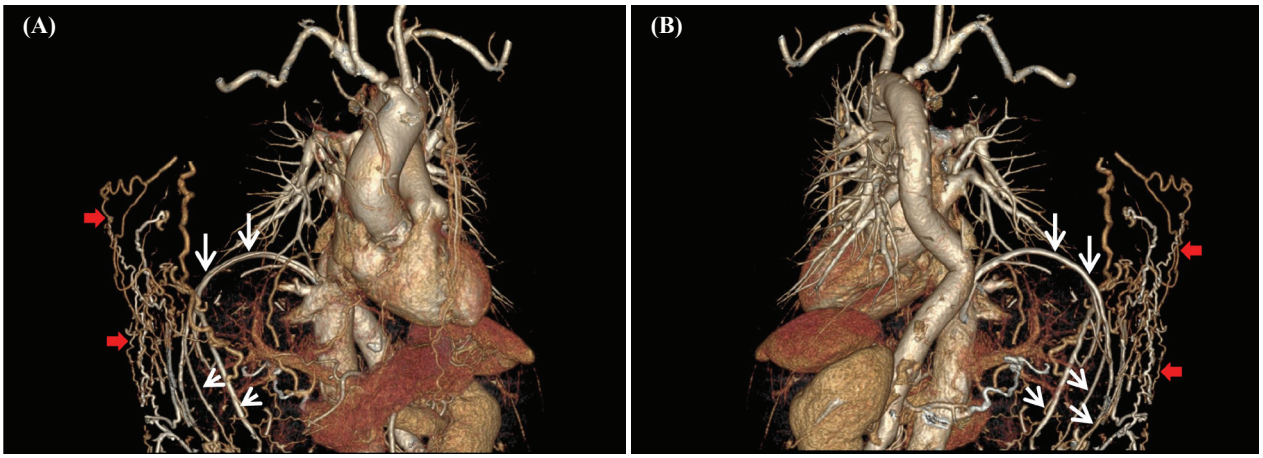

Fig. 2. Anterior view (A) and posterior view (B) of 3-dimensional reconstruction of the chest CT image showed right phrenic collateral (white arrows) and chest wall collateral (red arrows).

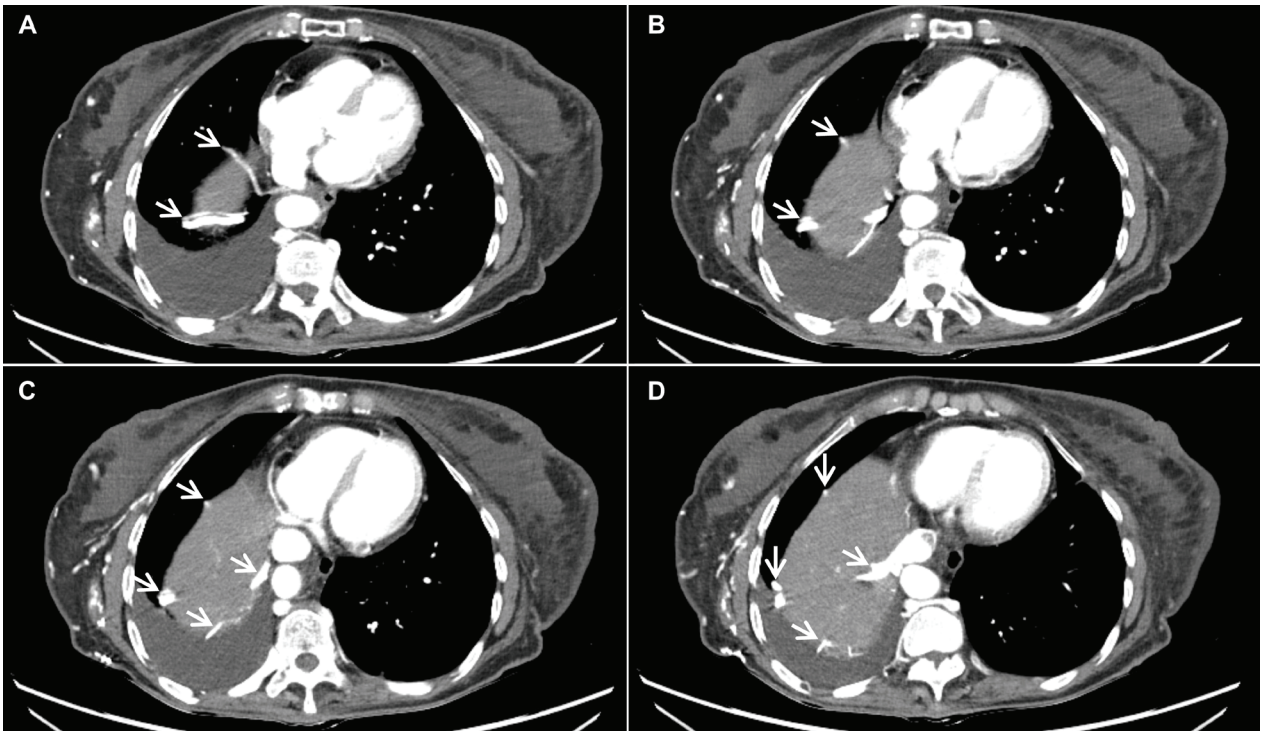

Fig. 3. Serial axial view of the chest CT image (A to D) showed 3 phrenic venous routes that passed through the liver surface.

Due to clinical stage IV disease, the patient participated in a clinical trial of third-generation EGFR-tyrosine kinase inhibitor (TKI) as first-line treatment [6]. She had a partial response initially and disease progression 1 year later. Upon disease progression, she presented with superficial vein engorgement at the right chest wall. Follow-up chest CT showed collateral venous circulations at the right anterior chest wall, right periscapular pathways, and phrenic venous pathway (Figure 2). The phrenic venous pathway included 3 prominent routes passing

through the liver surface and along the dome of the right diaphragm (Figure 3). The phrenic venous route finally drained into the inferior vena cava (Figure 4). The left supraclavicular lymph node rebiopsy revealed an exon 21 mutation (L858R) and positive immunohistochemical stain for C-mesenchymal epithelial transition factor (C-MET). Therefore, the patient received

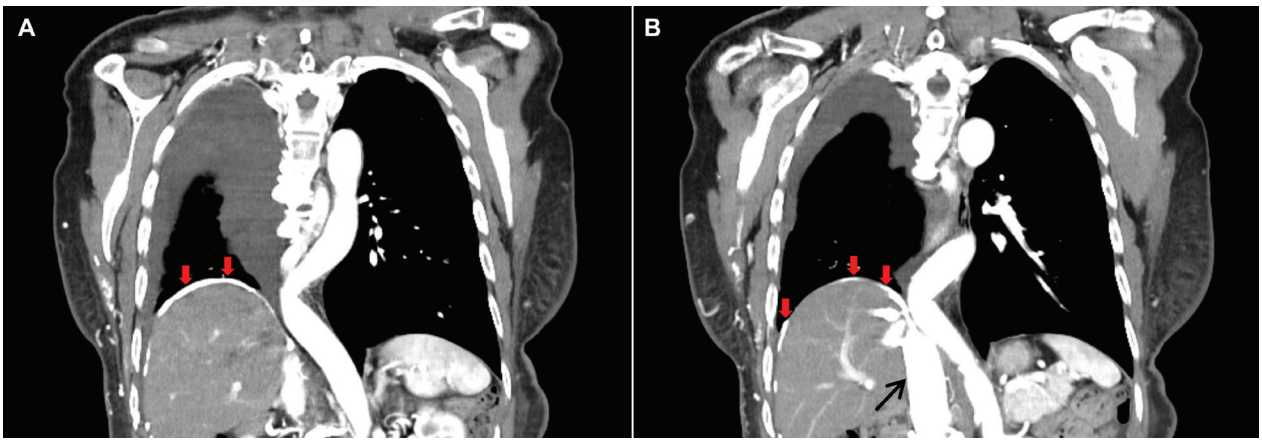

Fig. 4. Coronal view of the chest CT image (A and B) showed the right phrenic venous route (red arrows) drained into the inferior vena cava (black arrow).

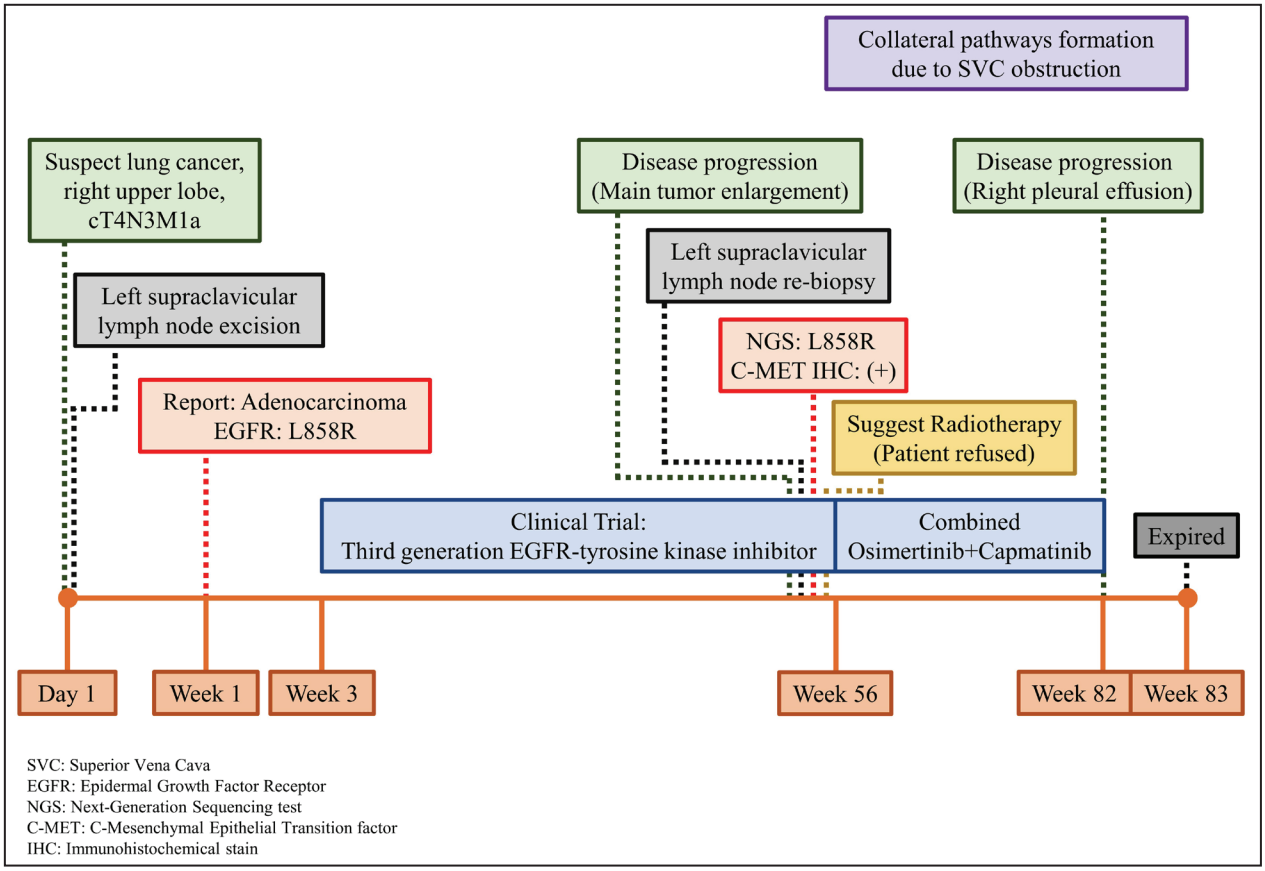

Fig. 5. Clinical course of the patient reported in this article.

second-line treatment with osimertinib and capmatinib, because MET overexpression may be a resistance mechanism of osimertinib.

However, the patient refused to receive palliative radiotherapy for the right upper lobe tumor. Three months later, the patient had stable disease with second-line treatment. Chest CT revealed no improvement in SVC syndrome or collateral circulations, particularly the engorged phrenic venous pathway. She developed disease progression with aggravated shortness of breath and right pleural effusion about 5 months later. She died soon after disease progression, with an overall survival of 18.9 months (Figure 5).

Discussion

SVC syndrome can result from compression or thrombosis of the SVC, which causes impaired venous drainage into the right atrium [2,7]. The etiologies of SVC syndrome are classified as non-malignant and malignant. Infectious diseases have accounted for most cases of non-malignant SVC syndrome in the past 60 years; however, in recent decades, SVC obstruction associated with an intravascular catheter or implantable cardiac devices has been more prevalent [2]. Benign mediastinal lesions, such as anterior mediastinal hematoma and pericardial hematoma, have also been reported [8,9]. Although the occurrence of non-malignant conditions is increasing, the most common causes of SVC syndrome remain malignant conditions [2,4]. Non-small cell lung cancer accounts for approximately half of the cases of SVC syndrome due to malignancy, and small cell lung cancer and lymphoma account for approximately 30% [2].

SVC syndrome can be classified into 4 types, based on the anatomic site of the obstruction: bilateral brachiocephalic vein (type I), supra-azygos SVC (type II), azygos SVC (type III), and infra-azygos SVC (type IV) [1]. SVC syndrome can induce the collateral circulation. Common collateral pathways are the azygos, vertebral, periscapular, and anterior cervical venous pathways [3,4]. Although collateral circulations are common in SVC syndrome, the pericardiophrenic pathway, with an incidence of 5%, has been very rarely reported [4]. A case involving the collateral vessel from the right subclavian vein to the left atrium, which is another form of an unusual collateral pathway, has also been reported [10].

The most frequent symptoms and signs of SVC syndrome are facial and arm edema, with a distended neck and chest veins. Stridor and vocal hoarseness are less frequent manifestations. The degree of dyspnea depends on the severity of SVC obstruction [2]. Patients with rapid progression of SVC obstruction may complain of severe shortness of breath. Chest CT with contrast enhancement can easily detect the SVC obstruction and collateral pathways [3,11,12]. The 3-dimensional reconstruction technique has advantages over conventional 2-dimensional CT [12]. In most cases, multiple collateral pathways were presented simultaneously [4].

Plekker et al. reported on the difference between clinical and radiological scoring systems. The clinical scoring system was used to assess clinical severity, with scores ranging from 0 to 36; cases with a score of more than 10 were classified as severe disease. The radiological score was defined as the degree of SVC obstruction minus collateral formation [3]. Another classification system that is based on the level of obstruction and the severity of vascular stenosis may be helpful to assess the clinical

condition [1]. The severity of SVC obstruction on chest CT should be reversely proportional to the formation of collateral circulations. The rationale is that the formation of collateral veins may reduce the congestive symptoms [3].

Management of SVC obstruction includes relief of symptoms and treatment of the underlying disease. Medicines, including loop diuretics and glucocorticoids, help to reduce edema and respiratory distress [2]. However, the effectiveness of these medications has not been well studied. In 1 study, the rate of clinical improvement was similar among patients receiving glucocorticoids, diuretics, or neither [13]. Endovascular stenting is another method of symptom relief. Two systematic reviews described a clinical success rate of 92.8%~98.8%, with a complication rate of 5.7%~7.5% [14,15]. SVC thrombosis due to a catheter-related condition can be treated with oral anticoagulants [15-16]. For patients with SVC syndrome caused by lung cancer, systemic chemotherapy with or without palliative radiotherapy usually reduces the tumor burden and improves clinical symptoms. The median survival of patients with SVC syndrome due to malignant diseases was approximately 4.7 months [14].

In the present case, the main collateral circulation was the phrenic venous pathway. No previous report has shown the formation of a single phrenic pathway. This venous route is always combined with other collateral circulations. No distinctive features were found to result in only 1 collateral pathway or another pattern, depending on the underlying cause or degree of obstruction [4]. Palliative radiotherapy to the bulky tumor of the present case might have reduced the severity of SVC compression, but the patient refused. Since the malignant condition in our patient was not well controlled, we could not identify the relationship between treatment response and reduction of the collateral pathways.

Conclusion

We presented a case with SVC syndrome, type III, due to lung cancer invasion to the azygos level. The patient had phrenic collateral circulation, which is a rare collateral circulation of SVC syndrome. The patient did not achieve a good response with second-line treatment, and refused to have palliative radiotherapy, which may have reduced the size of the bulky tumor and relieved some of her symptoms. Although the patient had an overall survival of 18.9 months, longer survival might have been achieved if a local treatment could have been added.

References

1. Azizi AH, Shafi I, Shah N, et al. Superior vena cava syndrome. JACC Cardiovasc Interv 2020; 13(24): 2896-910.
2. Wilson LD, Detterbeck FC, Yahalom J. Clinical practice. Superior vena cava syndrome with malignant causes. N Engl J Med 2007; 356(18): 1862-9.
3. Plekker D, Ellis T, Irusen EM, et al. Clinical and radiological grading of superior vena cava obstruction. Respiration 2008; 76(1): 69-75.
4. Meier A, Alkadhi H. Venous collateral pathways in superior thoracic inlet obstruction: a systematic analysis of anatomy, embryology, and resulting patterns. AJR Am J Roentgenol 2019; 213(1): 200-10.
5. Higdon ML, Atkinson CJ, Lawrence KV. Oncologic emergencies: recognition and initial management. Am Fam Physician 2018; 97(11): 741-8.
6. Cho BC, Felip E, Hayashi H, et al. MARIPOSA: phase 3 study of first-line amivantamab + lazertinib versus osimertinib in EGFR-mutant non-small-cell lung cancer. Future Oncol 2022; 18(6): 639-47.

7. Spring J, Munshi L. Oncologic emergencies: traditional and contemporary. Crit Care Clin 2021; 37(1): 85-103.
8. Ibrahim R, Yadav S, Waqar S, et al. Superior vena cava syndrome due to right anterior mediastinal hematoma: a case report. Cureus 2022; 14(7): e26994.
9. Saboe A, Pramanda AN, Hasan M, et al. Superior vena cava syndrome due to pericardial hematoma: a case report and mini-review of literature. SAGE Open Med Case Rep 2021; 9: 2050313X211057700.
10. Parsaee M, Pouraliakbar H, Ghadrdoost B, et al. Unusual collateral vessel from right subclavian vein to left atrium, a rare complication of superior vena cava obstruction. Echocardiography 2018; 35(8): 1233-6.
11. Kim HC, Chung JW, Yoon CJ, et al. Collateral pathways in thoracic central venous obstruction: three-dimensional display using direct spiral computed tomography venography. J Comput Assist Tomogr 2004; 28(1): 24-33.
12. Eren S, Karaman A, Okur A. The superior vena cava syndrome caused by malignant disease. Imaging with multi-detector row CT. Eur J Radiol 2006; 59(1): 93-103.
13. Schraufnagel DE, Hill R, Leech JA, et al. Superior vena caval obstruction. Is it a medical emergency? Am J Med 1981; 70(6): 1169-74.
14. Aung EY, Khan M, Williams N, et al. Endovascular stenting in superior vena cava syndrome: a systematic review and meta-analysis. Cardiovasc Intervent Radiol 2022; 45(9): 1236-54.
15. Azizi AH, Shafi I, Zhao M, et al. Endovascular therapy for superior vena cava syndrome: a systematic review and meta-analysis. EClinicalMedicine 2021; 37: 100970.
16. Mumoli N, Mazzone A, Evangelista I, et al. Superior vena cava syndrome after pacemaker implantation treated with direct oral anticoagulation. Thromb J 2021; 19(1): 84.

Variation in Oxygen Saturation Measured by a Wearable Device May Predict Response to Treatment in Patients with Community-Acquired Pneumonia

Yu-Cheng Wu[1], Chien-Chung Huang[2,3], Chiann-Yi Hsu[4], Wen-Cheng Chao[1,5,6,7], Chieh-Liang Wu[1,5]

Background: Community-acquired pneumonia (CAP) is 1 of the leading causes of death worldwide, and early prediction of response to treatment is crucial in managing patients with CAP. Wearable devices are increasingly being used to monitor physiological parameters continuously. Therefore, the aim of this study was to determine the ability of wearable devices to predict the outcome of treatment for patients with CAP.

Methods: We prospectively enrolled patients with CAP at a tertiary referral hospital in central Taiwan between 2020 and 2021, and used wearable devices to monitor oxygenation (SpO2) and physical activity for 2 days after admission. An unfavorable treatment outcome on Day 5 was determined by clinical deterioration, radiographic progression, or pneumonia-related complications. Multivariate logistic regression was used to determine the odds ratio (OR) and 95% confidence interval (CI).

Results: A total of 62 patients with CAP were enrolled, and 51.6% (32/62) of them were classified as having unfavorable treatment outcomes. The groups with favorable and unfavorable treatment outcomes had similar disease severities, including CURB-65 (1.13±0.82 vs. 1.06±0.8, *p*=0.719) and the pneumonia severity index (97.3±36.21 vs. 98.06±31.7, *p*= 0.983). We found a lower SpO_2, a higher variation in SpO_2, and lower physical activity in those with an unfavorable response compared to those with a favorable response. After adjusting for age, sex, and severity, we found that a lower average SpO_2 (OR: 0.91, 95% CI 0.62–1.33, *P*=0.624) and a greater variation in SpO_2 (OR: 1.87, 95% CI 1.02–3.42, *P*=0.044) on Day 2tended to be associated with an increased risk of an unfavorable treatment outcome.

Conclusion: In this study, we continuously monitored CAP patients using a wearable device and identified Day 2 SpO2 average and variation as potential early treatment outcome predictors. ***(Thorac Med 2024; 39: 13-23)***

Key words: Pneumonia, pulse oximetry, internet of things (IoT), wireless, monitoring

[1]Department of Critical Care Medicine, Taichung Veterans General Hospital, Taichung, Taiwan, [2]Computer &Communication Center of Taichung Veterans General Hospital, Taichung, Taiwan, [3]Department of Industrial Engineering and Enterprise Information, Tunghai University, Taichung, Taiwan, [4]Biostatistics Task Force of Taichung Veterans General Hospital, Taichung, Taiwan, [5]College of Medicine, Chung Hsing University, Taichung, Taiwan, [6]Department of Automatic Control Engineering, Feng Chia University, Taichung, Taiwan, [7]Big Data Center, Chung Hsing University, Taichung, Taiwan

Address reprint requests to: Dr. Chieh-Liang Wu, Taichung Veterans General Hospital, No. 1650, Section 4, Taiwan Boulevard, Xitun District, Taichung City, Taiwan 40705.

Background

Community-acquired pneumonia (CAP) is 1 of the leading causes of hospitalization and mortality worldwide, and is estimated to affect 24.8 patients per 10,000 person-years in the United States [1-2]. Several studies have found that clinical response to treatment, mainly defined by clinical outcome within approximately 5 days after admission, was about 70%; however, the early determinant for those with an unfavorable treatment response remains unclear [3-4].

Wearable devices are increasingly being used to provide autonomous, wireless, and continuous monitoring in medical care [5-7]. The continuous monitoring with these devices could reduce the workforce requirement and unnecessary contact in treating patients with coronavirus disease 2019 (COVID-19) [8]. In addition, silent hypoxia is a critical event in patients with COVID-19 infection, and continuous monitoring of oxygen saturation (SpO_2) by wireless pulse oximetry could provide timely detection of hypoxemia in patients with COVID-19 [9, 10].

However, wearable devices may produce high-volume stream data, and this big data may somehow lead to unexpected difficulties in the practical application of the wearable device, particularly the edge device. Therefore, it is important to identify the crucial indicator among the stream data of the wearable device in different practical applications. In the present study, we used a wearable device to collect continuous physiological parameters, including oxygenation and physical activity. Then, we attempted to identify early determinants, particularly SpO_2-relevant parameters, for treatment outcomes in patients with CAP.

Methods

Ethical approval

We prospectively enrolled patients with CAP at a tertiary referral hospital in central Taiwan between 2020 and 2021, and used wearable devices to monitor oxygenation (SpO_2) and physical activity for 2 days after admission. An unfavorable treatment outcome on Day 5 was determined by clinical deterioration, radiographic progression, or pneumonia-related complications. Multivariate logistic regression was used to determine the odds ratio (OR) and 95% confidence interval (CI).

This prospective study was approved by the Institutional Review Board of Taichung Veterans General Hospital (CE20182B). Informed consent was obtained from all participants before application of the wearable device and data collection.

Participants and clinical variables

We enrolled adult patients who met the criteria for CAP; that is, acute infiltrates on chest radiograph (CXR), accompanied by 2 or more symptoms, including fever, new cough, or change in color of respiratory secretions, chest discomfort, or dyspnea [3]. Demographic, laboratory, and microbiological data, as well as clinical data on comorbidities, medications, and variables for CAP severity scores, including the pneumonia severity index (PSI) and CURB-65 score, were collected [11, 12].

Definition of an unfavorable treatment outcome

Various criteria, including improvement in clinical symptoms, radiographic response, and development of adverse events, have defined the CAP outcome on day 4/5 after admission

[3, 13]. For example, the American Thoracic Society (ATS)used improvement in clinical symptoms and signs, including body temperature, heart rate, respiratory rate, systolic blood pressure, and SpO_2, on day 5 after admission to define the outcome of treatment in patients with CAP [3]. However, the guidance proposed by the United States Food and Drug Administration (FDA) for the industry in developing drugs to treat CAP recommended defining the outcome of treatment not only by evaluating the improvement in clinical symptoms on day 4, but also by checking the radiographic response and monitoring the development of complications related to pneumonia, including respiratory failure, hospital-acquired infection, progress to septic shock and upgrade of antibiotics [13].

To avoid underestimating unfavorable outcomes, we defined a favorable outcome of patients in the present study as a lack of clinical deterioration, radiographic progression, or pneumonia-relevant complications on day 5. For the evaluation of radiographic response, we used the Radiographic Assessment of Lung Edema (RALE) score, which was designed to quantify the density of consolidation of the 4 quadrants in patients with consolidative lung diseases, including acute respiratory distress syndrome (ARDS) and pneumonia [14-15]. In this study, the RALE scores were determined by 2 independent pulmonologists.

Wearable devices and collected parameters

We used 2 commercialized wireless wearable devices, including a finger pulse oximeter to monitor SpO_2, and a 3-axis accelerometer on the wrist to measure physical activity. The accelerometer exported an integrated digital output with the numeric data. The measured acceleration/deceleration scale range on the x, y, and z axes was 2 g, 4g, and 8g, respectively. The 2 wireless wearable devices used transmitted the signals gathered within 10 minutes to the gateway in the study hospital for a2-day period. We then transformed the data collected by the wearable device with 2 distinct indicators, including the mean value and the coefficient of variation (CoV), which is the ratio of the standard deviation to the mean value. Figure 1 shows the data collected from the wearable devices, wireless transmission, and data transfer to the server and analysis.

Statistical Analyses

The numbers of patients were expressed as percentages for categorical variables, and mean ± standard deviation was used for continuous variables. Given that the data collected by the

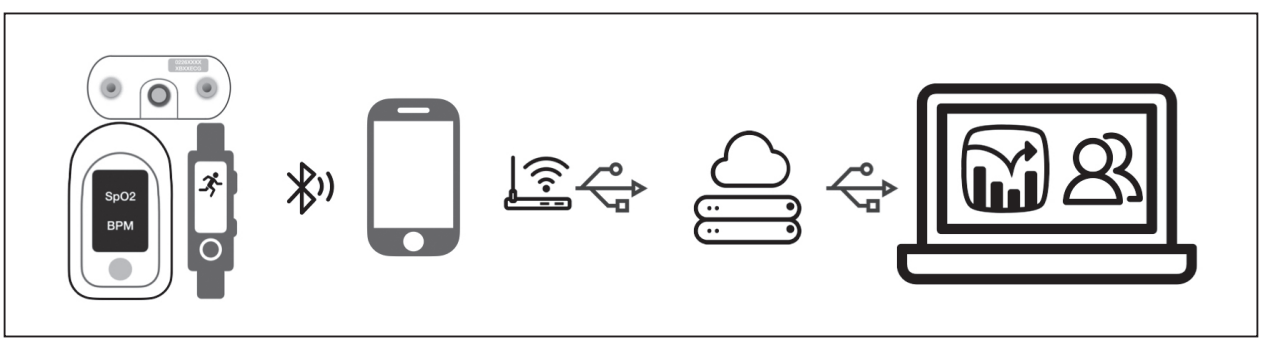

Fig. 1. Data collection from wearable devices, wireless transmission, and data transfer to the server and analysis

wearable device tended to be skewed to normal data, we used the Mann-Whitney U test and the exact test to determine the difference between those with distinct treatment outcomes. Multivariate logistic regression was used to determine the odds ratio (OR) and the corresponding 95% confidence interval (CI) for the unfavorable outcome. All data were analyzed using SPSS software version 22.0 (SPSS Inc., Chicago, IL, USA). A p-value less than 0.05 were considered statistically significant.

Results

Patient characteristics (including outcome of treatment)

A total of 62 CAP patients were enrolled between August 2020 and July 2021, and 51.6% (32/62) of them were classified as having unfavorable treatment outcomes on Day 5. The majority of the participants enrolled were elderly, with a mean age of 71.4±19.3 years, and 72.6% (45/62) of them were male. Given that the study hospital is a referral hospital in central Taiwan, the CAP severity scores were high, with PSI and CURB-6 scores of 97.7±33.7 and 1.1±0.80, respectively (Table 1). Comorbidities, severity scores, and laboratory data were compared between the favorable and unfavorable response groups. In particular, patients with unfavorable treatment results had a longer hospital stay than those with a favorable response (17.0±10.6 vs. 6.9±2.9 days, $p<0.01$).

The RALE scores on CXR and the pneumonia-associated complications among the enrolled participants were summarized in Table 2. We found that the RALE scores of the first CXR were similar between the 2 groups (9.3±6.5 vs. 7.4±4.5, $p=0.35$), but the RALE scores between Day 3 and Day 5 were higher in the unfavorable group than in the favorable group (10.3±5.9 vs. 4.9±3.5, $p<0.01$). Regarding pneumonia-associated complications, the numbers of participants with respiratory failure, hospital-associated infection, septic shock, and antibiotic upgrade were 3, 6, 1, and 19, respectively.

Dynamic data on days 1 and 2as measured by the wearable device

With respect to the dynamic data derived from the wearable device, we found high compliance with the use of the finger pulse oximeter; however, continued use of the wrist accelerometer tended to be suboptimal. We found that the level of compliance with use of the finger pulse oximeter at night was low, which may have resulted from the device being moved during the night.

The average SpO_2 was slightly lower in participants with unfavorable responses than in those with a favorable response on Day1 and Day2 during daytime (Day1: 95.8±2.0vs. 96.9±1.3, $p=0.01$; Day2: 96.0±1.8 vs. 96.7±1.6, $p=0.09$). Notably, we found a higher variation of SpO_2 on Day 2 daytime among participants with unfavorable treatment outcomes (CoV of SpO_2 on Day2 daytime: 2.25±1.15vs. 1.66±0.83, $p=0.03$). Physical activity as measured by the wrist accelerometer was lower among participants with an unfavorable treatment outcome, despite the aforementioned issue regarding the attrition of participants (Table 3). We then performed multivariate logistic regression (Table 4) to identify independent predictors of an unfavorable response to treatment on Day 5. We found that a lower variation of SpO_2 on Day 2 daytime could predict the response to treatment on Day 5.

Table 1. Demographic and Clinical Characteristics of Enrolled Subjects Categorized by the Treatment Outcome on Day5

	(Total (n=62)	Favorable outcome (n=30)	Unfavorable outcome (n=32)	*P* value
Demographic				
Age	71.4±19.3	72.6±20.6	70.3±18.3	0.39
Sex, male	45 (72.6%)	22 (73.3%)	23 (71.9%)	>0.99
Comorbidities				
Hypertension	38 (62.9%)	20 (66.7%)	18 (26.3%)	0.56
Diabetes mellitus	20 (32.6%)	11 (36.7%)	9 (28.1%)	0.66
Congestive heart failure	17 (27.4%)	9 (30.0%)	8 (25.0%)	0.88
Cerebrovascular disease	8 (12.9%)	3 (10.0%)	5 (15.6%)	0.71
Dementia	10 (16.1%)	3 (10.0%)	7 (21.9%)	0.30
COPD	22 (35.5%)	10 (33.3%)	12 (37.5%)	0.94
Moderate liver disease	4 (6.5%)	3 (10.0%)	1 (3.1%)	0.35
Chronic kidney disease	16 (25.8%)	12 (40.0%)	4 (12.5%)	0.03
Malignancy	11 (17.7%)	6 (20.0%)	5 (15.6%)	0.91
Severity scores				
Pneumonia severity index	97.7±33.7	97.3±36.2	98.1±31.7	0.98
CURB-65 score	1.10±0.80	1.13±0.82	1.06±0.80	0.72
Laboratory data				
White blood cell count (count/μl)	11205.1±4775.8	10573.7±4048.9	11816.1±5383.7	0.44
Hemoglobin (g/dL)	11.5±2.2	11.8±2.1	11.3±2.3	0.85
Platelets (103/μL)	228.0±84.9	210.7±74.4	243.6±91.9	0.17
Albumin (mg/dL)	3.5±0.5	3.9±0.5	3.3±0.5	0.10
Creatinine (mg/dL)	1.4±0.9	1.4±0.8	1.4±1.0	0.27
C-reactive protein (mg/dL)	7.6±7.5	5.3±4.9	10.2±8.9	0.04
Culture positivity				
Blood culture	9 (15.3%)	5 (17.2%)	4 (13.3%)	0.73
Sputum culture	14 (23.3%)	4 (13.8%)	10 (32.3%)	0.17
Hospital length of stay	12.1±9.3	6.9±2.9	17.0±10.6	<0.01

Abbreviations: COPD, chronic obstructive pulmonary disease

Table 2. Scoring of Sequential Chest X-ray and Pneumonia-Associated Complications of Enrolled Subjects Categorized by Treatment Outcome on Day5

	(Total (n=62)	Favorable outcome (n=30)	Unfavorable outcome (n=32)	*P* value
Day0 CXR				
Total score	8.4±5.7	7.4±4.5	9.3±6.5	0.35
Right upper lung score	1.5±2.5	1.0±2.0	1.9±3.0	0.28
Right lower lung score	2.6±2.4	2.1±1.6	3.2±2.9	0.21
Left upper lung score	0.4±1.1	0.4±1.3	0.4±1.0	0.45
Left lower lung score	3.9±3.7	3.9±3.6	3.8±3.9	0.61
Day3~5 CXR				
Total score	8.2±5.7	4.9±3.5	10.3±5.9	<0.01
Right upper lung score	1.6±2.6	0.8±1.6	2.1±3.0	0.07
Right lower lung score	2.8±2.9	1.8±1.6	3.4±3.1	0.19
Left upper lung score	0.5±1.4	0.1±0.3	0.8±1.8	0.13
Left lower lung score	3.3±3.3	2.2±3.0	4.0±3.3	0.03
Complications				
Respiratory failure		NA	3 (9.4%)	-
Hospital-associated infection		NA	6 (18.8%)	-
Septic shock		NA	1 (3.1%)	-
Upgrade of antibiotics		NA	19 (59.4%)	-

Discussion

CAP is 1 of the leading causes of death worldwide, but early predictors of treatment outcome are relatively underexplored. In this study, we prospectively enrolled participants with CAP and used 2 portable devices to monitor oxygenation and physical activity. We found that a high mean SpO_2 and a variation of SpO_2 on Day2were associated with unfavorable treatment on Day 5 in patients with CAP. Our findings provide evidence of the practical application of the wearable device to monitor SpO_2 in patients with CAP.

There is an increasing need for a wearable device in medical care after the COVID-19 pandemic, particularly for the continuous monitoring of SpO_2 to detect silent hypoxia [16, 17]. Silent hypoxia is currently recognized as a critical event in patients with COVID-19 infection, but measurement of SpO_2 is somehow affected by different clinical conditions. The fluctuation in SpO_2 measurement is high [18]. Therefore, continuous monitoring of SpO_2 is required to accurately detect, in a timely manner, silent hypoxia in patients with COVID-19 infection [19]. In addition to timely detection, lessening contact between patients and medical care staff with the remote patient monitoring sensor is another substantial unmet need for the wearable

Table 3. Data Mmeasured by the Wearable Device Within 2 Days Among Enrolled Subjects Categorizedby Treatment Outcome on Day5

	(Total (n=62)	Favorable outcome (n=30)	Unfavorable outcome (n=32)	*P* value
Day 1 Daytime				
SpO_2 (n=62)				
Mean (%)	96.3±1.8	96.9±1.3	95.8±2.0	0.01
CoV (%)	1.83±1.17	1.56±0.65	2.10±1.47	0.07
Accelerometry (n=49)				
Mean	20.9±13.2	26.0±14.7	16.7±10.2	<0.01
Day 1 Nighttime				
SpO_2 (n=53)				
Mean (%)	96.1±1.9	96.0±1.4	96.2±2.2	0.49
CoV (%)	1.23±0.89	1.10±0.48	1.34±1.15	0.29
Accelerometry (n=49)				
Mean	16.0±10.9	20.3±10.9	12.5±9.8	<0.01
Day 2 Daytime				
SpO_2 (n=61)				
Mean (%)	96.3±1.8	96.7±1.6	96.0±1.8	0.09
CoV (%)	1.96±1.05	1.66±0.83	2.25±1.15	0.03
Accelerometry (n=55)				
Mean	21.0±12.8	23.8±12.3	18.4±12.9	0.02
Day 2 Nighttime				
SpO_2 (n=55)				
Mean (%)	95.8±2.4	95.6±2.7	96.0±2.0	0.85
CoV (%)	1.95±0.73	1.93±0.87	1.97±0.59	0.85
Accelerometry (n=56)				
Mean	15.1±9.2	18.3±9.5	11.9±7.8	<0.01

Abbreviations: SpO_2, oxygen saturation; CoV, Coefficient of Variation.

Table 4. Crude and Adjusted Odds Ratios for the Association Between Variables and Unfavorable Treatment Outcome in Patients with CAP

	Crude OR (95% CI)	*P* value	Adjusted OR (95% CI)	*P* value
Age, per year increment	0.99(0.97-1.02)	0.630	0.98(0.94-1.02)	0.331
Sex (male)	1.08(0.35-3.29)	0.898	1.00(0.29-3.48)	0.995
PSI, per 1 score increment	1.00(0.99-1.02)	0.928	1.01(0.98-1.03)	0.645
Day2 daytime				
Mean of accelerometry	0.97(0.92-1.01)	0.127	0.95(0.90-1.01)	0.102
Mean of SpO_2	0.93(0.66-1.32)	0.695	0.91(0.62-1.33)	0.624
CoV of SpO_2	1.92(1.05-3.52)	0.035	1.87(1.02-3.42)	0.044

Abbreviations: CAP, community-acquired pneumonia; PSI, pneumonia severity index; SpO2, oxygen saturation; CoV, Coefficient of Variation; OR, odds ratio; CI, confidence interval.

device in treating patients with COVID-19 [5]. In this study, we used the wearable device and found that 2 parameters associated with SpO_2, including mean SpO_2 and the variation of SpO_2, on Day 2, can predict the response to treatment on Day 5 among CAP patients. This evidence highlights the practical application of the wearable device to monitor SpO_2 in patients with respiratory diseases, including CAP.

Notably, the wearable device may produce stream data. Retrieving key information from this data can be challenging, but is essential for the practical use of wearable devices in the medical facility. We used2 wearable devices and found that continuous monitoring of SpO_2, rather than physical activity, is crucial in patients with CAP. These data indicate the need to focus on continuously monitoringSpO_2in patients with respiratory tract diseases. In line with our data, a number of studies have shown an additional role for variability of SpO_2,in addition to the absolute/mean SpO_2 [20-23]. Al Rajeh, et al. recently conducted a proof-of-concept study with 11 patients with chronic obstructive lung disease (COPD) and reported that variability was an independent predictor of the exacerbation of COPD [21]. Similarly, Jiang, *et al*. enrolled 12 healthy men and used a network physiological approach to explore physiological alteration during normobaric hypoxia in healthy individuals [20]. They found that not only the average SpO_2 but also the fluctuation in SpO_2 was involved with respiratory control [20]. This evidence points to the previously ignored role of SpO_2 variation in patients with respiratory diseases, including CAP, as shown in this study.

The proportion of patients with CAP with unfavorable treatment outcomes appears to be high in the present study. Given that this study was carried out in a referral center, the enrolled patients seemed to be a population with multiple comorbidities, and had a high degree of severity of the disease. Furthermore, we defined an unfavorable response to treatment not only by the clinical parameters proposed by ATS [3], but also by the classification of the CXR and any incident adverse events encountered in the clinical trial [13]. Therefore, the proportion of unfavorable treatments tends to be high in the present study, and the use of strict criteria for unfavorable treatment outcomes can tend toward an overestimation, rather than an underestimation, of unfavorable treatment outcomes in patients with CAP.

The accelerometer has been used to measure the intensity of physical activity in different body positions, mainly when placed on the hip, thigh, and wrists [24-26]. However, the practical application of using an accelerometer depends on the sensor position, the intended user, and the proposed situation. For example, the wrist accelerometer was reported to measure physical activity in young and mobile patients with inflammatory bowel disease [27]. A hip-mounted accelerometer, however, was reported to be used to measure physical activity in patients with a risk of stroke [28].In the present study, the real-world application of wrist accelerometers tended to be suboptimal, with a relatively high proportion of patients refusing to wear wrist accelerometers continuously. We postulated that the patients enrolled in this study had an intravenous infusion apparatus on the hand/wrist, and this may have affected the use of wrist-wearable devices. In addition, patients with CAP tend to be on bed rest for a few days during admission for pneumonia, and some patients may require protective physical restraint with the wrist strap. Taken together, these clinical factors could limit the practical

use of wrist accelerometers in patients with CAP. In contrast, finger oximetry monitoring is a fundamental management in patients with pneumonia. Therefore, we focused on the analysis of finger pulse oximeter-derived parameters in the present study.

Of interest, the group with favorable outcomes showed slightly higher daytime SpO_2 levels, but lower nocturnal SpO_2 levels on both Day 1 and Day 2, compared to the group with unfavorable outcomes, although the differences did not reach statistical significance. We speculated that the nocturnal desaturation among patients with a favorable outcome could be attributed to sleep apnea, given that the enrolled population tended to be elderly patients [29, 30]. Studies have shown that obstructive sleep apnea was a risk factor for pneumonia [31, 32]. Therefore, nocturnal desaturation and increased activity among patients with a favorable outcome might potentially result from sleep apnea and wakefulness after sleep onset [33, 34].

There are limitations in this study. First, the study was prospective without blinding; therefore, more randomized and blinded studies may be warranted to validate our findings. Second, the wearable device in the present study was wireless but not contactless. However, the device can be easily sterilized; therefore, the infection control issue should be mitigated. Third, the measurement of physical activity with a biosensor or on the wrist may not reflect overall physical activity. More studies are needed to clarify the role of measuring physical activity by accelerometers in patients with CAP.

Conclusion

In conclusion, wearable devices are increasingly being applied in medical care, and the present prospective study demonstrates that the mean and variance of SpO_2 as measured by the wearable device were correlated with treatment on day 5 in patients with CAP. Our data highlight the crucial need for continuous monitoring of SpO2 in patients with lung diseases, including CAP. More randomized studies are warranted to validate our findings. In addition, more biomedical engineering efforts are needed to miniaturize the device and to design contactless monitors.

Declarations

Acknowledgments

We thank our colleague Dr. Po-Yu Liu, who completed a survey to help gather data.

Funding

This study was supported by the Special Research Project of the Ministry of Science and Technology (109WHA0510023). The funders had no role in the study design, data collection, analysis, decision to publish, or manuscript preparation.

Ethics approval and consent to participate

This study was approved by the Taichung Veterans General Hospital Ethics Review Committee (TCVGH: CE20182B). The study was conducted in accordance with the Declaration of Helsinki, and written informed consent was obtained from individual or guardians of the participants.

Authors' contributions

Study conception and design: Wen-Cheng Chao and Chieh-Liang Wu. Acquisition of data: Yu-Cheng Wu, Chien-Chung Huang, Wen-Cheng Chao and Chieh-Liang Wu. Analysis

and interpretation of data: Chien-Chung Huang. Drafting of manuscript: Yu-Cheng Wu, Wen-Cheng Chao and Chieh-Liang Wu. All authors read and approved the final manuscript.

Declaration of Competing Interest

The authors declare no competing interest.

References

1. Jain S, Self WH, Wunderink RG, et al.Community-acquired pneumonia requiring hospitalization among U.S. adults. N Engl J Med 2015;373(5):415-427.
2. Broulette J, Yu H, Pyenson B, et al.The incidence rate and economic burden of community-acquired pneumonia in a working-age population. Am Health Drug Benefits 2013;6(8): 494-503.
3. Metlay JP, Waterer GW, Long AC, et al.Diagnosis and treatment of adults with community-acquired pneumonia. An official clinical practice guideline of the American Thoracic Society and Infectious Diseases Society of America. Am J Respir Crit Care Med 2019;200(7): e45-e67.
4. Administration, FDA.Guidance for industry community-acquiredbacterial pneumonia: developing drugs for treatment. 2014. Available at: https://www.fda.gov/media/75149/download.
5. Kumar S, Dashtipour SK, Abbasi QH, *et al*. A review on wearable and contactless sensing for COVID-19 withpolicy challenges. Front Comms Net 2021;2.
6. Mitratza M, Goodale BM, Shagadatova A, *et al*.The performance of wearable sensors in the detection of SARS-CoV-2 infection: a systematic review. Lancet Digit Health 2022;4(5): e370-e383.
7. Kristinsson AO, Gu Y, Rasmussen SM, *et al*.Prediction of serious outcomes based on continuous vital sign monitoring of high-risk patients. Comput Biol Med, 2022;147: 105559.
8. Silva AF, Tavakoli M.Domiciliary hospitalization through wearable biomonitoring patches: recent advances, technical challenges, and the relation to Covid-19. Sensors 2020;20(23): 6835.
9. Min J, Sempionatto JR, Teymourian H, *et al*.Wearable electrochemical biosensors in North America.Biosens Bioelectron 2021;172: 112750.
10. Ngiam J, Chew N, Sia C, *et al*.Silent hypoxia: pulse oximetry and its relation to COVID-19 in Singapore. Singapore Med J 2021.
11. Fine MJ, Auble TE, Yealy DM, *et al*.A prediction rule to identify low-risk patients with community-acquired pneumonia. N Engl J Med 1997;336(4): 243-50.
12. Lim WS, van der Eerden MM, Laing R, *et al*. Defining community acquired pneumonia severity on presentation to hospital: an international derivation and validation study. Thorax 2003;58(5): 377-82.
13. Community-Acquired Bacterial Pneumonia: Developing Drugs for Treatment Guidance for Industry. FDA, US Department of Health and Human Services, Center for Drug Evaluation and Research, Editor. 2020.
14. Warren MA, Zhao Z, Koyama T, *et al*. Severity scoring of lung oedema on the chest radiograph is associated with clinical outcomes in ARDS. Thorax 2018;73(9): 840-846.
15. Torres-Vargas C, Legorreta-Soberanis J, Sanchez-GervacioBM, *et al*.Utility of a pulmonary oedema score for predicting the need for mechanical ventilation in COVID-19 patients in a general hospital. Arch Med Res 2022;53(4): 399-406.
16. Ding X, Clifton D, Ji N, *et al*.Wearable sensing and telehealth technology with potential applications in the Coronavirus pandemic. IEEE Rev Biomed Eng 2021;14: 48-70.
17. Tobin MJ, Laghi F, Jubra A.Why COVID-19 silent hypoxemia Is baffling to physicians.Am J Respir Crit Care Med 2020;202(3):356-360.
18. Luks AM, Swenson ER.Pulse oximetry for monitoring patients with COVID-19 at home. Potential pitfalls and practical guidance. Ann Am Thorac Soc 2020;17(9): 1040-1046.
19. Jeong H, Rogers JA, Xu S.Continuous on-body sensing for the COVID-19 pandemic: gaps and opportunities. Sci Adv 2020;6(36).
20. Jiang Y, Costello JT, Williams TB, *et al*. A network physiology approach to oxygen saturation variability during normobaric hypoxia. Exp Physiol 2021;106(1): 151-159.
21. Al Rajeh A, Bhogal AS, Zhang Y, *et al*. Application of oxygen saturation variability analysis for the detection of exacerbation in individuals with COPD: a proof-of-

concept study.Physiol Rep 2021;9(23): e15132.
22. Costello JT, Bhogal AS, Williams TB, *et al*. Effects of normobaric hypoxia on oxygen saturation variability. High Alt Med Biol 2020;21(1): 76-83.
23. Bhogal AS, Mani AR.Pattern analysis of oxygen saturation variability in healthy individuals: entropy of pulse oximetry signals carries information about mean oxygen saturation. Front Physiol 2017;8: 555.
24. de Leeuwerk ME, Bor P, van der Ploeg HP, *et al*.The effectiveness of physical activity interventions using activity trackers during or after inpatient care: a systematic review and meta-analysis of randomized controlled trials. Int J Behav Nutr Phys Act 2022;19(1): 59.
25. Montoye AHK, Pivarnik JM, Mudd LM, *et al*. Validation and comparison of accelerometers worn on the hip, thigh, and wrists for measuring physical activity and sedentary behavior. AIMS Public Health 2016; 3(2): 298-312.
26. Liu F, Wanigatunga AA, Schrack JA.Assessment of physical activity in adults using wrist accelerometers. Epidemiol Rev 2022;43(1): 65-93.
27. Lund K, Larsen MD, Knudsen T, *et al*. Physical activity measured by accelerometry in paediatric and young adult patients with inflammatory bowel disease. BMC Gastroenterol 2022;22(1): 290.
28. Hooker SP, Diaz KM, Blair SN, *et al*. Association of accelerometer-measured sedentary time and physical activity with risk of stroke among US adults. JAMA Netw Open 2022;5(6): e2215385.
29. Karhu T, Leppänen T, KorkalainenH, *et al*. Desaturation event scoring criteria affect the perceived severity of nocturnal hypoxic load. Sleep Med 2022;100: 479-486.
30. Karhu T, Myllymaa S, Nikkonen S, *et al*. Longer and deeper desaturations are associated with the worsening of mild sleep apnea: the Sleep Heart Health Study. Front Neurosci 2021;15: 657126.
31. Keto J, Feuth T, Linna M, *et al*. Lower respiratory tract infections among newly diagnosed sleep apnea patients. BMC Pulm Med 2023;23(1): 332.
32. Chiner E, Llombart M, Valls J, *et al*. Association between obstructive sleep apnea and community-acquired pneumonia. PLoS One 2016;11(4): e0152749.
33. Valko PO, Hunziker S, Graf K, *et al*.Sleep-wake misperception. A comprehensive analysis of a large sleep lab cohort.Sleep Med 2021;88: 96-103.
34. Bianchi MT, Williams KL, McKinney S, *et al*.The subjective-objective mismatch in sleep perception among those with insomnia and sleep apnea. J Sleep Res 2013;22(5): 557-68.

Patient with Classical Hodgkin's Lymphoma Presenting with Pulmonary Manifestations Mimicking Primary Pulmonary Hodgkin's Lymphoma

Yu-Cheng Lin[1,2], Chuan-Sheng Horng[1], Yao-Tung Wang[1,2], Ren-Tsung Ko[3], Shih-Ming Tsao[1,2]

Superior vena cava (SVC) syndrome is a common complication of lung cancer, including both non-small cell and small cell lung cancers. The formation of collateral circulation can reduce clinical symptoms, such as shortness of breath, a puffy face, and neck and arm swelling. Here, we report a case of SVC syndrome in a 70-year-old woman, a never-smoker, who presented with right neck and right arm numbness for 1 month. Right upper lobe lung cancer with partial compression of the SVC was diagnosed. Chest computed tomography revealed a rare collateral circulation pathway, i.e., the phrenic venous pathway. Collateral circulation was observed during the follow-up period. ***(Thorac Med 2024; 39: 31-35)***

Key words: Primary pulmonary Hodgkin's lymphoma, PPHL, clubbing of the fingers, diffuse nodular lesions.

Introduction

Primary pulmonary Hodgkin's lymphoma (PPHL) is uncommon, accounting for < 1% of all lymphomas. We reported a case that had pulmonary manifestations similar to PPHL, with an initial presentation of clubbing of the fingers and multiple lung nodules. This female patient underwent pulmonary biopsy using video-assisted thoracoscopic surgery. Histologic examination and immunohistochemical analysis assisted in reaching the diagnosis of classical Hodgkin's lymphoma. The diagnosis was challenging due to its rarity, as well as the nature of the disease.

Case Presentation

A 20-year-old female patient, a non-smoker with no past medical history, presented with a persistent productive cough lasting 3 months. There was no fever, poor appetite, fatigue, body weight loss or other systemic disease. On physical examination, she was found to have bilateral

[1]Department of Internal Medicine, Chung Shan Medical University Hospital, Taichung, Taiwan, [2]Division of Pulmonary Medicine, Chung Shan Medical University Hospital, Taichung, Taiwan, [3]Department of Pathology, Chung Shan Medical University Hospital, Taichung City, Taiwan
Address reprint requests to: Dr. Shih-Ming Tsao, Department of Internal Medicine, Chung Shan Medical University Hospital, Taichung, Taiwan (No. 110, Sec. 1, Jianguo N. Rd., South Dist., Taichung City 402, Taiwan (R.O.C.).

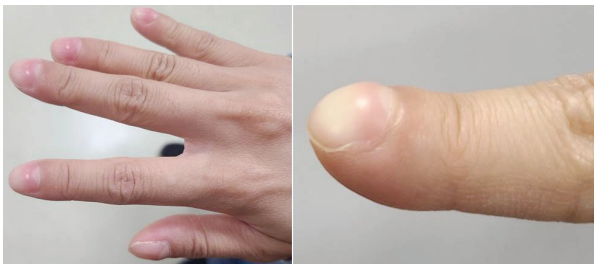

Fig. 1. Clubbing of the fingers.

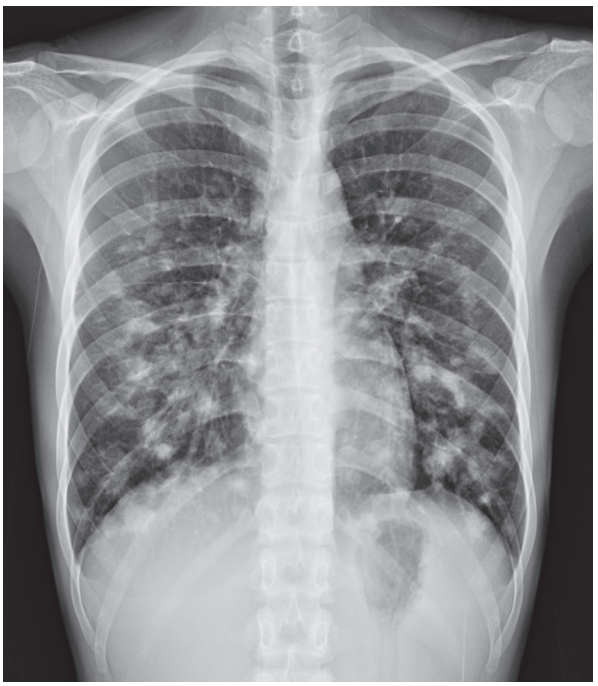

Fig. 1. Chest X-ray showing multiple diffuse nodules at the bilateral lungs, mainly at the middle and lower lung fields.

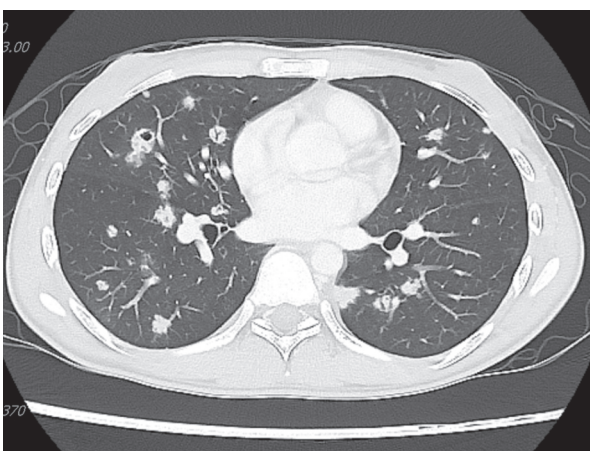

Fig. 3. Chest CT showing multiple bilateral nodules with cavitation.

clubbing of the fingers (Figure 1), without any palpable lymphadenopathy or hepatosplenomegaly. Her laboratory tests showed a white blood cell (WBC) count of 21,400/μL, a hemoglobin (Hb) level of 10.3 g/dl, and a C-reactive protein (CRP) level of 2.64 mg/dL. Chest X-ray revealed multiple diffuse infiltrative opacities in both lungs, primarily in the middle and lower lung fields (Figure 2). Chest computed tomography (CT) showed multiple small irregular nodules with cavitation throughout the bilateral lungs, without any obvious enlargement of the mediastinal or hilar lymph nodes (Figure 3).

The patient was initially treated with antibiotics and then antifungal medication, but minimal improvement was observed. Bronchoscopic investigations did not yield a diagnosis. The acid-fast bacilli stain and mycobacterial culture were both negative. A CT-guided biopsy was insignificant. Later on, she underwent pulmonary biopsy using video-assisted thoracoscopic surgery. Histologic examination and immunohistochemical analysis assisted in reaching the diagnosis of classical HL, mixed cellularity type, with mummified cells, and scattered large Reed-Sternberg (R-S) cells with prominent nucleoli in a mixed inflammatory background of small lymphocytes, histiocytes, eosinophils and neutrophils. Results of an immunohistochemistry stain showed PAX-5 (weak), CD15 (focal), and CD30(+), CD3(-), CD20(-), CK(-), CD1a(-), and CD68(-) in R-S cells (Figure 4). The Epstein-Barr encoding region (EBER) in situ hybridization was negative in tumor cells. The PAS, GMS and acid-fast stains revealed no microorganisms.

To further stage HL, the patient received a positron emission tomography (PET) scan examination, which revealed multiple focal areas of increased FDG uptake at the bilateral lung

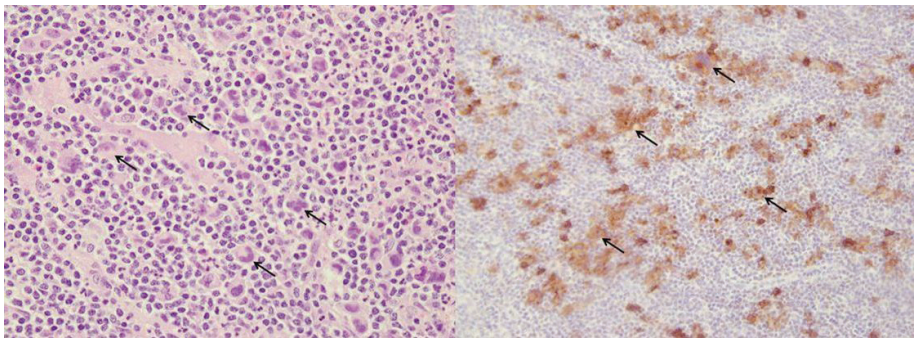

Fig. 4. Lymphocyte-rich classical Hodgkin's lymphoma. The neoplastic lymphocytes strongly expressed CD30.

Fig. 5. PET scan showing increased glucose metabolic lesions at the bilateral lungs, supraclavicular lymph nodes, and left iliac bone.

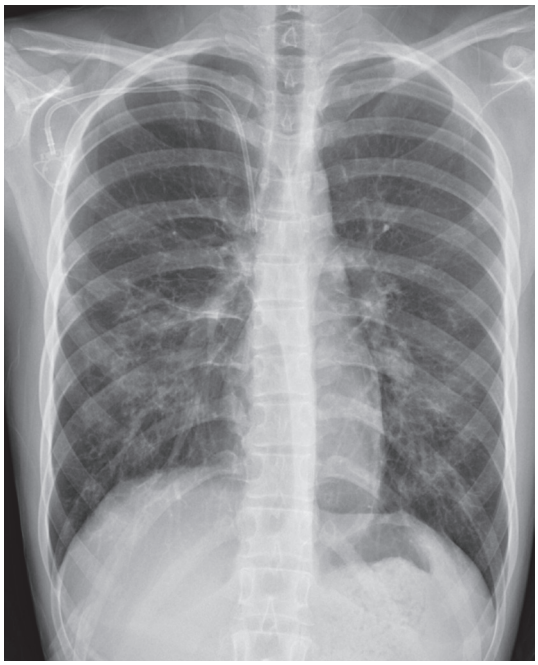

Fig. 6. Chest X-ray obtained after treatment.

regions, bilateral supraclavicular lymph nodes, and left iliac bone with bone destruction, compatible with HL involvement. The result was suggestive of stage IV disease (based on AJCC, 8th ed.) (Figure 5).

With classical HL diagnosed, the patient completed 4 cycles of chemotherapy with doxorubicin, bleomycin, vinblastine, and dacarbazine (ABVD), with significant improvement seen on her chest X-ray after treatment (Figure 6).

Discussion

Primary pulmonary Hodgkin's lymphoma is uncommon, consisting of < 1% of all lymphomas [7]. In order for PPHL to be diagnosed, the

following criteria must be fulfilled: (1) characteristic histological features of HL, (2) disease restriction to the lungs with or without minimal lymph node involvement, and (3) absence of extrapulmonary disease [4-7]. Even though our patient's HL did not completely meet the criteria of absence of extrapulmonary lesions, her condition is still valuable to report due to the unusual clinical characteristics.

In a literature review thus far, PPHL was found to be more common in females [7-8]. Clinical manifestations, such as cough, weight loss, chest pain, and dyspnea, were often nonspecific, and the patient could even be asymptomatic [6-7]. Our patient developed clubbing of the fingers. Due to minimal symptoms, she did not seek medical attention and was untreated for some time. The diagnostic process was challenging, as her chest CT showed multiple pulmonary nodules with cavities, which are less commonly associated with lymphoma. Thanks to aggressive diagnostic procedures and the use of video-assisted thoracoscopic lung biopsy, the diagnosis of Hodgkin's lymphoma with clinical manifestations essentially those of PPHL was achieved. The patient had significant improvement with a complete remission after the fourth cycle of chemotherapy.

Digital clubbing was first documented by Hippocrates nearly 2500 years ago, in a patient with empyema [9]. It is regarded as 1 of the oldest clinical signs that is still relevant in modern day medicine. Clubbing of the fingers may be associated with various clinical conditions; however, chronic lung diseases are most commonly the cause of clubbing [10-12]. The exact pathophysiology of clubbing of the fingers is still unclear, but 1 of the most notable theories is the local release of 'signal proteins' (VEGF and PDGF). Their actions, and those of prostaglandin E2, changes to fibroblasts, osteoclasts (acro-osteolytic) and osteoblasts (periostosis), and extracellular matrix deposition and angiogenesis, promote the features of clubbing and hypertrophic osteoarthropathy [13-14].

Radiologically, PPHL may appear as a single nodule, as multiple nodules, or as cavitated lesions. The most common finding in patients with pulmonary manifestations of HL were irregularly marginated soft tissue dense pulmonary nodules or masses. Cavitation was seen in less than 1% of nodules [15]. However, no radiological appearance is pathognomonic for PPHL. Sometimes, PPHL mimicks tuberculosis and other diseases, which makes diagnosis even more challenging [16].

In conclusion, our patient was diagnosed with classical HL, with pulmonary manifestations mimicking PPHL. After completing 4 cycles of treatment, the patient showed significant improvement on her chest X-ray.

References

1. Singh D, Vaccarella S, Gini A, *et al*. Global patterns of Hodgkin lymphoma incidence and mortality in 2020 and a prediction of the future burden in 2040. Int J Cancer 2022 Jun 15; 150(12): 1941-1947. doi: 10.1002/ijc.33948. Epub 2022 Feb 7. PMID: 35080783.
2. Siegel RL, Miller KD, Fuchs HE, *et al*. Cancer statistics, 2022. CA Cancer J Clin 2022 Jan; 72(1): 7-33. doi: 10.3322/caac.21708. Epub 2022 Jan 12. PMID: 35020204.
3. Berkman N, Breuer R, Kramer MR, *et al*. Pulmonary involvement in lymphoma. Leuk Lymphoma 1996 Jan; 20(3-4): 229-37. doi: 10.3109/10428199609051612. PMID: 8624461.
4. Lluch-Garcia R, Briones-Gomez A, Castellano EM, *et al*. Primary pulmonary Hodgkin's lymphoma. Can Respir J 2010 Nov-Dec; 17(6): e106-8. doi: 10.1155/2010/252746. PMID: 21165354; PMCID: PMC3006155.
5. McElnay PJ, Pawade J, Chandratreya L, *et al*. Giant

thoracic mass: an unusual presentation of primary pulmonary Hodgkin's lymphoma. BMJ Case Rep 2013 Sep 18; 2013: bcr2013200909. doi: 10.1136/bcr-2013-200909. PMID: 24049094; PMCID: PMC3794259.

6. Cooksley N, Judge DJ, Brown J. Primary pulmonary Hodgkin's lymphoma and a review of the literature since 2006. BMJ Case Rep 2014 Apr 7; 2014: bcr2014204020. doi: 10.1136/bcr-2014-204020. PMID: 24711477; PMCID: PMC3987623.
7. Radin AI. Primary pulmonary Hodgkin's disease. Cancer 1990 Feb 1; 65(3): 550-63. doi: 10.1002/1097-0142(19900201)65:3<550::aid-cncr2820650328>3.0.co;2-w. PMID: 2404558.
8. Yousem SA, Weiss LM, Colby TV. Primary pulmonary Hodgkin's disease. A clinicopathologic study of 15 cases. Cancer 1986 Mar 15; 57(6): 1217-24. doi: 10.1002/1097-0142(19860315)57:6<1217::aid-cncr2820570626>3.0.co;2-n. PMID: 3943043.
9. Adams F, translator. The genuine works of Hippocrates. New York: William Wood; 1981.
10. Lawry M, Daniel CR III. Nails in systemic disease. In: Scher RK, Daniel CR III, eds. Nails: Diagnosis, Therapy, and Surgery. Oxford: Elsevier Saunders, 2005:147.
11. Lovibond JL. Diagnosis of clubbed fingers. Lancet 1938; 231(5972): 363-364, ISSN 0140-6736,
12. Sarkar M, Mahesh DM, Madabhavi I. Digital clubbing. Lung India 2012 Oct; 29(4): 354-62. doi: 10.4103/0970-2113.102824. PMID: 23243350; PMCID: PMC3519022.
13. Rutherford JD. Digital clubbing. Circulation 2013 May 14; 127(19): 1997-9. doi: 10.1161/CIRCULATIONAHA.112.000163. PMID: 23671180.
14. Dubrey S, Pal S, Singh S, *et al*. Digital clubbing: forms, associations and pathophysiology. Br J Hosp Med (Lond) 2016 Jul; 77(7): 403-8. doi: 10.12968/hmed.2016.77.7.403. PMID: 27388379.
15. Diederich S, Link TM, Zühlsdorf H, *et al*. Pulmonary manifestations of Hodgkin's disease: radiographic and CT findings. Eur Radiol 2001; 11(11): 2295-305. doi: 10.1007/s003300100866. PMID: 11702175.
16. Chiu WC, Chen SH, Chen BJ, *et al*. Primary pulmonary Hodgkin's lymphoma: a rare etiology mimicking pulmonary tuberculosis. Pediatr Neonatol 2021 Sep; 62(5): 569-570. doi: 10.1016/j.pedneo.2021.03.017. Epub 2021 Apr 9. PMID: 33895095.

Multifocal Mass-like Pulmonary Consolidation in a Patient with Community-Acquired Pneumonia Caused by *Pseudomonas Aeruginosa*

Chang-Ching Lee[1], Sheng-Wei Pan[1,2]

Pseudomonas aeruginosa (*P. aeruginosa*) is a less common pathogen causing community-acquired pneumonia. However, patients with chronic airway disease are vulnerable to *P. aeruginosa* infection. *P. aeruginosa* infection is associated with a poor quality of life, frequent exacerbation, and a high mortality rate in patients with bronchiectasis. Ground-glass attenuation, peribronchial infiltration and consolidation, but not mass-like lesions, are the common radiographic features of *P. aeruginosa* pneumonia. Here, we reported a rare case of *P. aeruginosa* pneumonia with multifocal conglomerate mass-like consolidation. Ultrasound-guided transthoracic aspiration was performed to rule out malignancy, and pus was aspirated, which showed numerous inflammatory cells and yielded *P. aeruginosa*. The early diagnosis of *P. aeruginosa* pneumonia in this case helped in the initiation of appropriate antibiotic treatment and eliminated the need of an investigation for mass-like lesions. The mass-like lesions resolved after antibiotic use. In this case report, we reviewed the clinical presentations and radiographic patterns of *P. aeruginosa* pneumonia and the diagnostic value of sono-guided needle aspiration. ***(Thorac Med 2024; 39: 36-42)***

Key words: multifocal consolidation, bronchiectasis, community-acquired pneumonia, *Pseudomonas aeruginosa*, sono-guided needle aspiration.

Introduction

Pseudomonas aeruginosa (*P. aeruginosa*) infection is a less common causative microorganism in patients with community-acquired pneumonia (CAP); about 0.9%-1.9% of cases of CAP are caused by *P. aeruginosa* [1]. However, this infection can result in severe disease and is associated with a high risk of ICU admission [1-2]. Of note, in patients with cystic fibrosis (CF), non-CF bronchiectasis or other chronic lung disease, *P. aeruginosa* was a relatively prevalent pathogen [1, 3]. In a study on patients with bronchiectasis included from 10 different bronchiectasis clinical centers (n=2596), the prevalence of *P. aeruginosa* chronic infection

[1]Department of Chest Medicine, Taipei Veterans General Hospital, Taipei, Taiwan, [2]School of Medicine, National Yang Ming Chiao Tung University, Taipei, Taiwan
Address reprint requests to: Dr. Sheng-Wei Pan, Department of Chest Medicine, Taipei Veterans General Hospital 201, Section 2, Shih-Pai Road, Taipei, 112, Taiwan.

was 15% over a 5-year follow-up period [4]. In addition, the presence of *P. aeruginosa* in the airways has been associated with an accelerated decline in lung function, worsened quality of life, higher exacerbation frequency and higher mortality than other pathogen-related infections in patients with non-CF bronchiectasis [4-5]. Thus, early identification and treatment of *P. aeruginosa* pneumonia is of paramount importance in patients with bronchiectasis.

Diagnosis of *P. aeruginosa* pneumonia remains a challenge because of the non-specific image pattern and low sputum isolation rate [1, 6-7]. In Taiwan, the main causative pathogens of CAP are Streptococcus pneumoniae (23.26%), Mycoplasma pneumoniae (14.20%), Chlamydia pneumoniae (8.13%), Haemophilus influenzae, (5.9%), and Klebsiella pneumoniae (5.7%) [8]. Since the prevalence of *P. aeruginosa*-related CAP is around 0.9%-1.9% [1, 7, 9], the risk is usually neglected. The current practice guidelines for CAP suggest empirical antibiotic treatment for *P. aeruginosa* in those with prior respiratory isolation of *P. aeruginosa* or recent hospitalization (within 90 days) and previous receipt of parenteral antibiotics [7]. Empirical antibiotics covering *P. aeruginosa* for CAP is also suggested in patients with chronic lung disease, poor lung function (forced expiratory volume in 1 second (FEV_1) <30% predicted), and oral steroid use [8]. Thus, to avoid a delayed diagnosis and inappropriate management, it is worthwhile to expand our understanding of the clinical presentations of patients with *P. aeruginosa* pneumonia, especially in those with chronic lung disease.

Here, we report a patient with bronchiectasis who suffered from productive cough for 1 week and presented with multifocal mass-like consolidation in a chest radiograph (CXR) and chest computed tomography (CT). A diagnosis of CAP caused by *P. aeruginosa* was made quickly after sono-guided lung aspiration, and the patient was discharged uneventfully after antibiotic treatment and resolution of the lung lesions. In this report, we review the radiographic patterns of *P. aeruginosa* pneumonia and the diagnostic approach to patients with multifocal pulmonary consolidation.

Case Description

This 82-year-old woman, a non-smoker, had a history of bronchiectasis diagnosed for at least 13 years without exacerbation or regular medical treatment. She recently suffered from exacerbated productive cough with yellowish sputum for 1 week, with chest wall pain, chest tightness, night sweating, and poor appetite. Body weight loss, from 52 kg to 26 kg, also occurred in the most recent year. She visited the chest clinic and presented with tachycardia (heart rate: 113/min) and mild tachypnea (respiratory rate: 24/min), but no fever or hypotension. Chest auscultation revealed diffuse crackles and rhonchi. A CXR showed multiple mass-like consolidation in the peripheral lung fields at the right upper lobe, and left upper and left lower lobes (Figure 1). Due to mild respiratory distress and suspected atypical pneumonia during this COVID-19 pandemic era, she was referred to the emergency department for further investigation.

The laboratory investigation showed leukocytosis (23600/μL, segments 95.1%), elevated C-reactive protein (28.71 mg/dL), hyponatremia (122 mmol/L), and prolonged prothrombin time (International Normalized Ratio (INR) = 1.4). An atypical respiratory panel, including coronavirus tests, using the nasopharyngeal swab,

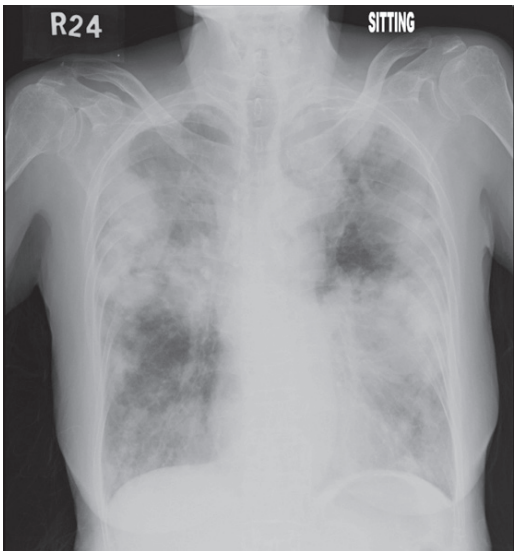

Fig. 1. CXR on the day of admission (day 0) showed multiple consolidative patches at the right upper lobe, and left upper and left lower lobes.

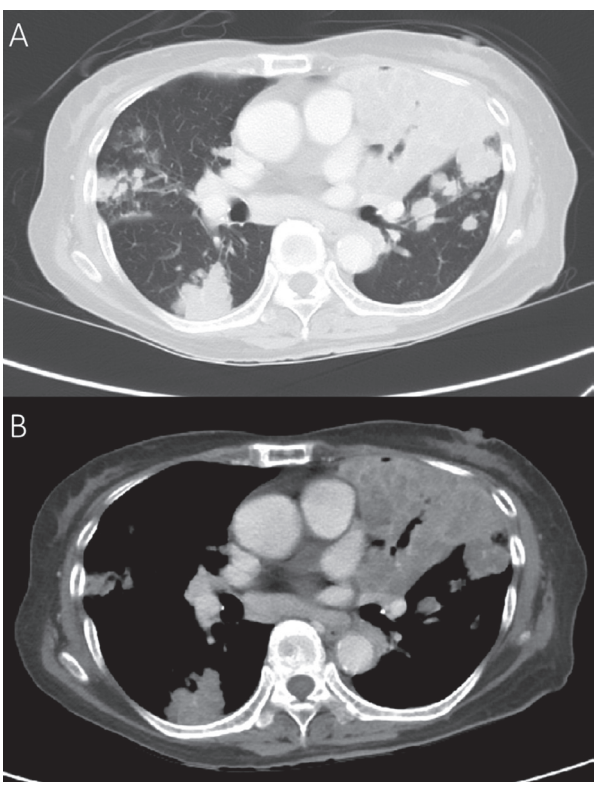

Fig. 2. Thoracic CT on the day of admission (day 0). (A) Lung window of thoracic CT showed multifocal, conglomerated soft tissue at the bilateral lungs, with upper lobes and left upper lobe lingual segment predominance, and a peripheral, wedge-shaped, acinar distribution. (B) Mediastinal window of thoracic CT showed multiple mass-like lesions at the bilateral lung fields. Some low-attenuating components and air bronchogram were also noted.

showed negative findings. Chest CT revealed a multifocal, conglomerated mass of soft tissue density at the bilateral lungs with low-attenuating components and air bronchogram, which generally imply a differentiated diagnosis of multifocal lung cancer and atypical pulmonary infection (Figure 2a-2b). The CURB-65 score (confusion status, blood urea nitrogen >19 mg/dL, respiratory rate more than or equal to 30, low blood pressure, age > 65) for CAP severity was 2 points. She was admitted under the tentative diagnosis of bilateral lung mass and pneumonia.

She received piperacillin and tazobactam combination treatment first, but the initial sputum culture revealed normal flora 3 days after admission. Thus, ultrasound-guided transthoracic needle aspiration was performed to assess the nature of the mass-like consolidation. Consolidative lung lesions with air bronchogram were noted in the chest sonography (Figure 3), and pus and some necrotic tissues were aspirated. Further biopsy was not performed because an infection process was favored. Cytology of aspirated fluid showed numerous inflammatory cells. Culture of the lung mass aspirate yielded *P. aeruginosa* on day 7. Antibiotic use was deescalated to ceftazidime based on the antibiotic sensitivity report. The clinical condition of the patient improved, and CXR on day 21 also showed improvement (Figure 4). The patient was discharged uneventfully after 3 weeks of treatment, and oral-form levofloxacin was prescribed. A follow-up CXR on day 44 showed significant regression of the mass-like consolidation and chronic change in the cystic bronchiectasis at the right upper lobe and left lingula (Figure 5). The antibiotic was discontinued after a 5-week treatment course.

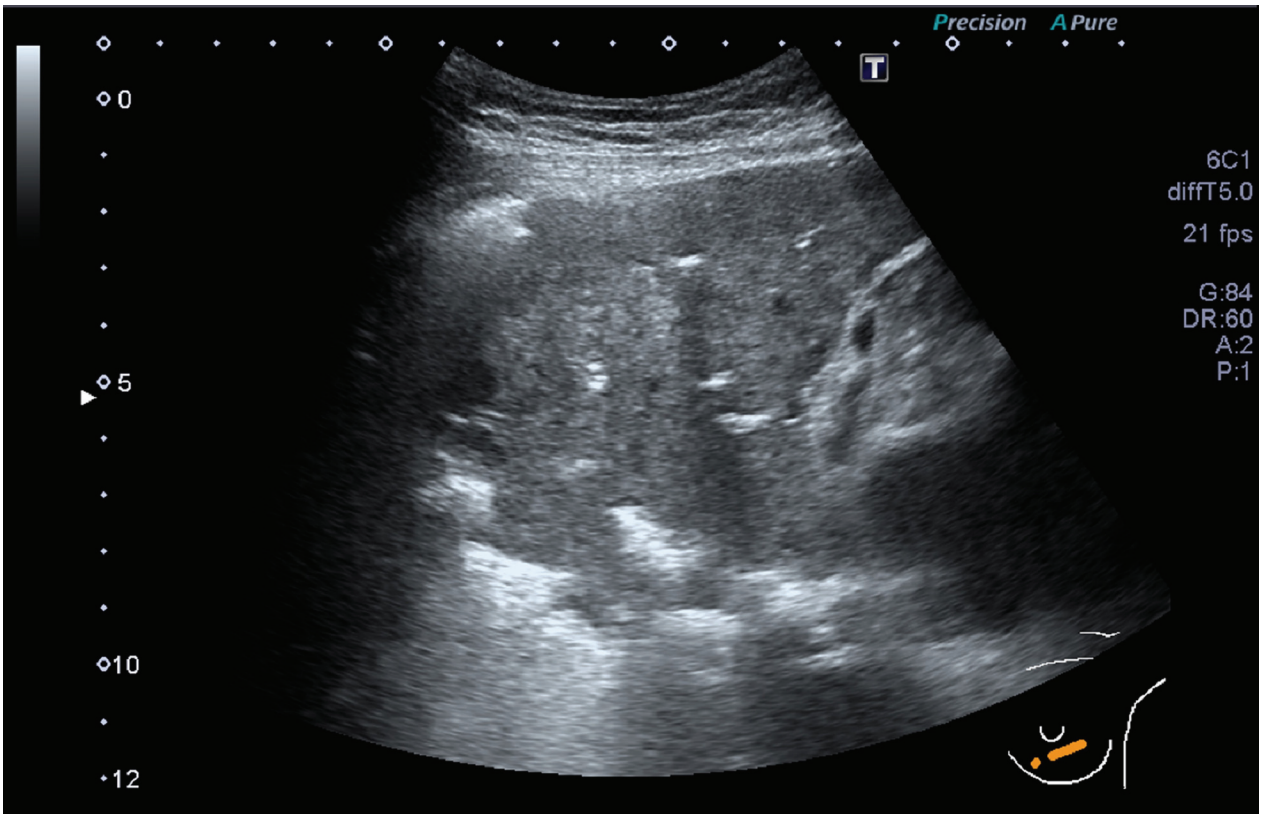

Fig. 3. Thoracic sonography showed a consolidative mass lesion, with air bronchogram.

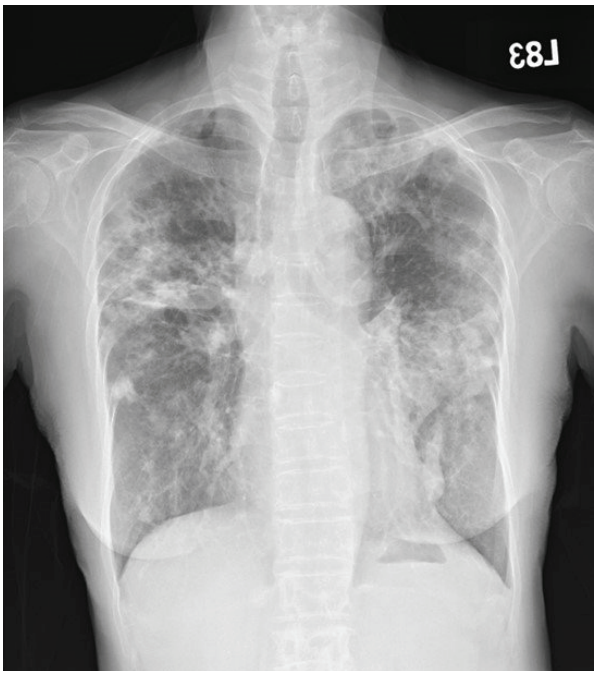

Fig. 4. CXR on day 21 (before discharge) showed improvement of the bilateral consolidation.

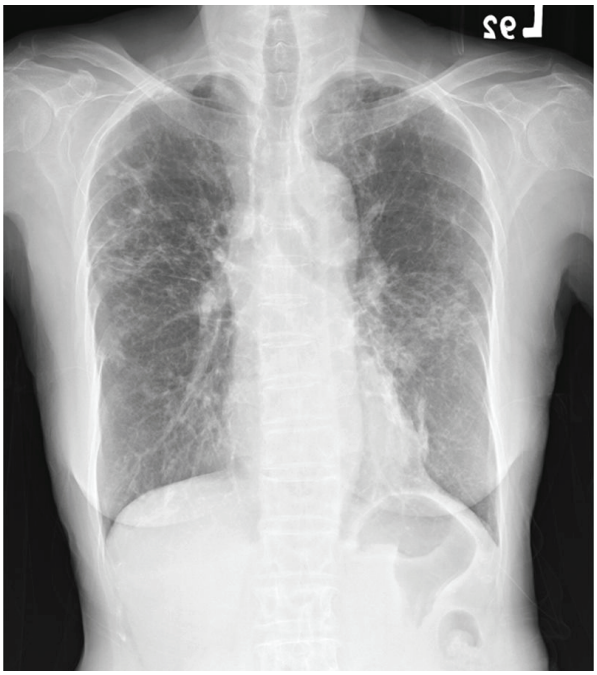

Fig. 5. CXR on day 44 showed marked regression of the bilateral mass-like lesions and chronic change of the cystic bronchiectasis at the right upper lobe and left lingula.

Discussion

The incidence and prevalence of *P. aeruginosa* infection are relatively higher in patients with bronchiectasis than in those without. Of note, *P. aeruginosa* infection is also associated with a higher exacerbation rate, worsened quality of life, and even higher hospital admission and mortality [1, 3-4, 10]. In a prospective study on 117 patients from south India with bronchiectasis, 53.8% of the patients were culture-positive for *P. aeruginosa*, and compared to those infected with non-P aeruginosa pathogens, they had a higher rate of bronchiectasis exacerbation (p: 0.007) [10]. These reports suggest the importance of *P. aeruginosa* infection in patients with bronchiectasis.

The classic radiologic features of P aeruginosa pneumonia were first described by Tillotson and Lerner in 1967 as diffuse bronchopneumonia with nodularity and micro-abscess with small areas of radiolucency [11]. However, subsequent studies have failed to confirm their conclusions [1]. Okada at el. analyzed the thoracic CT of 35 patients with *P. aeruginosa* pneumonia (mean age: 66.9 years, 21 males and 14 females) [6], and found that the main findings of *P. aeruginosa* pneumonia were ground-glass attenuation (97.1%) and bronchial wall thickening (88.6%), followed by consolidation (65.7%) and intralobular reticular opacity. Other findings included cavity (14.3%), centrilobular nodules (11.4%), and nodules (8.6%). It is uncommon to see mass-like lung lesions in patients with *P. aeruginosa* pneumonia [12].

In our report, the patient had a history of bronchiectasis, which was relatively stable without regular medication use. Although the radiographic findings and her weight loss may suggest a differential diagnosis of carcinoma, her initial clinical presentation implied a diagnosis of pneumonia. Because of the pre-existing cystic bronchiectasis at the bilateral upper lobes, the patient may have been at risk of *P. aeruginosa* colonization, resulting in subacute infection causing pus accumulation and abscess formation [10, 12]. With the multifocal consolidative radiographic findings noted in our case, the differential diagnosis should include pulmonary edema, interstitial lung disease, cryptogenic organizing pneumonia, drug-induced toxicity, diffuse alveolar hemorrhage, pulmonary alveolar proteinosis, infection, malignancy and COVID-19 pneumonia in this pandemic period. [13]. Some experts suggest using the 6-question rule checklist strategy, or FIBROVAKIM, to simplify the differential diagnosis of multiple lung parenchymal abnormalities [14]; this checklist would include: diffuse fibrosing (FI) disease; bronchial or bronchiolar (BRO) lesion; vascular or cardiac (VA) dysfunction; carcinomatous (K) process; infection (I); or medication-induced (M) disease. So, for patients with multiple lung parenchymal abnormalities, an infectious process should always be considered, and quick investigation is warranted to ensure appropriate and timely management.

With regard to diagnosis, imaging-guided transthoracic biopsy is a useful and accessible tool for newly found nodules, masses, and multiple unexplained mass-like consolidations, as in our case. Imaging-guided chest biopsy is generally indicated for a patient with a new or enlarging solitary nodule or mass, with multiple nodules without known neoplastic disease or in prolonged remission, focal parenchymal infiltrates in which an infectious organism cannot be isolated, diagnosis of hilar masses following negative bronchoscopy, an undiagnosed mediastinal mass, or biopsy or re-biopsy of malig-

nancy for targeted therapy [15]. In our patient, who presented with a multifocal conglomerate mass-like consolidation, which is seldom seen in CAP, imaging-guided thoracic biopsy was necessary to exclude lung cancer. Sono-guided aspiration is a safe and fast technique compared with CT-guided aspiration [15, 16]. In a published meta-analysis, sono-guided biopsy was found to be generally very well tolerated and safe, with a pooled incidence of pneumothorax and hemorrhage of 2.8% in sono-guided biopsy, compared to 20.5% in CT-guided biopsy [16]. Our patient underwent the procedure on day 3 of admission, and culture of the lung mass aspirate came out on day 7. The use of sono-guided aspiration helped the physicians make a correct diagnosis, and make an early decision on deescalating antibiotic treatment.

Conclusion

P. aeruginosa pneumonia is an important pathogen in patients with chronic airway disease, such as bronchiectasis. A diversity of radiographic findings are also found in *P. aeruginosa*, and the presence of a multifocal consolidative mass cannot exclude the possibility of *P. aeruginosa* pneumonia. Timely initiation of empirical antibiotics and selecting the proper tools to reach a diagnosis are important in patients with multifocal mass-like pulmonary consolidation and a suspicion of pulmonary infection.

References

1. Fujitani S, Sun HY, Yu VL, *et al*. Pneumonia due to Pseudomonas aeruginosa: part I: epidemiology, clinical diagnosis, and source. Chest 2011; 139(4): 909-919.
2. Wang T, Hou Y Wang R A case report of community-acquired Pseudomonas aeruginosa pneumonia complicated with MODS in a previously healthy patient and related literature review. BMC Infect Dis 2019; 19(1): 130.
3. Musher DM, Thorner AR. Community-acquired pneumonia. N Engl J Med 2014; 371(17): 1619-28.
4. Araujo D, Shteinberg M, Aliberti S, *et al*. The independent contribution of Pseudomonas aeruginosa infection to long-term clinical outcomes in bronchiectasis. Eur Respir J 2018; 51(2): 1701953.
5. Woo TE, Lim R, Surette MG, *et al*. Epidemiology and natural history of Pseudomonas aeruginosa airway infections in non-cystic fibrosis bronchiectasis. ERJ Open Res 2018; 4(2).
6. Okada F, Ono A, Ando Y, *et al*. Thin-section CT findings in Pseudomonas aeruginosa pulmonary infection. Br J Radiol 2012; 85(1020): 1533-8.
7. Metlay, J.P., Waterer GW, Long AC, *et al*. Diagnosis and treatment of adults with community-acquired pneumonia. An official clinical practice guideline of the American Thoracic Society and Infectious Diseases Society of America. Am J Respir Crit Care Med 2019; 200(7): e45-e67.
8. Chou CC, Shen CF, Chen SJ, *et al*. Recommendations and guidelines for the treatment of pneumonia in Taiwan. J Microbiol Immunol Infect 2019; 52(1): 172-199.
9. Neill AM, Martin IR, Weir R, *et al*. Community acquired pneumonia: aetiology and usefulness of severity criteria on admission. Thorax 1996; 51(10): 1010-6.
10. Chawla K, Vishwanath S, Manu MK, *et al*. Influence of pseudomonas aeruginosa on exacerbation in patients with bronchiectasis. J Glob Infect Dis 2015; 7(1): 18-22.
11. Tillotson JR, Lerner AM. Characteristics of nonbacteremic Pseudomonas pneumonia. Ann Intern Med 1968; 68(2): 295-307.
12. Gharabaghi MA, Abdollahi SMM, Safavi E, *et al*. Community acquired Pseudomonas pneumonia in an immune competent host. BMJ Case Rep 2012; 2012.
13. Parekh M, Donuru A, Balasubramanya R, *et al*. Review of the chest CT differential diagnosis of ground-glass opacities in the COVID era. Radiology 2020; 297(3): E289-E302.
14. Baque-Juston M, Mondot L, Leroy S, *et al*. Multiple lung parenchymal abnormalities: Don't panic, let's be pragmatic! The 6 question rule-a checklist strategy. Diagn Interv Imaging 2014; 95(4): 361-76.

15. Anzidei M, Porfiri A, Andrani F, *et al*. Imaging-guided chest biopsies: techniques and clinical results. Insights Imaging 2017; 8(4): 419-428.

16. DiBardino DM, Yarmus LB, Semaan RW. Transthoracic needle biopsy of the lung. J Thorac Dis 2015; 7(Suppl 4): S304-16.

Case Report: Metastatic Choriocarcinoma with Choriocarcinoma Syndrome Presenting as Massive Pulmonary Hemorrhage

Chiung-Hsin Chang[1], Chen-Yiu Hung[1,3], Ting-Chang Chang[2,3]

Diffuse alveolar hemorrhage (DAH) is a life-threatening disorder that may develop into respiratory failure. One of the various differential diagnoses of DAH is metastatic choriocarcinoma. We report the rare case of a 32-year-old woman who presented with pulmonary hemorrhage, liver and thoracic spine metastases of choriocarcinoma immediately after a normal delivery. Multiple hypervascular masses at the posterior wall of the uterus were found. She was then treated with cisplatin-etoposide chemotherapy. Hemothorax, hemoperitonium, and progressive pulmonary hemorrhage with a rapidly increasing choriogonadotropin level were noted soon after chemotherapy, and was diagnosed as choriocarcinoma syndrome. Thus, the patient was diagnosed as having metastatic choriocarcinoma with the initial presentation of massive pulmonary hemorrhage, and choriocarcinoma syndrome that presented during chemotherapy. ***(Thorac Med 2024; 39: 43-50)***

Key words: diffuse alveolar hemorrhage, gestational trophoblastic neoplasm, choriocarcinoma, choriocarcinoma syndrome.

Introduction

Diffuse alveolar hemorrhage (DAH) is a clinicopathologic syndrome presenting as hemoptysis, anemia, diffuse pulmonary infiltrates, and hypoxemic respiratory failure. DAH involves the accumulation of intraalveolar red blood cells originating from the alveolar capillaries. All causes of DAH have the common denominator of an injury to the alveolar microcirculation, including pulmonary capillary inflammation, bland pulmonary hemorrhage, and diffuse alveolar damage [1]. One of the rare causes of DAH is pulmonary metastatic choriocarcinoma, a hypervascular malignancy. Choriocarcinoma is a highly malignant gestational trophoblastic neoplasm; however, the incidence of non-gestational choriocarcinoma is very rare. It is characterized by vascular invasion and widespread metastasis at diagnosis,

[1]Department of Thoracic Medicine, Linkou Chang Gung Memorial Hospital, Taoyuan, Taiwan, [2]Department of Obstetrics and Gynecology, Linkou Chang Gung Memorial Hospital, Taoyuan, Taiwan, [3]Chang Gung University, College of Medicine, Taoyuan, Taiwan.
Address reprint requests to: Dr. Ting-Chang Chang, Department of Obstetrics and Gynecology, Linkou Chang Gung Memorial Hospital, Taoyuan, Taiwan.

and histologically consists of invasive, highly vascular, and anaplastic cytotrophoblasts and syncytiotrophoblasts accompanied with massive hemorrhage. The clinical presentation of choriocarcinoma depends upon the extent of disease and the location of metastasis, and is often associated with tumor bleeding. Hematogenous spreading is very common, and the lungs are the most frequent site of choriocarcinoma metastasis, followed by the vagina. The diagnosis of choriocarcinoma can be based on a high titer of human choriogonadotropin and the image pattern. Gestational choriocarcinoma may occur after any form of pregnancy, including mole pregnancy, abortion, and pre-term or term delivery. We present a rare case, with a complete survey of DAH etiology that was finally diagnosed as pulmonary metastatic choriocarcinoma.

Case Report

A 32-year-old female patient presented with hemoptysis and intermittent cough for 2 weeks. She was admitted to the hospital at 37 weeks' gestation due to frequent labor pain and blood-tinged vaginal discharge. She had a successful vaginal delivery 5 days after the initial symptoms were noted. However, she had deteriorated dyspnea, desaturation and hemoptysis a few hours after delivery. She had had a normal spontaneous delivery previously, and an uneventful prenatal course for the second pregnancy. She was then intubated and admitted to the intensive care unit (ICU) due to acute hypoxemic respiratory failure.

Her body height was 158 cm and body weight was 56 kg. On physical examination, she had a heart rate of 118 beats/min; blood pressure of 122/81 mmHg; temperature of 36.8°C; and respiratory rate of 15 breaths/min. Oxygen saturation was 98% with mechanical ventilation. The initial setting of the mechanical ventilator was the pressure control ventilation mode, with a peak pressure of 30 cmH_2O, positive end-expiratory pressure of 10 cmH_2O, and FiO_2 of 40%. Crackles were heard at the bilateral lung fields. The abdomen was soft, but not tender. No skin lesions were noted. Pelvic examination on the bed showed a postpartum uterus, and 19 mm of necrotic flesh tissue that had passed out of the vagina. There were no skin lesions.

The chest radiograph upon emergency department arrival showed diffuse coarse nodular infiltrates over bilateral lungs (Fig. 1a). The computed tomography (CT) image showed multiple ground glass opacities with consolidation and multiple hypodense intrahepatic tumors with a perihepatic blood clot (Fig. 2a-2c). Laboratory study showed a white blood cell count of 21,400 cells/mm^3, a hemoglobin level of 9 g/dL, a platelet count of 119,000/mm^3, a d-dimer level of 2869 ng/mL, fibrinogen level of 524 mg/dL, C-reactive protein level of 188mg/L, and an albumin level of 2.79 g/dL. The electrolytes, creatinine, liver function markers, procalcitonin, prothrombin time and activated partial thromboplastin time were within normal ranges. Influenza virus, human immunodeficiency virus, and cytomegalovirus were not detected. The galactomannan antigen, antinuclear antibody, C3, C4, rheumatic factor, anti-neutrophil cytoplasmic antibodies (ANCA), and anti-phospholipid antibodies were all within their normal ranges. The alpha fetoprotein level was 43.3 ng/mL. The sputum and blood cultures reported negative findings. The CA-125 level was 42.6 U/mL. The β-human chorionic gonadotropin (β-hCG) level was 79,008

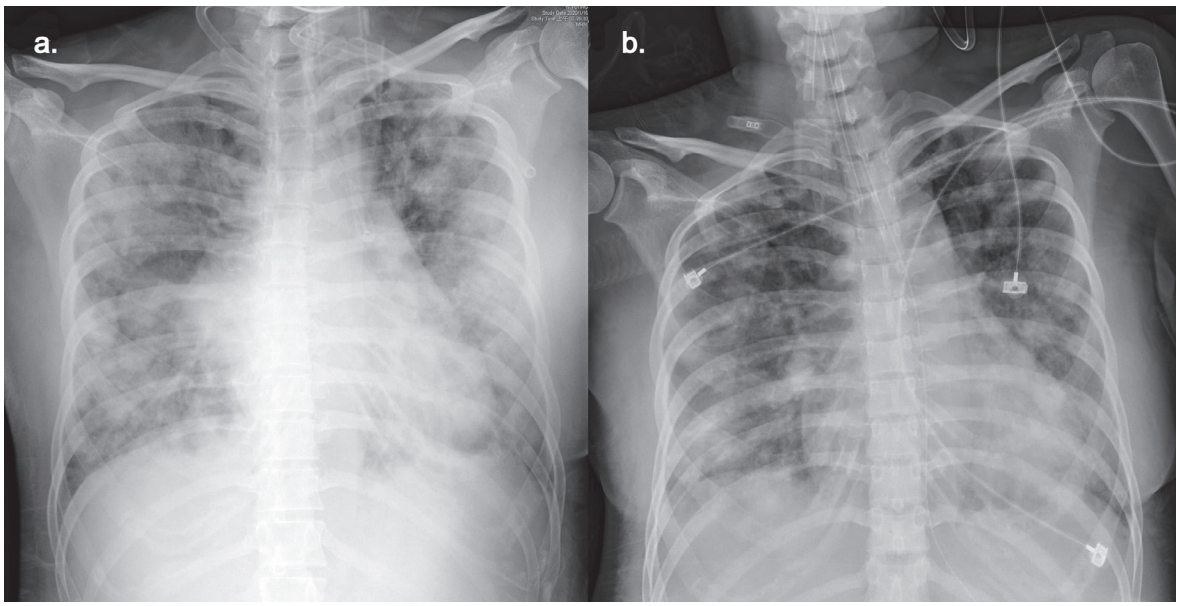

Fig. 1. Chest radiographs during admission. a. Chest radiograph at admission revealed diffused cotton ball nodular lesions over the entire lung field bilaterally on the 1st day of admission. b. Chest radiographs showed much improvement in the bilateral lung lesions a month after chemotherapy was initiated.

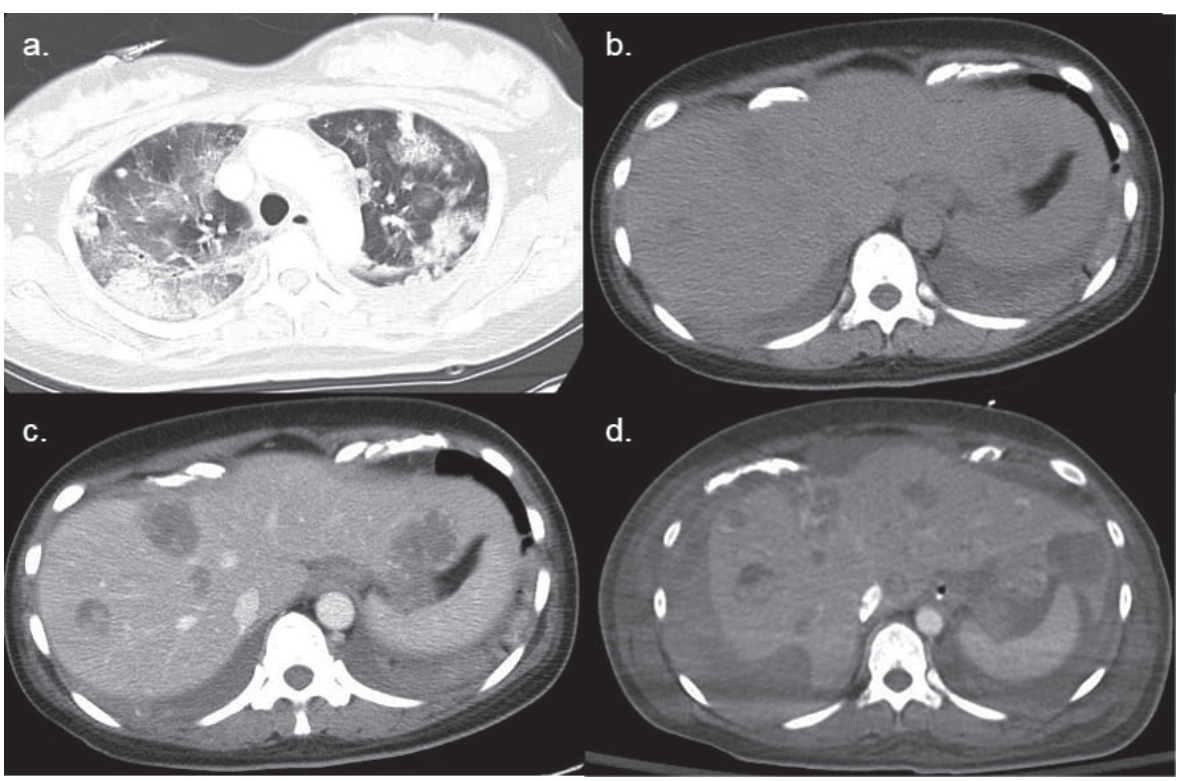

Fig. 2. CT image of chest and abdomen. a. Chest CT of the lung window showed multiple ground-glass opacities and consolidations in bilateral lungs (1st day of admission); b. The artery phase of the liver CT (1st day of admission); c. The venous phase of the liver CT (1st day of admission). d. CT angiography of the liver showed multiple progressive hypervascular liver tumors with rupture, leading to subcapsular hematoma and hemoperitoneum (13th day of admission).

IU/L. Abdominal echo revealed bilateral multiple hyperechoic nodules. Transabdominal pelvic ultrasound showed multiple posterior wall masses with increasing vascularity. Fiberoptic bronchoscopy revealed blood oozing from the right middle lung, and no endobronchial lesion or active bleeding. Hemosiderin-laden macrophages were not seen in the bronchioalveolar lavage (BAL) fluid. Cytology and microbiology of the BAL specimens had negative findings. A diagnosis of choriocarcinoma was reported by the pathologist (Fig. 3).

Acute respiratory distress syndrome (ARDS) occurred during ICU admission. The ventilator setting was adjusted according to the ARDS protocol [2]. The modified World Health Organization (WHO) prognostic score of this patient was 14 and the International Federation of Gynecology and Obstetrics (FIGO) staging of gestational trophoblastic neoplasia was stage IV [3]. At this point, induction chemotherapy at a low dosage or with modified regimens is suggested to avoid aggravated tumor bleeding caused by chemotherapy-induced massive tumor necrosis [4-6]. Under the diagnosis of choriocarcinoma with diffuse pulmonary metastasis, resulting in respiratory failure, and with multiple hepatic metastatic tumors, low-dose cisplatin chemotherapy was started on the 4th admission day, along with bevacizumab. The details of the chemotherapy, using cisplatin, etoposide, and bevacizumab, are listed in Table 1.

One week after initiation of chemotherapy, the patient's serum β-hCG level was 144,415 IU/L, along with hemothorax, progressive hemoptysis, hypoxia, hemoperitoneum and anemia. The follow-up CT angiography revealed multiple hypervascular liver tumors with tumor rupture leading to subcapsular hematoma and hemoperitoneum (Fig. 2d). Attempted weekly, low-dosage chemotherapy was interrupted by aggravated hemoptysis, hemoperitoneum and vaginal bleeding. Decreased β-hCG levels and improved chest radiography results (Fig. 1b) were noted after chemotherapy. The clinical course is summarized and illustrated in Figure 4. Tracheostomy was performed on the 35th admission day. She was successfully liberated from mechanical ventilation with a tracheal mask after 40 days of intubation, and could easily read a book on the ICU bed, though vaginal

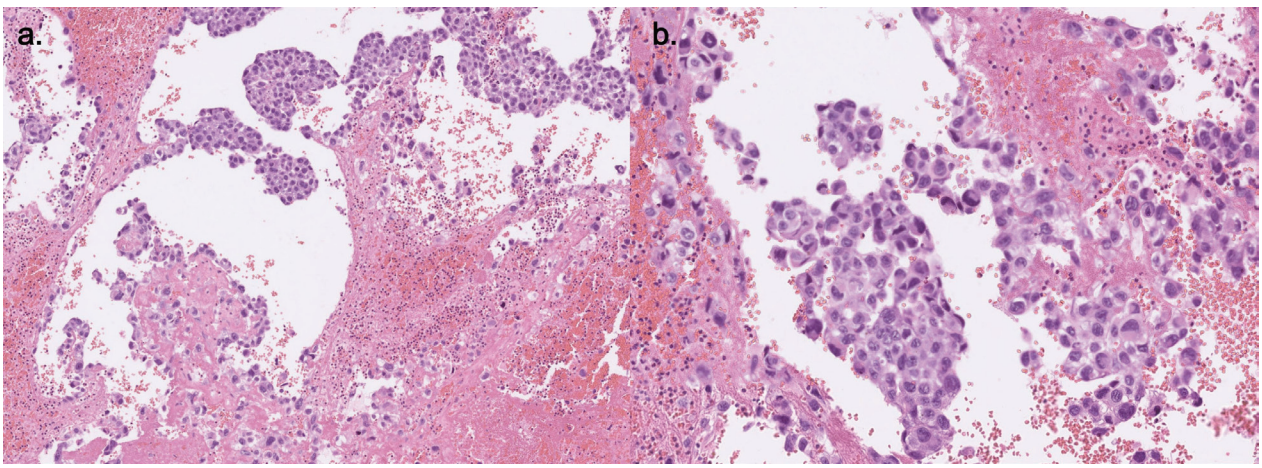

Fig. 3. Abundant blood clots and clusters of trophoblastic tumor cells with marked nuclear pleomorphism were noted in the vaginal mass specimen. No chorionic villi were identified. (hematoxylin-eosin stain, original magnifications, 200 [a] and 400[b]).

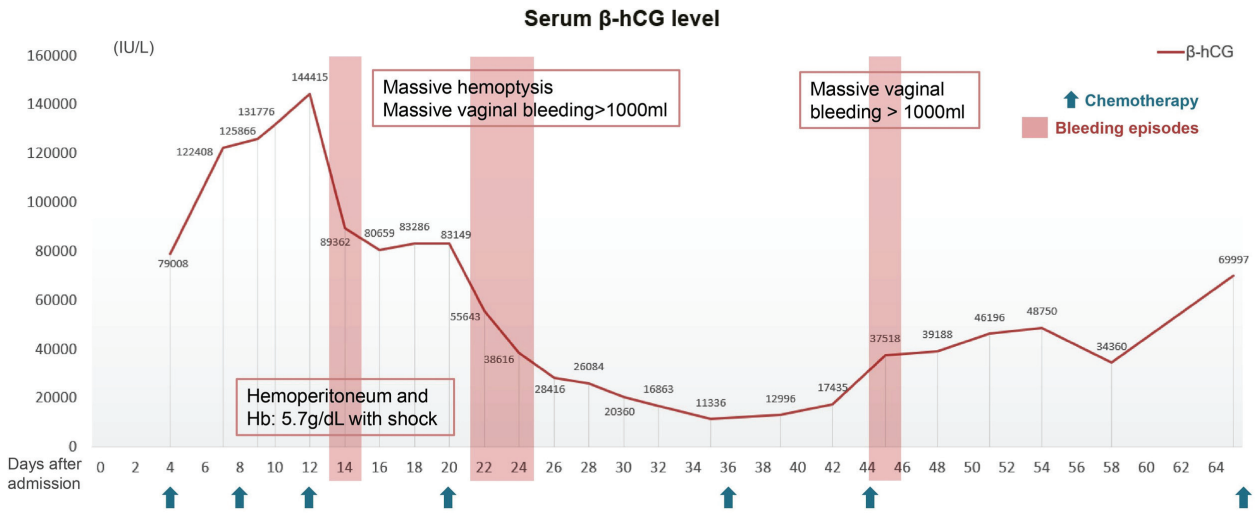

Fig. 4. Serum β-hCG (β-human chorionic gonadotropin), chemotherapy and the clinical course of a 32-year-old woman with ultra-high risk gestational choriocarcinoma.

bleeding persisted. A large amount of vaginal bleeding, up to 1500 ml/day, occurred after the third etoposide regimen and continued, which, along with subsequent fever episodes, hampered further chemotherapy.

The patient complained of numbness over bilateral lower limbs on the 66th admission day. The deep tendon reflex of the bilateral lower limbs was decreased and muscle power was absent within a few days. Magnetic resonance imaging (MRI) revealed T6 and T11 spine and epidural tumors with cord compression. Progressive dyspnea recurred, and the patient responded poorly to mechanical ventilator support. The patient died of T-spinal cord compression-related respiratory failure on the 70th day of admission.

Discussion

We reported the clinical course of a patient with advanced pulmonary metastatic choriocarcinoma after term pregnancy, with life-threatening pulmonary hemorrhage, tumor lysis syndrome, and finally successful liberation from the mechanical ventilator. Although the patient was successfully liberated from the mechanical ventilator after treatment, she eventually died of disease progression.

With the finding of bilateral multiple diffused hazy-rimed nodules in the initial chest radiography with hemoptysis, DAH syndrome was taken into consideration in this patient. Various diseases, including infections, autoimmune diseases, drugs, and metastatic malignancies, are associated with DAH syndrome. The high alpha fetoprotein level in this case helped us focus on the diagnosis of gestational trophoblastic neoplasm [7].

The radiologic findings of pulmonary metastasis in the chest radiograph are usually multiple diffuse ill-defined nodules with irregular margins in the bilateral lung fields. When accompanied by peritumoral hemorrhage, pulmonary metastatic choriocarcinoma has the relatively characteristic CT findings of nodular attenuation surrounded by a halo of ground-glass opacity (CT halo sign) or ill-defined fuzzy

margins [8]. Fragility of the neovascular tissue that leads to a rupture of the vessel is a probable cause of hemorrhage around the metastasis [9].

Respiratory failure is a rare but lethal complication of choriocarcinoma with pulmonary metastasis. It is usually caused by extensive pulmonary hemorrhage and may progress rapidly. Kelly *et al*. found several factors that contributed to respiratory failure and early death within 1 month of starting treatment in patients with choriocarcinoma, including >10 metastatic lung lesions, chest X-ray opacification >50%, and an initial hCG level >105 IU/L. The most important step in reducing mortality is early diagnosis [10]. For the management of DAH, general supportive therapies including correction of the known coagulation abnormalities, oxygen supplementation and even mechanical ventilation are necessary. Metastasis involving the level of the phrenic motoneurons (C3, 4, and 5) or high levels of the thoracic spinal cords (T1-T6), which innervate the diaphragm and respiratory muscles, also contribute to the subsequent respiratory failure in such patients [11].

Extracorporeal membrane oxygenation (ECMO) has been used in a few patients with refractory hypoxemic respiratory failure due to DAH, mostly with the etiologies of ANCA-associated vasculitis and systemic lupus erythematosus [12]. Although successful bridging ECMO support has also been reported in several patients with metastatic choriocarcinoma and ARDS, there has been no reported ECMO experience in patients with metastatic choriocarcinoma and massive pulmonary hemorrhage, to the best of our knowledge [12, 13]. In addition, recurrent hemothorax, hemoperitoneum and massive vaginal bleeding was noted during this patient's admission. ECMO use was controversial for this patient due to the necessity of anticoagulation for ECMO and the risk of worsening multiple massive hemorrhage.

Choriocarcinoma is a highly vascular tumor, and hemorrhage of the uterus and organs undergoing metastasis is common. Although most cases of choriocarcinoma responded to chemotherapy, and patients with distant metastases may be able to enjoy an uneventful life and preserve their fertility potential after successful chemotherapy, patients with a WHO prognostic score of ≥13 (defined as "ultra-high risk") had a significantly increased risk of early death, defined as mortality within 4 weeks after treatment initiation. The mortality rate was 4.9% in cases with a score of <13, and 38.4% in those with a score ≥13 [14]. Standard chemotherapy with etoposide, methotrexate, and dactinomycin alternating weekly with cyclophosphamide and vincristine (EMA/CO) for high-risk patients (a WHO prognostic score ≥7) with gestational trophoblast neoplasm has been suggested [15]. However, standard chemotherapy may cause sudden tumor necrosis with severe bleeding, metabolic acidosis, myelosuppression, septicemia, and multiple organ failure, resulting in early death. To avoid this, the use of initial partial rather than full-dose chemotherapy is suggested. The Charing Cross Group introduced induction low-dose etoposide at 100 mg/m2 and cisplatin at 20 mg/m2 on days 1 and 2 every 7 days for selected patients with a high tumor burden [16, 17]. We scheduled a weekly induction of alternating cisplatin and etoposide, which was initially complicated with aggravated hemoptysis and hemoperitoneum. Since vascular endothelial growth factor and its receptors are highly expressed in gestational trophoblastic disease [18], and bevacizumab plus chemotherapy was shown to be highly effective for malignant pleu-

ral effusion [19-21], we added bevacizumab at a very low dose to the chemotherapy.

Massive bleeding episodes occurred several times soon after the administration of chemotherapy in this case, which was suspected to be "choriocarcinoma syndrome". Life-threatening tumor necrosis following induction chemotherapy was first described by Logothetis as "choriocarcinoma syndrome" in 1984. Choriocarcinoma syndrome was defined as a clinical presentation of advanced germ cell tumors with high-volume choriocarcinoma elements and a markedly elevated β-hCG level, over 50,000 IU/L [22]. Choriocarcinoma syndrome usually occurs shortly after the administration of chemotherapy. It has a high risk of fatal bleeding from metastatic lesions, and frequently involves acute respiratory failure and a high mortality rate in the early phase of induction treatment due to massive tumor lysis. The symptoms and signs are associated with hemorrhage from metastatic sites in any organ that has tumor involvement [23-25].

Conclusion

Patients with choriocarcinoma with multiple metastases may present with diffuse alveolar hemorrhage with acute respiratory failure. Metastasis of choriocarcinoma involving high levels of the T spine may also contribute to respiratory failure in such patients. The occurrence of choriocarcinoma syndrome should be considered a possibility after the administration of chemotherapy to patients with a high choriocarcinoma volume and high hCG level.

Conflict of interest statement

No conflict of interest is declared.

Ethics statement

The authors declare that appropriate written informed consent was obtained for the publication of this manuscript and accompanying images. This study was approved by the Institutional Review Board of Chang Gung Medical Foundation (IRB No. 202200163B0).

References

1. Lara AR, Schwarz MI. Diffuse alveolar hemorrhage. Chest 2010; 137(5): 1164-71.
2. Thompson BT, Chambers RC, Liu KD. Acute respiratory distress syndrome. N Engl J Med 2017; 377(6): 562-72.
3. Oncology FCoG. Current FIGO staging for cancer of the vagina, fallopian tube, ovary, and gestational trophoblastic neoplasia. Int J Gynaecol Obstet 2009; 105(1): 3-4.
4. Shen Y, Ren T, Feng F, *et al*. Treatment of respiratory failure in metastatic pulmonary choriocarcinoma: an experience at Peking Union Medical College Hospital, China. Chin Med J 2012; 125(7): 1214-8.
5. Vaccarello L, Apte SM, Diaz PT, *et al*. Respiratory failure from metastatic choriocarcinoma: a survivor of mechanical ventilation. Gynecol Oncol 1997; 67(1): 111-4.
6. Coleman RE, Seckl MJ. Ultra-high risk GTN: what is it and HOW should we manage it? Int Soc Study Trophoblast Dis (ISSTD) GTD book 2015; 1-12.
7. Abelev G. Alpha-fetoprotein in ontogenesis and its association with malignant tumors. Adv Cancer Res 1971; 14: 295-358.
8. Hirakata K, Nakata H, Nakagawa T, *et al*. CT of pulmonary metastases with pathological correlation. Seminars in Ultrasound, CT and MRI; 1995: Elsevier.
9. Seo JB, Im JG, Goo JM, *et al*. Atypical pulmonary metastases: spectrum of radiologic findings. Radiographics 2001; 21(2): 403-17.
10. Kelly M, Rustin G, Ivory C, *et al*. Respiratory failure due to choriocarcinoma: a study of 103 dyspneic patients. Gynecol Oncol 1990; 38(2): 149-54.
11. Winslow C, Rozovsky J. Effect of spinal cord injury on

the respiratory system. Am J Phys Med Rehabil 2003; 82(10): 803-14.
12. Abrams D, Agerstrand CL, Biscotti M, *et al*. Extracorporeal membrane oxygenation in the management of diffuse alveolar hemorrhage. ASAIO J 2015; 61(2): 216-8.
13. Sekandarzad A, Udi J, Waller CF, *et al*. Extracorporeal membrane oxygenation support as a bridge to recovery during chemotherapy in a young patient with metastatic choriocarcinoma and severe acute respiratory distress syndrome. Oncol Res Treat 2020; 43(10): 559-64.
14. Bolze PA, Riedl C, Massardier J, *et al*. Mortality rate of gestational trophoblastic neoplasia with a FIGO score of ≥13. Am J Obstet Gynecol 2016; 214(3): 390.e1-8.
15. Lurain JR. Gestational trophoblastic disease II: classification and management of gestational trophoblastic neoplasia. Am J Obstet Gynecol 2011; 204(1): 11-8.
16. Ngan HY, Seckl MJ, Berkowitz RS, *et al*. Diagnosis and management of gestational trophoblastic disease: 2021 update. Int J Gynecol Obstet 2021; 155: 86-93.
17. Alifrangis C, Agarwal R, Short D, *et al*. EMA/CO for high-risk gestational trophoblastic neoplasia: good outcomes with induction low-dose etoposide-cisplatin and genetic analysis. J Clin Oncol 2013; 31(2): 280-6.
18. Singh M, Kindelberger D, Nagymanyoki Z, *et al*. Vascular endothelial growth factors and their receptors and regulators in gestational trophoblastic diseases and normal placenta. J Reprod Med 2012; 57(5-6): 197-203.
19. Jiang L, Li P, Gong Z, *et al*. Effective treatment for malignant pleural effusion and ascites with combined therapy of bevacizumab and cisplatin. Anticancer Res 2016; 36(3): 1313-8.
20. Tao H, Meng Q, Li M, *et al*. Outcomes of bevacizumab combined with chemotherapy in lung adenocarcinoma-induced malignant pleural effusion. Thorac Cancer 2018; 9(2): 298-304.
21. Worley Jr MJ, Elias KM, Horowitz NS, *et al*. Durable remission for a woman with refractory choriocarcinoma treated with anti-endoglin monoclonal antibody and bevacizumab: a case from the New England Trophoblastic Disease Center, Brigham and Women's Hospital and Dana-Farber Cancer Institute. Gynecol Oncol 2018; 148(1): 5-11.
22. Logothetis C. Choriocarcinoma syndrome. Cancer Bull 1984; 36: 118-20.
23. Benditt JO, Farber HW, Wright J, et al. Pulmonary hemorrhage with diffuse alveolar infiltrates in men with high-volume choriocarcinoma. Ann Intern Med 1988; 109(8): 674-5.
24. Shintaku M, Hwang MH, Amitani R. Primary choriocarcinoma of the lung manifesting as diffuse alveolar hemorrhage. Arch Pathol Lab Med 2006; 130(4): 540-3.
25. Durieu I, Berger N, Loire R, et al. Contralateral haemorrhagic pulmonary metastases ("choriocarcinoma syndrome") after pneumonectomy for primary pulmonary choriocarcinoma. Thorax 1994; 49(5): 523-4.

What to Expect When You're Not Expecting it: Reexpansion Pulmonary Edema Following Tube Thoracostomy for Pneumothorax

Yu-Lin Hsieh[1]

Symptomatic reexpansion pulmonary edema (RPE) is an extremely rare complication following tube thoracostomy for pneumothorax, with a mortality rate up to 20% [1]. It can occur in chronic pneumothorax with rapid decompressive treatment or pleural effusion with excessive tapping. Ultimately, the risk factors remain unclear.

A 61-year-old man suffered from chest tightness and shortness of breath for about a week. Chest X-ray showed significant right-side pneumothorax. Coughing and desaturation developed 20 minutes after tube thoracostomy. Follow-up X-ray revealed a partial reexpanded right lung. The patient was given diuretics and hydrocortisone, along with CPAP support. The pulmonary edema resolved gradually over 4 days, and the patient underwent VATS bullectomy successfully. ***(Thorac Med 2024; 39: 51-54)***

Key words: Pneumothorax, tube thoracostomy, reexpansion pulmonary edema (RPE).

Introduction

Symptomatic reexpansion pulmonary edema (RPE) is an extremely rare complication following tube thoracostomy for pneumothorax, with a mortality rate up to 20% [1]. It can occur in cases of chronic pueumothorax post-chest tube insertion or pleural effusion with excessive tapping. Ultimately, the risk factors remain unclear.

Case Report

A 61-year-old chronic smoker with no past medical history visited the outpatient department with the complaint of chest tightness and shortness of breath for about a week. Auscultation revealed an absence of right breathing sounds. Chest X-ray showed massive pneumothorax with atelectasis of the right lung. The patient was referred to the emergency room (ER)

[1]Mackay Memorial Hospital, Department of Surgery, Division of Thoracic surgery
Address reprint requests to: Dr. Wen-Chien Huang,Mackay Memorial Hospital, Department of Surgery, Division of Thoracic surgery, No.92, Sec.2, Zhongshan N. Rd., Zhongshan Dist., Taipei City

for evaluation, and chest tube insertion was performed. Vital signs showed blood pressure 168/140 mmHg, heart rate 77 bpm, and respiratory rate 21/min. A 24 French chest tube was inserted smoothly by the emergency physician. Then, 20 minutes post-procedure, the patient developed tachycardia, coughing and desaturation. His peripheral oxygen saturation dropped from 96% to 89%, despite 2 L/min of oxygen that had been supplied via nasal cannula. The thoracic surgeon was called to the ER, and a repeated chest X-ray confirmed that the chest tube had been placed in the right pleural cavity with the right lung partially re-expanded with increased lung opacity. With the tentative diagnosis of reexpansion pulmonary edema, the patient's oxygen supply was adjusted to maintain adequate oxygenation. A routinely used low-pressure suction post-chest tube insertion was not employed in this case.

The next day, the patient maintained clear consciousness, but complained of occasional shortness of breath, despite the oxygen supply. Follow-up chest X-ray showed both partial expansion and diffuse pulmonary edema of the right lung. Arterial blood gas revealed PaO_2 around 75-78 mmHg with the O_2 aerosal mask at 100% use. Based on the images and clinical symptoms, the diagnosis of RPE was confirmed. Diuretics and hydrocortisone 100 mg q6h were added to the treatment, and fluid intake was restricted. The oxygen mask was replaced by a CPAP ventilator, with expiratory positive airway pressure (EPAP) at 7 cmH_2O, and additional positive pressure support. The patient was placed under close monitoring in the observation ward, and was able to maintain his O_2 saturation at around 95-98%.

On the 4th day under CPAP ventilation, chest X-ray showed resolution of the pulmonary edema, and the patient was in stable condition. A persistent airleak was noted, and chest CT was arranged, which revealed multiple blebs on the apex of the right lung. The patient then underwent surgical intervention with VATS for bullectomy and pleurodesis on the 5th day. The

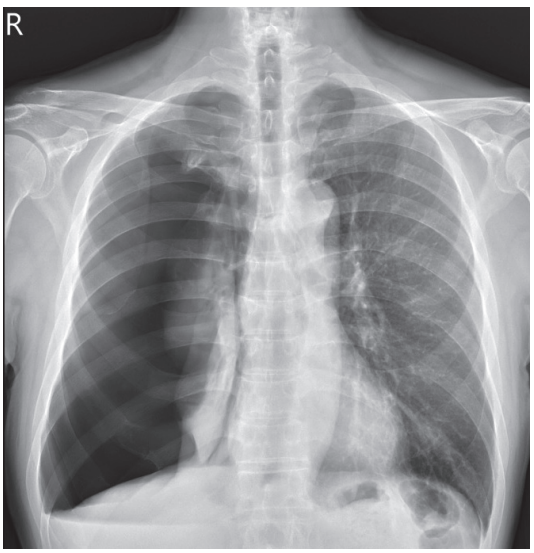

Fig. 1. Complete right-side pneumothorax.

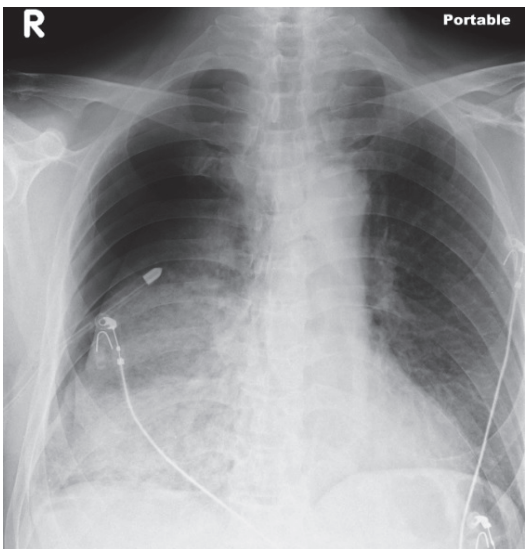

Fig. 2. Post-chest tube insertion with poor expansion.

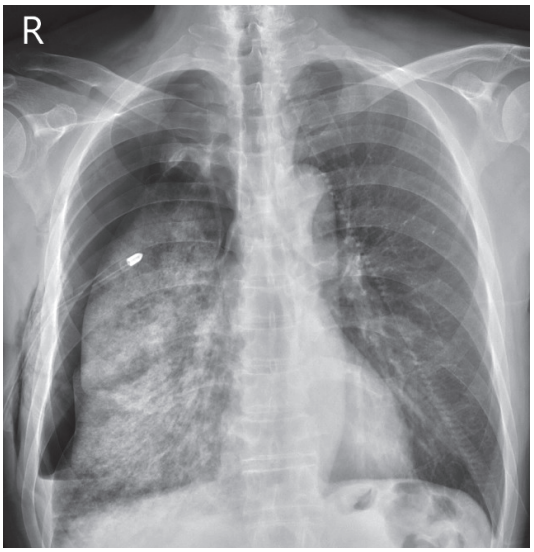

Fig. 3. Diffuse alveolar opacities 12 hours post-chest tube insertion.

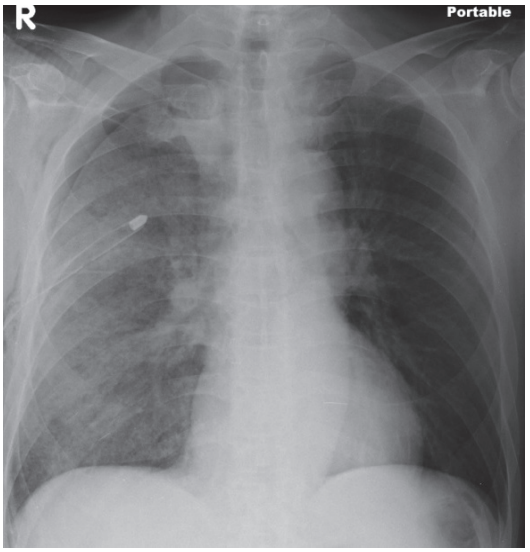

Fig. 4. Pulmonary edema resolved 4 days after aggressive.

patient's recovery was uneventful post-surgery and he was discharged 9 days after admission.

Discussion

Symptomatic RPE is extremely rare and is considered to be an iatrogenic complication with no definite risk factors. Published case reports have suggested that the duration of symptoms, a large size of the pnumothorax, and a rapid rate of reexpansion were significant risk factors [2]. However, a series study by Naohiro Taira *et al*, showed that pleural effusion coincident with pneumothorax was the most significant contributor to the development RPE [3].

For the majority of stable spontaneous pneumothorax cases, the guideline has suggested that a small thoracostomy tube (16-22 Fr) or catheter (14 Fr) would be sufficient to evacuate the air; larger tubes (>24 Fr) are for patients who are unstable or with hemopneumothorax. The size of the tube, however, is believed not to be a factor causing RPE. The negative pressure suction that connects to the chest tube bottle can speed up the drainage process, which would initiate the development of RPE.

According to Mahfood *et al*, 64% of patients experience symptoms within 1 hour of tube insertion, and in all cases, the onset occurred within the next 24 hours [1]. Symptoms included new onset cough, tachycardia, dyspnea and oxygen saturation drop. It is crucial for the physician to recognize the early signs and symptoms of RPE, and identify radiographic changes post-procedure. Treatment for RPE is generally conservative and guided by the severity of the presentation. If the patient experiences hypoxemia, noninvasive ventilation with positive airway pressure can be initiated. This noninvasive mechanical ventilation permits a higher capillary oxygen concentration, increases mean airway pressure, and improves ventilation to collapsed areas of the lung, thereby permitting more complete emptying, which can speed up the recovery process. [5] In severe cases, if the patient develops respiratory distress, intubation for mechanical ventilation will be required.

The exact pathophysiology behind RPE re-

mains unclear. Limited studies have suggested that the disruption of the alveolar-capillary barrier and excessive hydrostatic forces contribute to the development RPE [5]. Lung reexpansion can promote an influx of inflammatory cells into the newly inflated lung, and in these cases, steriod can play a crucial role [7]. High-dose steroid therapy, also known as methyprednisolone pulse therapy (1000 mg/day), administered for 3 days, has been suggested for patients in an unstable condition, or with pleural effusion, followed by thoracentesis [6].

In our case, assuming the patient had been experiencing right lung collapse for a week, the duration and size of the atelectasis itself might indicate a high risk for developing RPE. A 24 French large-bore chest tube provided a rapid rate of reexpansion, which added another risk factor to the condition, and resulted in RPE developing within 20 minutes post-tube thoracostomy. It is crucial to recognize the associated symptoms post-tube thoracostomy and not to add negative pleural suction routinely.

References

1. Mahfood S, Hix WR, Aaron BL, *et al*. Reexpansion pulmonary edema. Ann Thorac Surg 1988; 45: 340-5.
2. Tan HC, Mak KH, Johan A, *et al*. Cardiac output increases prior to development of pulmonary edema after re-expansion of spontaneous pneumothorax. Respir Med 2002; 96: 461-5.
3. Taira N, Kawabata T, Ichi T, *et al*. An analysis of and new risk factors for reexpansion pulmonary edema following spontaneous pneumothorax. J Thorac Dis 2014 Sep; 6(9): 1187-1192.
4. MacDuff A, Arnold A, Harvey J, *et al*. Management of spontaneous pneumothorax: British Thoracic Society Pleural Disease Guideline 2010. Thorax 2010 Aug; 65 Suppl 2: ii18-31.
5. Kotoulas C, Siklis T, Nastoulis C, *et al*. Unilateral reexpansion pulmonary edema: report of a case successfully treated with continuous positive airway pressure. Pneumon 2004; 17(2): 213-6.
6. Walter JM, Matthay MA, Gillespie C, *et al*. Acute hypoxemic respiratory failure after large-volume thoracentesis. Ann Thorac Soc 2016 Mar; 13(3): 438-43.
7. Yoshikawa K, Miyata M, Sueoka N, *et al*. Effective steroid therapy for reexpansion pulmonary edema. JMA J 2019 Mar 4; 2(1): 97-98.

Typical carcinoid Neuroendocrine Tumors of the Lung, a Rare Type of Lung Neoplasm: A Case Report and Literature Review

Yi-Fang Chen[1], Chiao-Hung Wang[1], Hsiu-Ling Cheng[2], Yih-Yiing Wu[3]

Lung neuroendocrine tumors (NETs) are a rare type of tumor that affects the lungs. These tumors tend to occur more frequently in women and in white populations, with incidence rates ranging from 0.2-2 cases per 100,000 people per year. It is important for doctors to distinguish between low-grade (typical and atypical carcinoids) and high-grade (large cell neuroendocrine and small cell carcinoma) NETs in the lung, as the prognosis and treatment for these tumors can differ significantly. We reported the case of a patient who was incidentally found to have a lung nodule that was diagnosed as a lung NET. The patient underwent surgery and had a successful recovery thereafter. ***(Thorac Med 2024; 39: 55-63)***

Key words: lung neuroendocrine tumor, typical lung carcinoid tumor, atypical carcinoid tumor, carcinoid syndrome

Introduction

Neuroendocrine tumors (NETs) of the lung are a rare type of lung neoplasm that is characterized by neuroendocrine differentiation, and typically has a slow-growing clinical course. Like NETs of other organs, pulmonary NETs are derived from neuroendocrine cells that produce peptides and amines, including in the gastrointestinal tract, lung, thymus, and ovaries. Lung NETs are the second most common type of this tumor, and account for about 25% of all NETs. They also make up about 1-2% of all lung cancers [1].

Case Description

A 51-year-old female patient had a history of hyperthyroidism. She received a regular health examination yearly, and was incidentally found to have a nodular lesion of the lung in July 2021. According to her statement, she felt mild shortness of breath while walking upstairs, but otherwise, no other discomfort was noted.

[1]Division of Chest Medicine, Department of Internal Medicine, Taipei City Hospital Renai Branch, Taiwan, [2]Division of Chest Surgery Medicine, Department of Surgery, Taipei City Hospital Renai Branch, [3]Department of Pathology, Taipei City Hospital Renai Branch.
Address reprint requests to: Dr. Yi-Fang Chen, Division of Chest Medicine, Department of Internal Medicine, Taipei City Hospital Renai Branch.

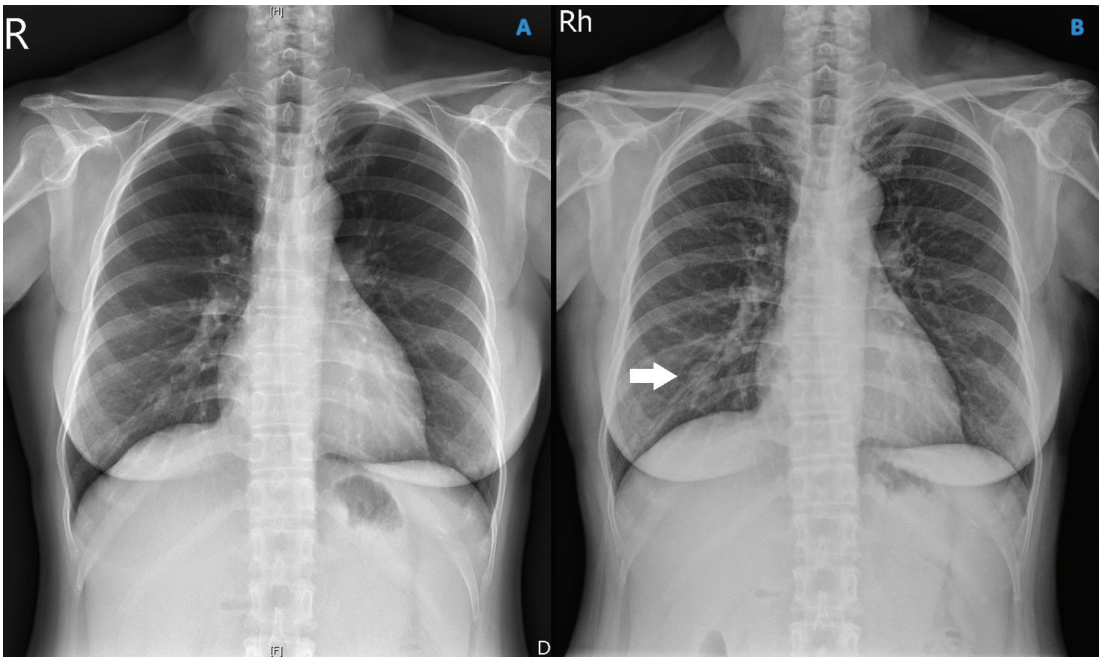

Fig. 1. Patient's chest X-ray. (A). March 2018. (B). August 2021. Compared with the earlier chest X-ray, the more recent chest X-ray shows a nodular opacity at the right lower lung (white arrow).

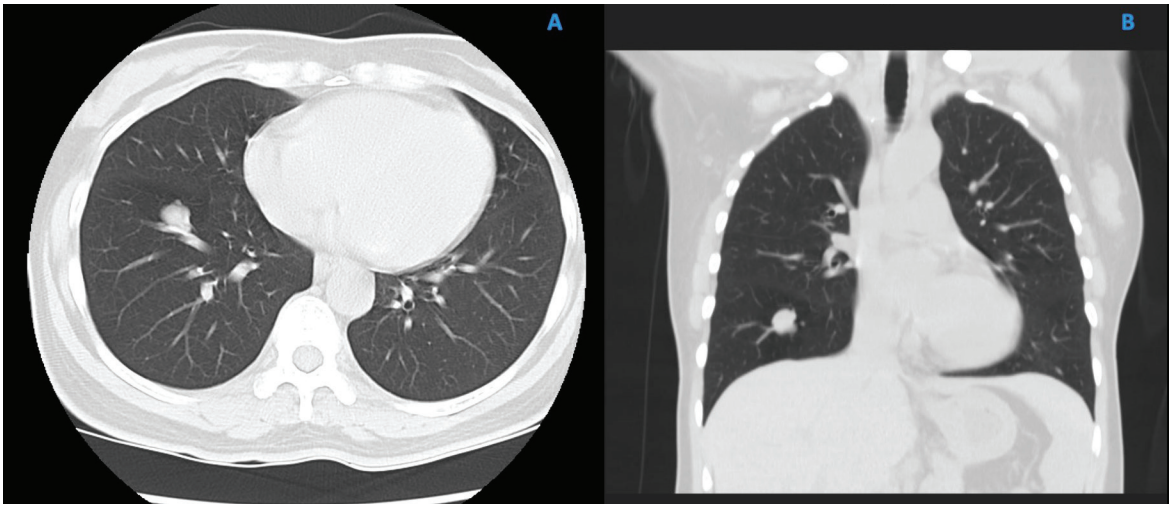

Fig. 2. Patient's chest CT showed a 1.5-cm lobulated nodule in the right lower lobe. (A). Axial view. (B). Coronal view.

She did not smoke, drink alcohol, or have a history of allergies. Thus, she went to our chest clinic for a second opinion in August 2021. Chest X-ray in August 2021 showed a nodular opacity in the right lower lung (Figure 1). Non-contrast medium-enhanced chest CT was arranged, which showed a 1.5-cm lobulated nodule in the right lower lobe (Figure 2).

Laboratory test results of tumor markers, including CEA, CA-153, CA-125, and CA-199, were reviewed, and all were within a normal range. We consulted the chest surgeon for a

surgical evaluation. VATS and RB7 segmentectomy were suggested, and the patient was admitted for surgery in September 2021. An indurated nodule, approximately 2 cm in diameter, was found in the medial basal segment of the right lower lobe. There was no pleural retraction and no lymph node enlargement. Her vital signs were stable after surgery, and her surgical wound showed no signs of infection. The patient then was discharged, and she was regularly followed up at our outpatient department.

The specimen was sent for pathological examination. Grossly, the tumor was relatively well-circumscribed, gray to brown, and solid. Microscopically, it was composed of relatively monotonous hyperchromatic neoplastic cells, growing in acinar and ribbon-like patterns without necrosis (Fig. 3). There were inconspicuous nucleoli and rare mitoses. In the immunohistochemical study, the neoplastic cells were diffusely and strongly positive for CK7, TTF-1, synaptophysin, chromogranin A, and CD56 (Fig. 4). As a result, the specimen was identified as a carcinoid/NET, grade 1.

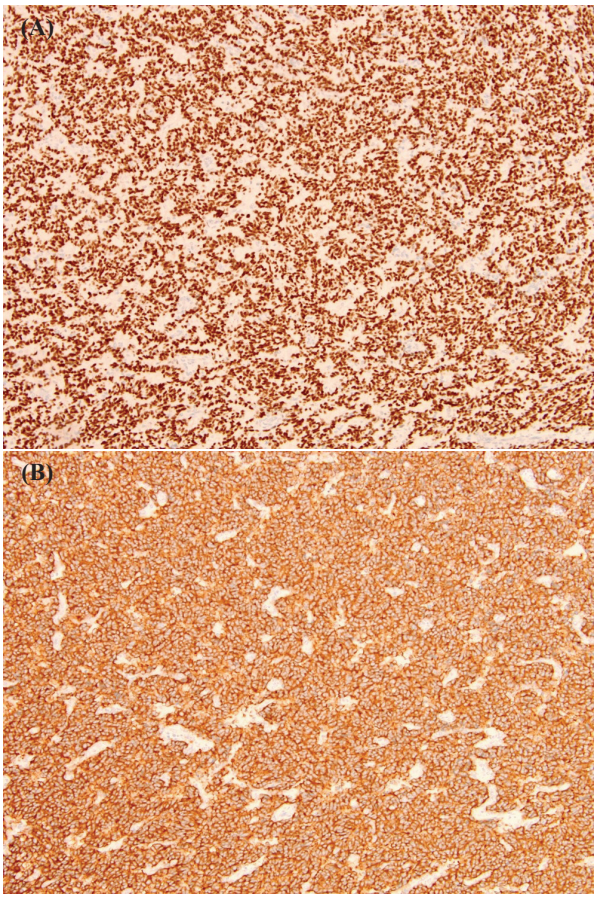

Fig. 3. (A).TTF-1 100x. (B).Synaptophysin 100x. The neoplastic cells showed diffuse and intense immunopositivity for TTF1, with all cells exhibiting brown nuclear staining. They also displayed diffuse and intense synaptophysin immunopositivity, with all cells showing orange membranous staining.

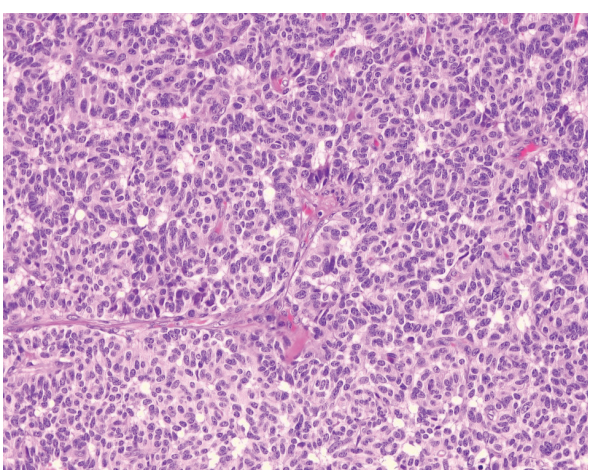

Fig. 3. HE 200x. Relatively monotonous hyperchromatic neoplastic cells arranged in acinar and ribbon-like patterns, with inconspicuous nucleoli, rare mitoses and no necrosis.

After learning that the patient had a typical carcinoid, we conducted a retrospective inquiry to determine if the patient had experienced symptoms associated with carcinoid syndrome, such as flushing and diarrhea. Fortunately, the patient did not exhibit these symptoms.

Surgery was performed for this tumor initially based on the suspicion that it could be lung cancer. Therefore, we opted for an RB7 segmentectomy, which is a standard treatment for typical carcinoid, as well. During the follow-up period, there was no evidence of tumor recurrence.

Discussion

Lung NETs are a rare type of tumor that affects the lungs. These tumors tend to occur more frequently in women and in white populations, with incidence rates ranging from 0.2-2 cases per 100,000 people per year [1]. There have been reports suggesting that the incidence of lung NETs may be increasing, which could be due to the increased use of advanced medical imaging techniques that can detect these tumors earlier. The typical age at diagnosis for an adult with a typical lung NET is 45 years, while those with atypical tumors tend to be around 10 years older [2].

There is some evidence that smoking may be associated with the development of lung NETs, but the relationship is not well understood. Some studies have found that between one-third and two-thirds of patients with lung NETs have been smokers [2]. However, the evidence linking smoking to the development of NETs is not as strong as it is for other types of lung cancer. No other known carcinogens or environmental exposures have been identified as potential risk factors for the development of lung NETs.

Most cases of lung NETs are sporadic, but they can occasionally be seen in people with multiple endocrine neoplasia type 1 (MEN1). There have also been rare instances of families with a history of lung NETs that are not related to the MEN syndrome [2].

According to the 2021 World Health Organization (WHO) classification, lung NETs can range from pre-cancerous conditions such as diffuse idiopathic pulmonary neuroendocrine cell hyperplasia (DIPNECH) to carcinoid tumors and high-grade neuroendocrine carcinomas (NECs) such as small cell and large cell NECs [3] (Table 1).

Grading system

Unlike NETs that occur in the gastrointestinal system, the terms "typical" and "atypical" are still used to describe low-grade versus intermediate-grade tumors in the lung. The grade of these tumors is primarily determined by the mitotic rate (rather than the Ki-67 index) and the presence of necrosis. However, it is more accurate to refer to these tumors as well-differentiated NETs of a low grade (typical carcinoids) and well-differentiated NETs of an intermediate grade (atypical carcinoids) [1, 4].

Table 1. WHO Classification of Lung Neuroendocrine Neoplasms and Some Clinicopathologic Correlates

Variable	Typical carcinoid	Atypical carcinoid	Large cell neuroendocrine carcinoma	Small cell lung carcinoma
Mitoses per 2 mm^2	0-1	2-10	≥ 11	≥ 11
Necrosis	No	Punctate	Extensive	Extensive to geographic
Cytological details	Variable	Variable	Large cells	Small cells
IHC for NE markers	Contributory to diagnosis	Contributory to diagnosis	Defining for diagnosis	Contributory to diagnosis
Combined variants	No	No	Yes	Yes
Paraneoplastic syndrome association	Uncommon	Rare	Rare	Frequent

Acronyms: IHC: immunohistochemical, NE: neuroendocrine

It is important for doctors to distinguish between low-grade (typical and atypical carcinoids) and high-grade (large cell neuroendocrine and small cell carcinomas) NETs in the lung, as the prognosis and treatment for these tumors can differ significantly. Low-grade tumors, including typical carcinoids, have a more benign appearance under the microscope and have fewer than 2 mitoses per 2 mm^2 without necrosis. Atypical carcinoids also have a similar appearance, but have a higher mitotic rate (between 2 and 10 per 2 mm^2) and may have necrosis. These tumors are graded as G1 and G2, respectively. In contrast, high-grade tumors, including large cell NECs and small cell carcinomas, have large cells with a low nucleus-to-cytoplasm ratio and frequent nucleoli, and have a mitotic rate of more than 10 per 2 mm^2 with necrosis. These tumors are graded as G3 [1].

There are several different grades of NETs in the lung, with different prognoses and treatment recommendations. G1 NETs (typical carcinoids) make up 2% of thoracic malignancies, and have a 10%-15% chance of spreading to distant sites. G2 NETs (atypical carcinoids) represent 0.2% of thoracic malignancies, and have a 20% chance of spreading. G3 large cell NETs have an incidence of 3%, while G3 small cell NETs, the most aggressive type, have an incidence of 20% [1].

Clinical features

Lung NETS can be classified as either central or peripheral based on their location in relation to the bronchial tree. Central-type lung NETs can cause symptoms such as coughing, wheezing, hemoptysis (coughing up blood), chest pain, and recurrent pneumonia in the same part of the lung or lobe due to blockage. These tumors may be misdiagnosed as infections, leading to patients receiving multiple courses of antibiotics before the true diagnosis is made. Pulmonary NETs can often be seen on chest X-ray as round or oval-shaped areas of increased density, ranging 2-5 cm in size. These tumors may be accompanied by a mass in the hilum (the area where the bronchus divides into smaller branches) or near the hilum. If the tumor is causing a blockage in the bronchus, the X-ray may show atelectasis and a build-up of mucus in the affected area. Cavitation is uncommon. These tumors may also cause pleural effusions in some cases, particularly if the patient has developed obstructive pneumonia [4-5].

About 25% of pulmonary NETs present as an asymptomatic solitary pulmonary nodule in the periphery of the lung. These tumors are often found incidentally on a routine chest X-ray, usually as a single nodule. They may not cause any symptoms [2].

There are several syndromes that can occur as a result of peptide production by lung NETS, depending on the specific peptide involved and the underlying cause of excessive peptide production. Here are a few examples:

Carcinoid syndrome and carcinoid crisis

Carcinoid syndrome is a condition caused by the release of certain hormones, such as serotonin, from tumors called carcinoid tumors. Symptoms can include flushing of the skin, diarrhea, and difficulty breathing. Long-term effects of high hormone levels can include small vein abnormalities on the skin, heart valve damage, and fibrous tissue buildup in the abdominal area and other parts of the body [6-8].

Lung NETs produce lower levels of serotonin than tumors in the small intestine (midgut NETs), which results in a lower incidence of carcinoid syndrome. The condition is uncom-

mon in patients with localized lung NETs, and is more likely to occur in those with large tumors or liver metastases. Even in patients with advanced disease, the incidence of carcinoid syndrome is low, with studies showing that only 8% of patients with lung NETs have carcinoid syndrome at the time of initial diagnosis, compared to 31% of patients with small bowel NETs. And even within the lung NETs patient population, carcinoid syndrome is relatively less common in the localized stage (8%), but increases to 15% in those with distant metastases [2, 4].

Unlike other NETs, the risk of a severe reaction -- known as a carcinoid crisis -- is very low in lung NETs, and prophylactic treatment is typically not needed. However, healthcare providers should be aware of the potential for a crisis and be prepared to provide treatment if necessary [1, 6-8].

Cushing's syndrome

Approximately 1-2% of lung NETs can cause a condition called Cushing's syndrome, which occurs when the tumor produces ACTH. This is the most common cause of Cushing's syndrome that occurs outside of the pituitary gland. The onset is usually sudden, and it often causes low potassium levels in the blood; it can be confirmed by measuring cortisol and ACTH levels in the blood [2, 4, 9].

Acromegaly

Acromegaly, a condition caused by the production of growth hormone-releasing hormone (GHRH) or insulin-like growth factor 1 (IGF-1) by a tumor, is uncommon in patients with lung NETs, but lung NETs are the most common cause of acromegaly that occurs outside of the pituitary gland [2, 10-12].

Diagnostic approach

Compared to a chest radiograph, CT provides a more detailed and accurate view of the size, location, and spread of lung NETs. CT can also help distinguish tumors from other conditions such as obstructive atelectasis or bronchial obstruction-related mucoid impaction. CT can show if the tumors have lobulated or irregular borders, or punctate or eccentric calcification, and can show if the tumors are intraluminal, extraluminal, or a mixture of both. CT scans can also show marked enhancement due to the vascular nature of the tumors. However, CT may not be highly specific in detecting metastatic lymph nodes, with a positive predictive value of only 20%.

Approximately 80% of low-grade (typical) lung NETs and 60% of intermediate-grade (atypical) lung NETs express somatostatin receptors, which can be imaged using gallium-68 DOTATATE, gallium-68 DOTATOC, or copper-64 DOTATATE positron emission tomography (PET) scans or somatostatin receptor scintigraphies (OctreoScan). These imaging techniques can detect metastatic disease throughout the body and are more sensitive than CT or MRI. However, it is important to note that non-NETs can also express somatostatin receptors, although at lower levels [2, 4].

Serum levels of chromogranin A (CgA) are lower in lung NETs than in NETs in other areas of the body, and they can be similar to levels seen in patients with non-cancerous conditions that are associated with increased CgA levels. Therefore, measuring CgA is not useful for patients with localized tumors, and it is not routinely done. Even in cases of metastatic disease, the usefulness of measuring CgA in addition to radiographic assessments is questionable [2, 4,

5, 13].

For NETs that appear as single lung nodules, a common first diagnostic step is to use CT-guided needle aspiration. The main risk of this approach is pneumothorax. In some cases, if the likelihood of malignancy is high, patients may skip the CT-guided needle aspiration step and proceed directly to surgery [2].

Surgery is the preferred treatment option for lung NETs. The goal is to remove the tumor while preserving as much lung tissue as possible. The type of surgery performed will depend on the size, location, and tissue type of the tumor [1].

For patients with peripheral lung tumors, the recommended surgical approach is complete anatomic resection, such as lobectomy or segmentectomy, and systematic nodal dissection. This should include at least 6 nodes/stations, 3 of which should be in the mediastinum, including the subcarinal station. In patients with limited lung function, a standard segment resection is preferred over a broad wedge resection [2, 4, 5].

For patients with central airway tumors, the preferred surgical approach is lung parenchymal-sparing surgery and systematic nodal dissection. This is because these tumors have a low malignancy and recurrence potential, and are???? almost exclusively typical carcinoid. If possible, bronchial sleeve resection or sleeve lobectomy should be performed instead of pneumonectomy, with intraoperative frozen section of the resection margins. In case of distant pneumonitis and destroyed lung parenchyma, an initial local endobronchial resection to clear the airway may be performed before re-evaluating for lung parenchymal-sparing surgery. Systemic nodal dissection should also be performed, since lymph node metastases may be present in up to 25% of cases of typical carcinoid and in more than 50% of atypical carcinoid cases. If the cancer is not suitable for surgery, local resection such as endobronchial or peripheral ablation techniques may be used for palliative purposes [2, 4-5].

Low-grade lung NETs have a good prognosis when surgically removed, with high 5 and 10-year survival rates. Recurrence rates are low at 3%. The impact of lymph node involvement on the prognosis is not yet clear, but most studies show that it is associated with a worse outcome. The only widely accepted negative prognostic factor is incomplete resection. A nomogram has been developed to predict survival for low-grade lung NETs based on factors such as age, gender, prior malignancy, tumor location, TNM stage, and performance status. In other words, localized low-grade lung NETs have a good prognosis after surgery, but lymph node involvement and incomplete resection may negatively impact outcomes. A nomogram can help predict survival based on various patient and tumor characteristics [4-5, 14-16].

Intermediate-grade (atypical) lung NETs have a worse prognosis than low-grade tumors. The 5-year survival rates range widely, from 30%-95%, and the 10-year survival rates range from 35%-56%. These tumors are more likely to spread (16%-23%) and recur locally (3%-25%). Distant metastases to the liver or bone are more common than local recurrence [5, 15, 17].

Radiation therapy (RT) can provide effective palliation for patients with locally unresectable primary lung NETs, but it is not a curative option. Some experts recommend using chemotherapy plus RT for patients with locally advanced unresectable lung NETs, similar to the treatment for intrathoracic neuroendocrine

small cell lung cancer; however, response rates for this approach are lower than for small cell lung cancer, and its superiority over RT alone remains uncertain. Platinum-based chemotherapy may be most appropriate for patients with histologically aggressive tumors with relatively high proliferative activity. For patients with small, peripheral, low-grade (typical) lung NETs, who are not suitable for surgical resection, stereotactic body radiation may be a reasonable therapeutic option, although there are no clinical series to verify the benefit. In summary, RT can provide effective palliation for locally unresectable primary lung NETs, but the role of chemotherapy and other treatments such as stereotactic body radiation is not yet clear and more data is needed [13, 15, 18].

For patients with a lung NET that cannot be surgically removed and who have carcinoid syndrome, we recommend using a medication known as a somatostatin analog (SSA), such as octreotide or lanreotide. These medications bind to receptors on tumor cells and are very effective at reducing the release of bioactive amines. They are also highly effective at improving flushing and diarrhea symptoms in over 80% of patients with carcinoid syndrome [1-2, 4-5].

For those patients with slowly progressive, metastatic, somatostatin-receptor-positive lung NETs, it is suggested to start treatment with an SSA, as these have been shown to inhibit tumor growth in patients with advanced gastrointestinal NETs. However, there have not been any randomized studies of SSAs versus placebo specifically in lung NETs, and 2 phase III trials involving gastrointestinal NETs excluded patients with lung NETs [1-2, 5].

Systemic therapy is appropriate for patients with progressive, disseminated, or SSA-refractory NETs. The therapeutic options include everolimus, cytotoxic chemotherapy, or peptide receptor radioligand therapy using the radiolabeled SSA (177Lu-dotatate), where available, for patients with somatostatin-receptor-positive tumors [1-2, 4-5].

Everolimus is a recommended treatment for progressive metastatic lung NETs, especially for those that do not show positive results on somatostatin receptor-based imaging. Everolimus may also be used in combination with SSA therapy as a second-line option for slowly progressive lung NETs after SSA alone has failed, particularly in patients with carcinoid syndrome. This information is based on data from the RADIANT 4 trial [1-2, 4-5, 19].

For patients with rapidly progressive or treatment-resistant NETs of the lung, cytotoxic chemotherapy may be recommended as a treatment option. Regimens such as cisplatin or carboplatin-based chemotherapy are used for highly aggressive tumors, and temozolomide-based chemotherapy is used for tumors with more indolent growth. However, the evidence supporting the use of these drugs in this setting is limited. Participation in clinical trials for new treatments is encouraged [1-2, 5].

In conclusion, it is important to distinguish the grade of lung NETs. The prognosis and treatment recommendations for NETs in the lung vary depending on the grade of the tumor.

References

1. Melosky B. Advanced typical and atypical carcinoid tumours of the lung: management recommendations. Curr Oncol 2018 Jun; 25(S1): S86-S93.
2. Caplin ME, E. Baudin E, P. Ferolla P, *et al*. Pulmonary neuroendocrine (carcinoid) tumors: European Neuroendocrine Tumor Society expert consensus and recommendations for best practice for typical and atypical pulmonary carcinoids. Ann Oncol 2015; 26(8):

1604-1620.

3. Nicholson AG, Tsao MS, Beasley MB, *et al*. The 2021 WHO Classification of Lung Tumors: impact of advances since 2015. J Thorac Oncol 2022; 17(3): 362-387.
4. Randhawa S, Trikalinos N, Patterson GA. Neuroendocrine tumors of the lung. Thorac Surg Clin 2021 Nov; 31(4): 469-476.
5. Prinzi N, Rossi RE, Proto C, *et al*. Recent advances in the management of typical and atypical lung carcinoids. Clin Lung Cancer 2021 May; 22(3): 161-169.
6. Clement D, Ramage J, Srirajaskanthan R. Update on pathophysiology, treatment, and complications of carcinoid syndrome. J Oncol 2020 Jan 21; 2020: 8341426.
7. Bardasi C, Benatti S, Luppi G, *et al*. Carcinoid crisis: a misunderstood and unrecognized oncological emergency. Cancers (Basel) 2022 Jan 28; 14(3): 662.
8. Fischer S, Kruger M, McRae K, *et al*. Giant bronchial carcinoid tumors: a multidisciplinary approach. Ann Thorac Surg 2001 Jan; 71(1): 386-93.
9. Jones JE, Shane SR, Gilbert E, *et al*. Cushing's syndrome induced by the ectopic production of ACTH by a bronchial carcinoid. J Clin Endocrinol Metab 1969 Jan; 29(1): 1-5.
10. Phillips JD, Yeldandi A, Blum M, *et al*. Bronchial carcinoid secreting insulin-like growth factor-1 with acromegalic features. Ann Thorac Surg 2009 Oct; 88(4): 1350-2.
11. Filosso PL, Donati G, Rena O, *et al*. Acromegaly as manifestation of a bronchial carcinoid tumour. Asian Cardiovasc Thorac Ann 2003 Jun; 11(2): 189.
12. Bhansali A, Rana SS, Bhattacharya S, *et al*. Acromegaly: a rare manifestation of bronchial carcinoid. Asian Cardiovasc Thorac Ann 2002 Sep; 10(3): 273-4.
13. Divisi D, Crisci R. Carcinoid tumors of the lung and multimodal therapy. Thorac Cardiovasc Surg 2005 Jun; 53(3): 168-72.
14. Ferguson MK, Landreneau RJ, Hazelrigg SR, *et al*. Long-term outcome after resection for bronchial carcinoid tumors. Eur J Cardiothorac Surg 2000 Aug; 18(2): 156-61.
15. Filosso PL, Oliaro A, Ruffini E, *et al*. Outcome and prognostic factors in bronchial carcinoids: a single-center experience. J Thorac Oncol 2013 Oct; 8(10): 1282-8.
16. Fink G, Krelbaum T, Yellin A, *et al*. Pulmonary carcinoid: presentation, diagnosis, and outcome in 142 cases in Israel and review of 640 cases from the literature. Chest 2001 Jun; 119(6): 1647-51.
17. Harpole DH Jr, Feldman JM, Buchanan S, *et al*. Bronchial carcinoid tumors: a retrospective analysis of 126 patients. Ann Thorac Surg 1992 Jul; 54(1): 50-5.
18. Mackley HB, Videtic GM. Primary carcinoid tumors of the lung: a role for radiotherapy. Oncology (Williston Park) 2006 Nov; 20(12): 1537-49.
19. Yao JC, Fazio N, Singh S, *et al*. Everolimus for the treatment of advanced, non-functional neuroendocrine tumours of the lung or gastrointestinal tract (RADIANT-4): a randomised, placebo-controlled, phase 3 study. Lancet 2016 Mar 5; 387(10022): 968-977.

Treatment Experience with Inhaled Amikacin in Mycobacterium Abscessus-Pulmonary Disease: A Case Report

Yen-Jung Li[1], Sheng-Wei Pan[2,3]

Mycobacterium abscessus is one of the major etiologic pathogens causing nontuberculous mycobacterial pulmonary disease in susceptible patients. We reported a 57-year-old woman with connective tissue disease, structural lung disease, and *M. abscessus*-pulmonary disease. After 1 month of initial macrolide-based combination antibiotic therapy, the patient started inhaled amikacin (parenteral formulation) during the continuous phase of treatment and maintained sputum culture conversion. Without any complications, she was able to tolerate 12 months of inhaled amikacin and had a successful treatment outcome for *M. abscessus*-pulmonary disease. In addition to presenting the case, we reviewed the efficacy and potential side effects of using inhaled amikacin for the treatment of *M. abscessus*-pulmonary disease. ***(Thorac Med 2024; 39: 64-71)***

Key words: *Mycobacterium abscessus*-pulmonary disease; nontuberculous mycobacteria (NTM)-pulmonary disease; inhaled amikacin

Introduction

Nontuberculous mycobacteria pulmonary disease (NTM-PD) is increasing in prevalence worldwide, particularly in those with specific host factors [1-5]. In Taiwan, NTM-PD is most commonly caused by Mycobacterium avium complex (MAC), Mycobacterium abscessus (Mabs), and Mycobacterium kansasii, with variations in distribution based on geographic location [6]. Compared to MAC- or M. kansasii-PD, the treatment outcome of Mabs-PD is relatively poor. Treating patients with Mabs-PD can be challenging due to bacteria's constitutional and inducible resistance to macrolide, and the requirement of combined and prolonged antibiotic therapy, including amikacin injection in the initial months. Of note, even with the initial use of amikacin injection and a continuous macrolide-based multidrug regimen for Mabs-PD treatment [6, 7], only 40% of patients achieve microbiologic cure [8-10].

[1]Department of Chest Medicine, Taipei Veterans General Hospital, Taipei, Taiwan, [2]School of Medicine, College of Medicine, National Yang Ming Chiao Tung University, Taipei, Taiwan, [3]Division of Pulmonary Immunology & Infectious Diseases, Department of Chest Medicine, Taipei Veterans General Hospital, Taipei, Taiwan
Address reprint requests to: Dr. Sheng-Wei Pan, Division of Pulmonary Immunology & Infectious Diseases, Department of Chest Medicine, Taipei Veterans General Hospital, No. 201, Section 2, Shi-Pai Road, Taipei 112, Taiwan.

To improve treatment response, the 2 latest NTM-PD guidelines, published in 2017 and in late 2020, both suggest adding inhaled amikacin in the continuous phase of treatment for Mabs-PD [6, 7]. However, the effectiveness and potential side effects of this treatment for Mabs-PD are not yet well understood. Although amikacin liposome inhalation suspension (ALIS) is FDA-approved for inhalation therapy in the US, it is currently indicated only for patients with refractory MAC-PD, and not for those with Mabs-PD [11]. Inhaled amikacin through nebulization of the parenteral formulation is recommended for Mabs-PD and is available in Taiwan and in most other countries. Here, to share our treatment experience using inhaled amikacin, we present the case of a patient with Mabs-PD who received inhaled amikacin, and review the current evidence on the efficacy and safety of inhaled amikacin for the treatment of Mabs-PD.

Case Report

A 57-year-old woman had a medical history of Sjogren syndrome, bronchiectasis and emphysema (Figure 1A and 2A). She had experienced chronic dyspnea for years, and it had worsened during the 3 weeks before admission in early 2020. She eventually presented to the emergency department with drowsiness, and was intubated and placed on mechanical ventilation due to hypercapnic respiratory failure. In addition, she developed right-side pneumothorax and received tube thoracotomy upon admission. The chest plain film and chest computed tomography (CT) scan showed bilateral bronchiectasis, fibrotic and emphysematous changes in both lungs, and left lower lobe (LLL) consolidations. The consolidation had progressed, compared to the 2016 chest CT, which showed LLL nodular opacities (Figure 1B and 2B).

After receiving intensive care, the patient

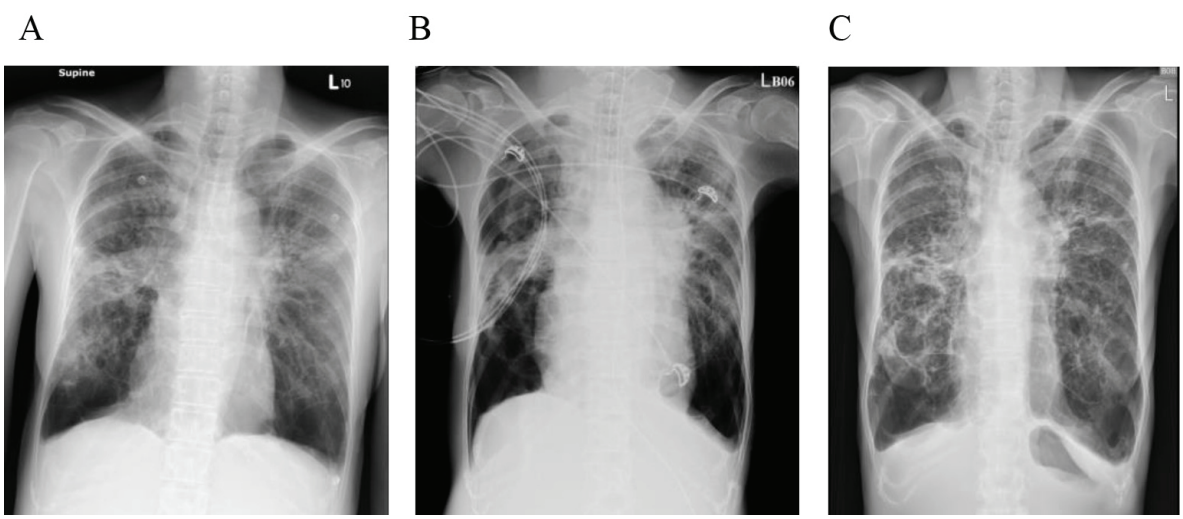

Fig. 1. Serial Chest Plain Film from 2016 to 2022. A. Chest plain film from 2016 revealed bilateral upper lung and right middle lobe (RML) fibrotic changes with bronchiectasis and bilateral lower lung emphysematous changes. B. Chest plain film in 2020 revealed right-side pneumothorax and an endotracheal tube in situ. Bronchiectasis, and fibrotic and emphysematous changes were observed in bilateral lung fields. Consolidations in bilateral upper lung fields, and the RML and left lower lobe (LLL) showed progression. C. Chest plain film in 2022 revealed that the fibrotic changes and bronchiectasis in the bilateral upper lung fields had remained stable, whereas the consolidation had resolved.

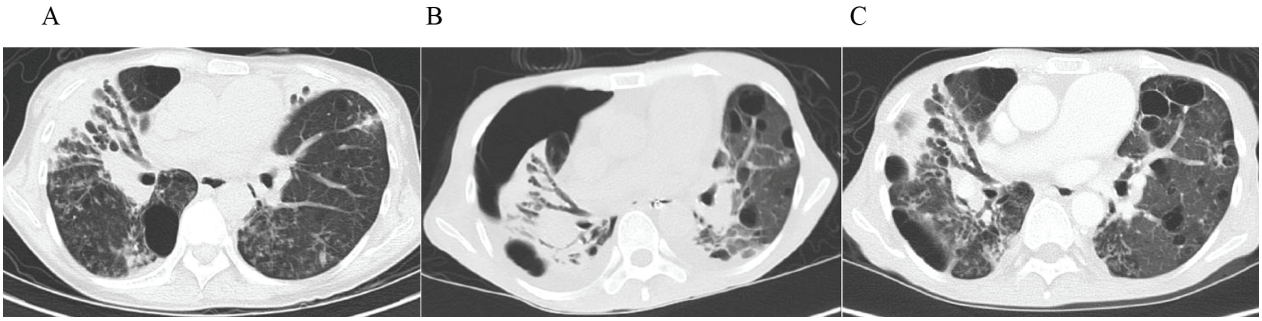

Fig. 2. Serial Chest Computed Tomography (CT) from 2016 to 2022 A. Chest CT from 2016 revealed bronchiectasis at the bilateral lung fields and nodular opacities at the left lower lobe (LLL).B. Chest CT in 2020 revealed right-side pneumothorax, a collapsed right lung and LLL consolidation. C. Chest CT in 2022 showed improvement in the LLL nodular and consolidative opacities.

was successfully weaned off the ventilator on hospital day 6. A series of microbiologic surveys found that her sputum was positive for acid-fast bacilli, and Mabs was isolated in 4 sets of sputum mycobacterial cultures between hospital days 1 and 29. The microbiologic findings fulfilled the diagnostic criteria for NTM-PD, although subspecies identification and drug susceptibility testing were not available at this hospital. Due to the worsening of the patient's clinical symptoms and radiographic findings, treatment for Mabs-PD was commenced on hospital day 30, after providing a detailed explanation of the treatment course, potential benefits, and risks to the patient.

During the initial phase, the patient was given combination therapy consisting of intravenous (IV) cefoxitin, IV amikacin, and oral azithromycin, in accordance with the guidelines. No significant adverse events were observed with this treatment regimen. After 1 month of receiving IV cefoxitin and amikacin, the patient began receiving the continuous phase of NTM treatment. Thus, in addition to a device for home oxygen therapy, a jet nebulizer was prepared for inhaled amikacin delivery. Then, the patient was started on a continuous phase regimen consisting of oral azithromycin, moxifloxacin, and inhaled amikacin (parenteral formulation, 500 mg, once daily, with the addition of normal saline, 2 mL) upon discharge on day 60, based on the 2017 BTS guideline [7].

During the outpatient follow-up, the patient continued with her oral regimen and inhaled amikacin. Her sputum amount decreased and her shortness of breath improved. Sputum culture for mycobacteria was performed regularly every 2 to 3 months. Sputum conversion was achieved uneventfully 1½ months after discharge, and the continuous phase of NTM treatment was continued for another year after sputum conversion. Throughout the treatment course, in both inpatient service and outpatient clinic settings, the patient was closely monitored for potential side effects, such as renal injury, arrhythmia, and ototoxicity. Baseline assessment revealed no evidence of hearing impairment, and audiometry was performed after the initial phase of treatment. Electrocardiograms were performed monthly for the first 6 months of treatment, and then the follow-up interval for the second half of the year was extended to3 to 4 months. QTc prolongation was observed during treatment, and as a result, moxifloxacin was replaced with minocycline for weeks. The patient tolerated the other oral

medication and inhaled amikacin well, without obvious gastrointestinal upset or upper respiratory tract discomfort. Furthermore, there were no symptoms of sore throat, hoarseness, cough, tinnitus, or hearing loss during the period of amikacin inhalation therapy.

After completing the NTM treatment course, follow-up chest plain film and chest CT scans showed regression of the nodular opacities and consolidation at the LLL, and the bronchiectasis, and fibrotic and emphysematous changes at the bilateral lung fields showed no interval change in 2022 (Figure 1C and 2C). The patient remained sputum culture-negative for NTM 1½ years after completing treatment for Mabs-PD.

Discussion

NTM are generally free-living organisms in our environment, in the soil, dust and water. To date, almost 200 species of NTM have been identified, including pathogenic species [12-13]. Among NTM-related human diseases, NTM-PD is the most common clinical manifestation. Host factors for NTM-PD, including structural lung disease (e.g., bronchiectasis, chronic obstructive pulmonary disease, and cystic fibrosis), thoracic skeletal abnormalities, neoplasms, rheumatoid arthritis, and the use of steroid or immunomodulatory drugs, are all significant contributors to the development of NTM-PD [2]. Our patient, who had both autoimmune disease (Sjogren syndrome) and structural lung disease (emphysema), was at high risk of developing NTM-PD.

Indeed, with the advances in microbiologic techniques and the increase in health awareness, there has been a steady rise in the numbers of reported cases of NTM-PD and of identified NTM species. Various studies have reported on the increase in the incidence and prevalence of NTM-PD worldwide, and in Taiwan [2, 3, 14, 15]. The hospital-based incidence of NTM-PD in Taiwan has shown a significant increase, from 1.26 to 7.94 per 100,000 patients, from 2000 to 2008 [15]. Between 2010 and 2014, the average incidence rate was 46.0 episodes per 100,000 hospital-based patient-years [14].

According to 2007 ATS/IDSA guidelines [12], the diagnostic criteria for NTM-PD comprise both clinical and microbiologic factors. The clinical criteria include compatible radiographic findings and pulmonary symptoms with appropriate exclusion of other diagnoses. The typical radiographic features include nodular or cavitary opacities on chest radiograph or a high-resolution CT scan that shows multifocal bronchiectasis with multiple small nodules. In some studies, patchy, poorly defined consolidations are also reported as compatible findings for NTM-PD [16-17].

The pulmonary symptoms are variable and nonspecific, and include chronic or recurrent cough, sputum production, fatigue, malaise, dyspnea, fever, hemoptysis, chest pain, and weight loss.

The microbiologic criteria should include 1) positive culture results from at least 2 separate expectorated sputum samples, 2) positive culture results from at least 1 bronchial wash or lavage, or 3) transbronchial or other lung biopsy with mycobacterial histopathologic features and positive culture for NTM.

Our symptomatic patient fulfilled the diagnostic criteria for NTM-PD because of her multifocal bronchiectasis with consolidative patches and expectorated sputum samples that were culture-positive for Mabs.

Mabs is a rapidly growing mycobacteria

(RGM) that exhibits a high degree of genotypic heterogeneity among its subspecies, M. abscessus, M. bolletii and M. massiliense, which lead to different treatment responses [13]. In Taiwan, Mabs is the second most common NTM species causing NTM-PD, and it is more prevalent than MAC as a pathogen in southern Taiwan [14]. Notably, the specific mutations in the drug-resistant gene in the subspecies of Mabs can lead to bacterial constitutional and inducible resistance to macrolide, which is the backbone regimen for Mabs-PD [18, [18]. As a result of multiple drug resistance, treatment success rates have been unsatisfactory, at around 30% for M. abscessus and 50% for M. massiliense [8-10].

According to the 2020 ATS/ERS/ESCMID/IDSA guideline, a macrolide and amikacin-based multidrug regimen was suggested in the initial and continuous phases of Mabs-PD treatment, based on its macrolide susceptibility pattern (mutational or inducible resistance). The initial phase is defined as the time that parenteral agents are given, and the continuous phase is defined as the subsequent phase of therapy that includes oral and/or inhaled agents.

The following is the regimen from the 2020 ATS guideline. The initial phase of treatment for Mabs-PD without mutational or inducible resistance (typically M. massiliense) should contain at least 3 active drugs with a macrolide-containing multidrug regimen, including 1-2 kinds of parenteral drugs, amikacin, imipenem or cefoxitin, tigecycline, and 2 kinds of oral drugs, azithromycin, or clarithromycin, clofazimine, linezolid. For those with inducible or mutational macrolide resistance, at least 4 active drugs are suggested in the initial phase as a multi-drug regimen, including 2-3 kinds of parenteral drugs and 2-3 kinds of oral drugs. Macrolide is not counted as an active drug in this situation but can serve as an immunomodulator [6]. For the continuation phase, 2-3 kinds of active drugs are suggested for use, including inhaled amikacin and oral azithromycin, clofazimine, and linezolid. Moreover, the 2017 BTS guideline suggests moxifloxacin, minocycline, and co-trimoxazole as alternative options for treatment during the continuation phase. The recommended dose of inhaled amikacin (parenteral formulation), according to the guideline, is 250-500 mg per day [7].

The reported therapeutic options for refractory Mabs-PD include azithromycin, clarithromycin, moxifloxacin, doxycycline, meropenem, doripenem, linezolid, tigecycline and inhaled amikacin [19, 20]. However, the standardized regimen and duration of salvage therapy for refractory Mabs-PD are not yet established.

Our patient with Mabs-PD received amikacin inhalation therapy with nebulization of the parenteral formulation, but not ALIS. ALIS has been approved by U.S. Food and Drug Administration for refractory MAC-PD treatment since 2018, but the only available form of amikacin that can be inhaled in Taiwan is the parenteral formulation. Emerging evidence for the inhaled parenteral formulation of amikacin for refractory NTM-PD has been reported in recent years. Several case series in HIV-negative patients with refractory NTM-PD, more than half of which had Mabs-PD, showed that additional inhaled amikacin correlated with clinical response [21], culture conversion (40%), and symptoms improvement (45%) [19]. In a cohort study of 77 patients with refractory NTM-PD, 62% of whom had Mabs-PD, the patients received inhaled amikacin (initially treated with 250 mg daily, uptitrated to 500 mg twice weekly to once daily) over a median duration 12 months (IQR 6.8-12 months); 49% of

them experienced symptomatic improvement, but only 18% achieved sputum conversion [22]. Although the case numbers were relatively small and the dose, duration, efficacy and safety of inhaled amikacin were heterogeneous across different studies, inhaled amikacin showed positive treatment responses in cases with refractory NTM-PD.

Inhaled amikacin in the continuation treatment phase for patients with Mabs-PD, but not in cases with a refractory response, is recommended as part of a multidrug regimen for primary therapy in Mabs-PD, according to guidelines since 2017 [6-7]. A prospective observational cohort study enrolled 82 treatment-naïve patients with Mabs-PD. They received guideline-based treatment during the initial phase with IV amikacin, IV imipenem or cefoxitin, and oral azithromycin for 2 to 4 weeks. Continuation phase treatment included azithromycin, inhaled amikacin (500 mg/mL, once daily, 3 times weekly), and/or clofazimine, and/or oral linezolid. Specifically, 56% of the patients had M. massiliense-PD and 44% had M. abscessus-PD. Finally, 96% of patients with M. massiliense-PD, and only 33% of patients with M. abscessus-PD, achieved sputum culture conversion ($p<0.001$). Patients with M. massiliense-PD also showed greater improvements in symptoms, radiology, and sputum culture conversion, compared to those with M. abscessus-PD. However, 23% of patients with Mabs-PD experienced adverse effects from inhaled amikacin, primarily ototoxicity. Overall, this cohort study suggests that a multidrug regimen containing inhaled amikacin in the continuous phase can result in favorable outcomes and tolerable adverse effects, particularly in patients with M. massiliense-PD. For those with M. abscessus-PD, more effective therapeutic options are needed [23].

Various nebulizing mechanisms are capable of transforming bulk liquids into droplets. Jet nebulizers, which compress gas to generate droplets, are inexpensive and simple devices. However, they are not portable and have a large residual volume of medication. Ultrasonic nebulizers aerosolize suspension by acoustic wave, but the substantial heat might degrade proteins or heat-sensitive materials. Mesh nebulizers, which force liquid to flow through small apertures of a plate or membrane, are efficient, portable and with minimal residual volume. Smart nebulizers utilize the aforementioned nebulizing techniques to generate aerosols, while also analyzing the patient's breathing cycle. This enables them to deliver droplets during inhalation, thereby reducing drug loss [24, 25]. Our patient was administered amikacin inhalation therapy through a jet nebulizer due to its accessibility and cost-effectiveness.

Subspecies identification data for Mabs and drug resistance results for our patient were not available. However, the patient exhibited a favorable treatment response, as evidenced by improved symptoms and sputum conversion, since she continued azithromycin-based combination therapy, in accordance with the 2017 BTS guideline, and used inhaled amikacin in the continuation phase for 1 year. If refractory Mabs-PD had developed, linezolid and clofazimine were agents that could be considered for salvage treatment. Fortunately, our patient tolerated the treatment well and did not experience any significant adverse effects associated with inhaled amikacin therapy. The occurrence of adverse effects of inhaled amikacin have been reported as 8% to 38% in various case series. These side effects may include hoarseness, throat irritation, bitter taste, oral thrush, tinnitus,

vertigo, ototoxicity, and nephrotoxicity. Ototoxicity is the most common side effect, often leading to the discontinuation or dose reduction of inhaled amikacin [19, 21-23]. Nevertheless, inhaled amikacin appears to be generally well-tolerated, but the adverse effects should be regularly monitored.

Our patient with Mabs-PD had a positive treatment response with the use of an inhaled parenteral formulation of amikacin during the continuous phase. A guideline-based regimen that includes inhaled amikacin improves treatment outcomes in patients with Mabs-PD.

Conclusion

Mabs is a common pathogen that causes NTM-PD. Recent guidelines recommend a multidrug treatment approach that includes oral macrolides and inhaled amikacin after IV amikacin for Mabs-PD. Inhaled amikacin appears to be an effective treatment for Mabs-PD, particularly for patients with M. massiliense-PD. Although generally safe and well-tolerated, monitoring for any adverse effects of inhaled amikacin is still necessary.

References

1. Chan ED, Iseman MD. Underlying host risk factors for nontuberculous mycobacterial lung disease. Seminars in respiratory and critical care medicine. 2013;34(1): 110-123.
2. Prevots DR, Marras TK. Epidemiology of human pulmonary infection with nontuberculous mycobacteria: a review. Clinics in chest medicine. 2015;36(1): 13-34.
3. Lee MR, Chang LY, Ko JC, *et al*. Nontuberculous mycobacterial lung disease epidemiology in Taiwan: A systematic review. J Formos Med Assoc. 2020;119 Suppl 1: S4-S12.
4. Honda JR, Knight V, Chan ED. Pathogenesis and risk factors for nontuberculous mycobacterial lung disease. Clinics in chest medicine. 2015;36(1): 1-11.
5. Feng JY, Chen WC, Chen YY, *et al*. Clinical relevance and diagnosis of nontuberculous mycobacterial pulmonary disease in populations at risk. J Formos Med Assoc. 2020;119 Suppl 1: S23-S31.
6. Daley CL, Iaccarino JM, Lange C, *et al*. Treatment of Nontuberculous Mycobacterial Pulmonary Disease: An Official ATS/ERS/ESCMID/IDSA Clinical Practice Guideline. Clin Infect Dis. 2020;71(4): e1-e36.
7. Haworth CS, Banks J, Capstick T, *et al*. British Thoracic Society Guideline for the management of non-tuberculous mycobacterial pulmonary disease (NTM-PD). BMJ Open Respir Res. 2017;4(1): e000242.
8. Kwak N, Dalcolmo MP, Daley CL, *et al*. Mycobacterium abscessus pulmonary disease: individual patient data meta-analysis. 2019;54(1): 1801991.
9. Pasipanodya JG, Ogbonna D, Ferro BE, *et al*. Systematic Review and Meta-analyses of the Effect of Chemotherapy on Pulmonary Mycobacterium abscessus Outcomes and Disease Recurrence. Antimicrobial agents and chemotherapy. 2017; 61(11).
10. Diel R, Ringshausen F, Richter E, *et al*. Microbiological and Clinical Outcomes of Treating Non-Mycobacterium Avium Complex Nontuberculous Mycobacterial Pulmonary Disease: A Systematic Review and Meta-Analysis. Chest. 2017;152(1): 120-142.
11. Kurz SG, Zha BS, Herman DD, *et al*. Summary for Clinicians: 2020 Clinical Practice Guideline Summary for the Treatment of Nontuberculous Mycobacterial Pulmonary Disease. Ann Am Thorac Soc. 2020;17(9): 1033-1039.
12. Griffith DE, Aksamit T, Brown-Elliott BA, *et al*. An official ATS/IDSA statement: diagnosis, treatment, and prevention of nontuberculous mycobacterial diseases. Am J Respir Crit Care Med. 2007;175(4): 367-416.
13. Johansen MD, Herrmann JL, Kremer L. Non-tuberculous mycobacteria and the rise of Mycobacterium abscessus. Nat Rev Microbiol. 2020;18(7): 392-407.
14. Huang HL, Cheng MH, Lu PL, *et al*. Epidemiology and Predictors of NTM Pulmonary Infection in Taiwan - a Retrospective, Five-Year Multicenter Study. Scientific reports. 2017;7(1): 16300.
15. Lai CC, Tan CK, Chou CH, *et al*. Increasing incidence of nontuberculous mycobacteria, Taiwan, 2000-2008. Emerg

Infect Dis. 2010;16(2):294-296.
16. Koh WJ, Kwon OJ, Jeon K, *et al*. Clinical significance of nontuberculous mycobacteria isolated from respiratory specimens in Korea. Chest. 2006;129(2): 341-348.
17. Shu CC, Lee CH, Wang JY, *et al*. Nontuberculous mycobacteria pulmonary infection in medical intensive care unit: the incidence, patient characteristics, and clinical significance. Intensive Care Med. 2008;34(12): 2194-2201.
18. Nash KA, Brown-Elliott BA, Wallace RJ, Jr. A novel gene, erm(41), confers inducible macrolide resistance to clinical isolates of Mycobacterium abscessus but is absent from Mycobacterium chelonae. Antimicrobial agents and chemotherapy. 2009;53(4): 1367-1376.
19. Olivier KN, Shaw PA, Glaser TS, *et al*. Inhaled amikacin for treatment of refractory pulmonary nontuberculous mycobacterial disease. Ann Am Thorac Soc. 2014;11(1): 30-35.
20. Yagi K, Ishii M, Namkoong H, *et al*. The efficacy, safety, and feasibility of inhaled amikacin for the treatment of difficult-to-treat non-tuberculous mycobacterial lung diseases. BMC Infect Dis. 2017;17(1): 558.
21. Safdar A. Aerosolized amikacin in patients with difficult-to-treat pulmonary nontuberculous mycobacteriosis. Eur J Clin Microbiol Infect Dis. 2012;31(8): 1883-1887.
22. Jhun BW, Yang B, Moon SM, *et al*. Amikacin Inhalation as Salvage Therapy for Refractory Nontuberculous Mycobacterial Lung Disease. Antimicrobial agents and chemotherapy. 2018; 62(7).
23. Kang N, Jeon K, Kim H, *et al*. Outcomes of Inhaled Amikacin-Containing Multidrug Regimens for Mycobacterium abscessus Pulmonary Disease. Chest. 2021;160(2): 436-445.
24. Carvalho TC, McConville JT. The function and performance of aqueous aerosol devices for inhalation therapy. J Pharm Pharmacol. 2016;68(5): 556-578.
25. Ari A, Fink JB. Recent advances in aerosol devices for the delivery of inhaled medications. Expert opinion on drug delivery. 2020;17(2): 133-144.

Klebsiella Pneumoniae Invasive Liver Abscess Syndrome with Metastatic Septic Embolism in a Patient with Newly Diagnosed Diabetes: A Case Report

Jung-Fu Tzeng[1], Jiunn-Min Shieh[1], Shyh-Ren Chiang[1]

Klebsiella pneumoniae can produce a variety of infectious disease and is also the most common cause of septic emboli. *K. pneumoniae* invasive liver abscess syndrome (KPIS), characterized by primary liver abscess associated with metastatic infections, including metastatic septic emboli, is a life-threatening condition without appropriate management. We reported a young male patient with KPIS, whose symptoms and chest plain films mimicked pneumonia initially. The diagnosis of diabetes was established during this hospitalization. Liver abscess and thrombosis of the right common femoral vein were found. *K pneumoniae* was isolated from the liver abscess. The clinical manifestations, radiologic features, and management were reviewed. ***(Thorac Med 2024; 39: 72-77)***

Key words: *Klebsiella pneumoniae* invasive liver abscess syndrome (KPIS), septic emboli, diabetes mellitus

Introduction

Klebsiella pneumoniae can produce a variety of infectious diseases. It is also associated with a community-acquired primary invasive liver abscess syndrome, and complicated metastatic infections. *K. pneumoniae* invasive liver abscess syndrome (KPIS) with metastatic septic embolism could flare abruptly and become life-threatening. We report a patient with KPIS; the clinical manifestations, risk factors and management were reviewed.

Case Report

A 36-year-old Taiwanese male was admitted to the Emergency Department of Chimei Medical Center with the chief complaint of fever, dry cough, and general weakness for 1 week, followed by progressive shortness of breath for 1 day. He had a past medical history of right femoral head avascular necrosis, and a history of smoking 1 pack of cigarettes per day for 10 years. He denied recent travelling, tick bites, contact with ill persons, drug use, or diarrhea.

[1]Departments of Internal Medicine, Chi Mei Medical Center, Tainan City, Taiwan
Address reprint requests to: Dr. Shyh-Ren Chiang, Department of Internal Medicine, Chi Mei Medical Center, 901, Chung-Hwa Road, Yung-Kang City, Tainan City, Taiwan.

On admission, his initial vital signs included a body temperature of 38.5°C, heart rate of 92 beats/min, blood pressure of 136/76 mmHg, respiratory rate of 20 breaths/min, and an oxygen saturation of 96% on 3 L/min oxygen. His sclera were anicteric and there were bilateral crackles in the lungs, but there was no audible murmur on cardiac auscultation. His abdominal and neurologic examinations revealed nothing unusual, and no skin rash was observed.

A complete blood count test showed a white blood cell count of 21,300/uL, with an elevated neutrophil ratio of 90.9%. Blood biochemical test results were as follows: aspartate aminotransferase: 16 IU/L; alanine aminotransferase: 67 IU/L; total bilirubin: 0.39 mg/dL; creatinine: 0.63 mg/dL, glucose: 261 mg/dL, with a hemoglobin A1c (HbA1c) test result of 12.6%. The chest X-ray showed multiple consolidations in bilateral lower lung fields (Figure 1). Two sets of peripheral blood cultures were obtained, and moxifloxacin was prescribed. This patient was admitted to the ward with the diagnosis of bilateral pneumonia, and a new diagnosis of diabetes mellitus (DM).

On the 2nd day after admission, the patient continued to have high fever, up to 38°C, and chills. Due to the persistent fever, an abdominal sonogram study was done that revealed a single abscess in the right lobe of the liver (68.2 mm x 41.3 mm x 46.6 mm) (Figure 2). The patient was diagnosed with primary liver abscess. He was immediately treated with sonogram-guided percutaneous drainage of the liver abscess (pigtail catheter, 8 French), which drained 120 mL of yellow pus over the first 24 h. The liver pus was submitted for Gram stain and both aerobic and anaerobic culture. Antibiotic therapy was shifted to ceftriaxone for the suspected invasive liver abscess syndrome.

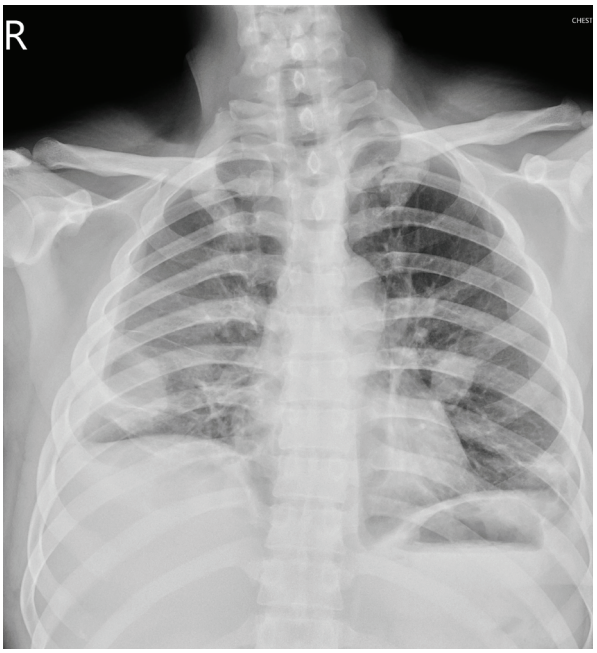

Fig. 1. Chest X-ray showed bilateral consolidations and right pleural effusion.

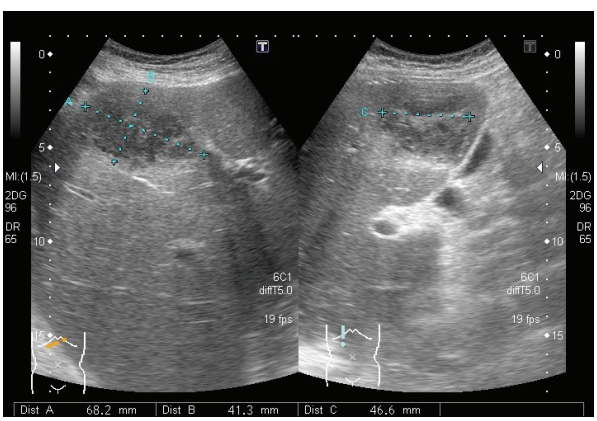

Fig. 2. Abdominal sonography with a positive finding of abscess formation (68.2 mm x 41.3 mm x 46.6 mm) at the left liver lobe.

On the 3rd day of admission, severe pain and swelling of the right lower limb were noted, and therefore, an extremities sonogram was done, which showed partial thrombosis of the right common femoral vein, and complete thrombosis of the right superficial femoral vein to the popliteal vein (Figure 3). Pulmonary embolism could not be excluded, so, for further imaging examination, chest computed tomog-

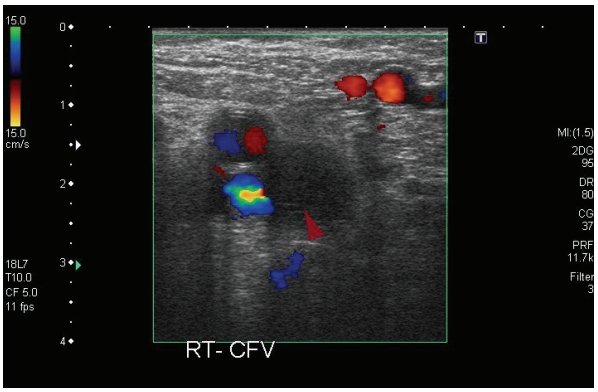

Fig. 3. Partial thrombosis (red arrowhead) of the common femoral vein seen under extremity sonography.

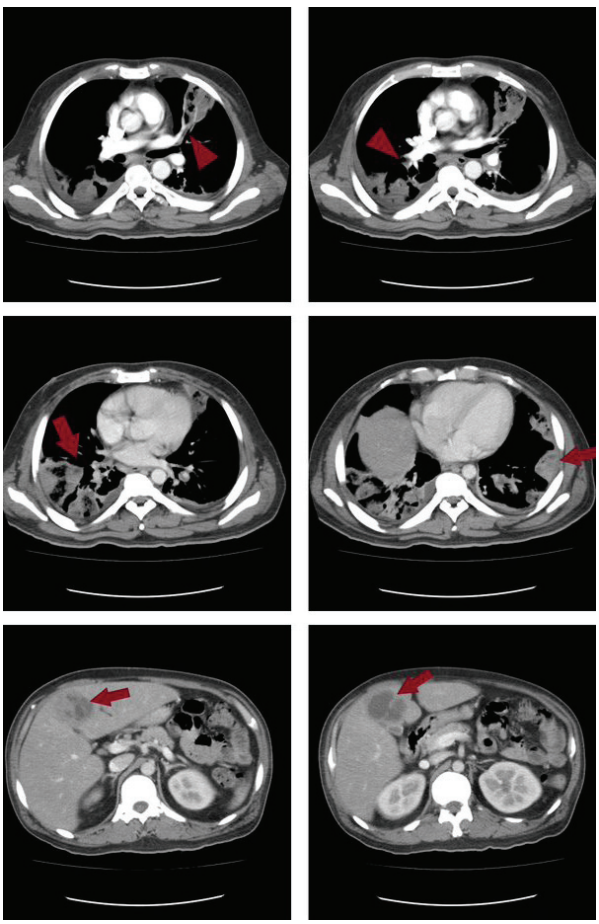

Fig. 4. Chest computed tomography shows bilateral septic emboli (red arrowhead) with abscess formation (red arrow) and a left liver abscess (red arrow).

raphy (CT) was performed, which discovered bilateral septic emboli with abscess formations and a left liver abscess (Figure 4). Low molecular weight heparin was added for deep vein thrombosis.

K. pneumoniae were isolated from blood, sputum and liver pus samples subsequently. The isolates were susceptible to broad-spectrum antibiotics such as cephalosporin, ampicillin-sulbactam, levofloxacin, aminoglycosides, and meropenem, but resistant to ampicillin. The follow-up white blood cell count showed 21,300/uL, and treatment was shifted to ceftazidime, based on the antibiotic susceptibility test. After these treatments, his fever subsided, and the follow-up imaging examinations showed improvement of the lung and liver abscesses (Figure 5). Even though negative conversion was detected on blood culture 10 days after initiating antimicrobial treatment, the total intravenous antibiotics duration was maintained for 4 weeks. Rivaroxaban, vildagliptin, and metformin were used for deep vein thrombosis and DM treatment, and education on diabetic control was also arranged. After the patient's condition had stabilized, the pigtail tube was removed, and cefuroxime was maintained for the entire antibiotics course. The patient was then discharged with outpatient department follow-up.

Discussion

This patient was a young male who had no known systemic disease other than alcohol abuse, who presented to our hospital with fever, dry cough, general weakness, and progressive shortness of breath. He later underwent chest CT, abdominal sonography and lower extremity sonography. Pulmonary emboli with lung abscess of bilateral lung fields were found. Liver

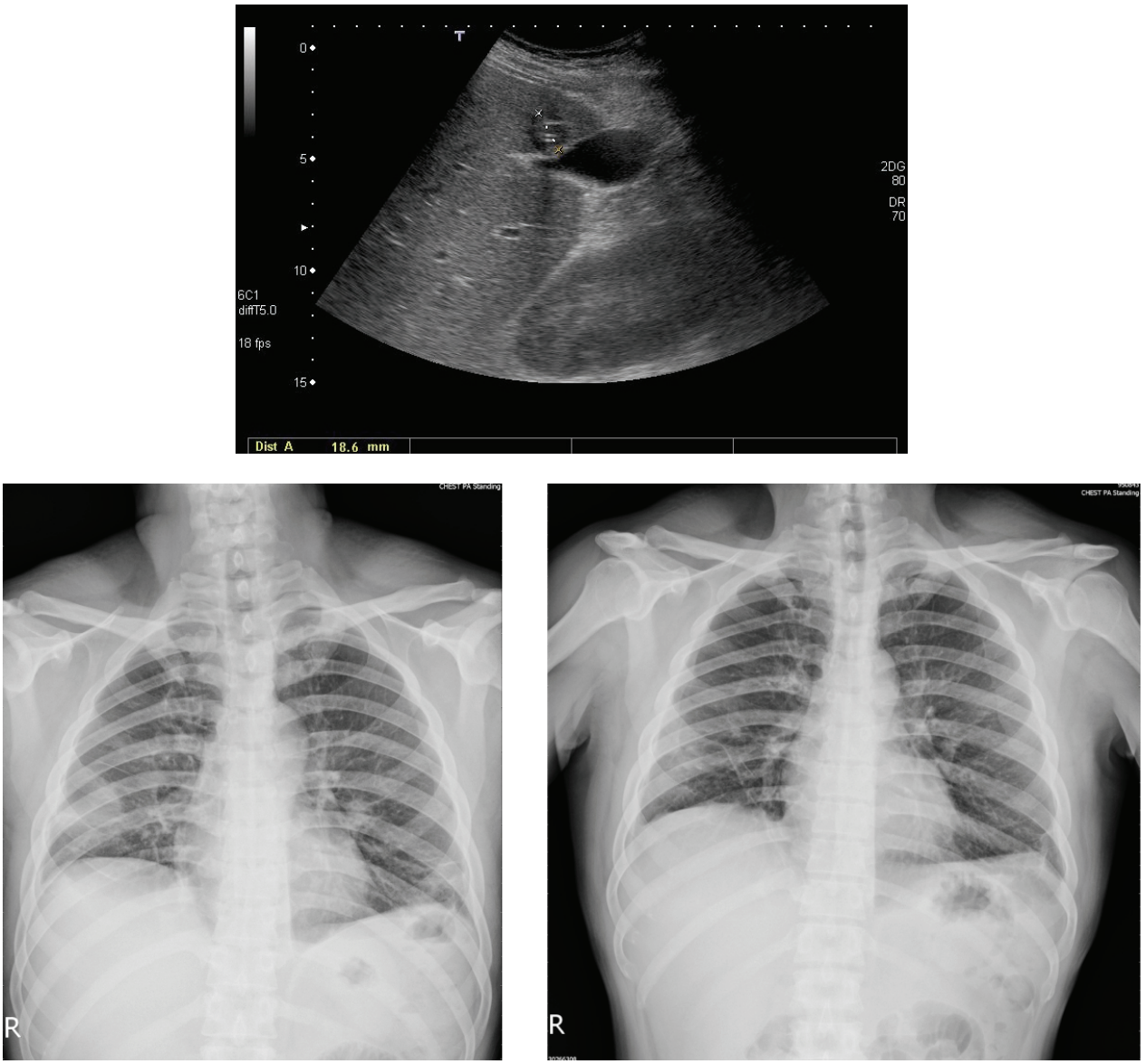

Fig. 5. Abdominal sonography 1 month after pigtail drainage (upper column), which showed decreased diameter of the abscess (18.6 mm), and chest plain film 1 month (lower left column) and 2 months (lower right column) after initiating antimicrobial treatment.

abscess and partial thrombosis of the right common femoral vein were also found. DM was diagnosed during this hospitalization, and *K. pneumoniae* was isolated from blood, sputum, and liver pus. *K. pneumoniae* invasive syndrome was suspected. The patient received liver abscess drainage with pigtail, and antimicrobial treatment with ceftazidime. He recovered smoothly and was discharged with outpatient department follow-up for diabetes control.

K pneumoniae is the most common cause of septic emboli, and typically originates from liver abscess [1]. KPIS, characterized by primary liver abscess associated with metastatic infections, is a life-threatening condition without appropriate management [2].

Several medical risks, such as DM, alcoholism, malignancy, chronic obstructive pulmonary disease, and glucocorticoid therapy, characterized by impaired host defenses, can prime a patient for KPIS. Among these risks, DM, especially poorly controlled diabetes, is very common [3, 4]. Diagnosis of KPIS may often be delayed, due to a lack of clinical suspicion when there are only lung consolidations mimicking pneumonia. The clinical manifestations of lung infections in KPIS, including fever, dry cough, and general weakness, were nearly nonspecific [5, 6].

Since the medical records, past history, and initial chest X-ray films of this patient had no hints of septic emboli, the KPIS diagnosis was confirmed after isolating K pneumoniae from blood cultures, followed by abdominal sonogram. Therefore, it is important to clarify the origin of fever in K pneumoniae infections. The prevalence of septic emboli might be underestimated, since the clinical manifestations were nonspecific in most cases [1, 7].

Without a prior medical history of DM for this patient, a new diagnosis of uncontrolled DM was established based on his blood HbA1C of 12.6%. Of note, diabetic patients with a high HbA1C concentration (> 9.0%) have an association with metastatic complications that are associated with KPIS [8].

There was clinical relevance between the uncontrolled diabetes, liver abscess, and K pneumoniae bacteremia in this patient [3]. Another point worth mentioning is the alcohol abuse history of the patient, which also worked as a predisposing factor for the formation of liver abscess [9]. Third-generation cephalosporins are the main choice of antibiotics, and drainage of the liver abscess has played an important role in the treatment of these patients [5, 6, 10, 11]. Thus, the use of appropriate antibiotics based on the results of culture, drainage of the liver abscess, surveying of the possibility of extrapulmonary septic emboli, and combining lifestyle and pharmaceutical education are needed to achieve good clinical outcomes [5, 6, 9, 10]. It is noteworthy that some strains of 'hypervirulent' K pneumoniae liver abscess may be associated with high mortality relative to multidrug-resistant and classical Klebsiella infections [12]. When dealing with KPIS, early diagnosis, detection of risk factors, and appropriate management are points worthy of our attention.

To summarize, KPIS is a rare but severe condition, the incidence of which might be underestimated, since the clinical presentations currently reported show no specific characteristics, such as fever, dry cough, general weakness, or focal infiltrates mimicking nodules or pneumonia on chest plain film [5, 6, 10]. Clinicians should be alert for any risk factor such as uncontrolled diabetes, chronic liver disease, alcoholism, malignancy, chronic obstructive pulmonary disease, or being on glucocorticoid therapy. Among these conditions, uncontrolled diabetes is a strong predisposing factor for hepatic venous thrombophlebitis and metastatic infection [8]. Early recognition of the disease, with early intervention with antimicrobial therapy and liver abscess drainage, could lead to satisfactory outcomes [5-6].

Conclusion

KPIS is a life-threatening syndrome, originating from pyogenic liver abscess. Severe complications may reveal disseminated septic emboli in the hosts. Among the predisposing factors, uncontrolled diabetes and chronic liver disease are the main concerns. Early diagnosis,

initiation of appropriate antibiotics and abscess drainage should be implemented promptly for better outcomes.

References

1. Chou DW, Wu SL, Chung KM, *et al*. Septic pulmonary embolism requiring critical care: clinicoradiological spectrum, causative pathogens and outcomes. Clinics (Sao Paulo) 2016; 71(10): 562-569.
2. Evangelista V, Gonçalves CV, Almeida R, *et al*. Klebsiella pneumoniae invasive syndrome. Eur J Case Rep Intern Med 2018; 5(3): 000800.
3. Lin YT, Wang FD, Wu PF, *et al*. Klebsiella pneumoniae liver abscess in diabetic patients: association of glycemic control with the clinical characteristics. BMC Infect Dis 2013; 13: 56.
4. Thomsen RW, Jepsen P, Sørensen HT. Diabetes mellitus and pyogenic liver abscess: risk and prognosis. Clin Infect Dis 2007; 44(9): 1194-201.
5. Ye R, Zhao L, Wang C, *et al*. Clinical characteristics of septic pulmonary embolism in adults: a systematic review. Respir Med 2014; 108(1): 1-8.
6. Tian LT, Yao K, Zhang XY, *et al*. Liver abscesses in adult patients with and without diabetes mellitus: an analysis of the clinical characteristics, features of the causative pathogens, outcomes and predictors of fatality: a report based on a large population, retrospective study in China. Clin Microbiol Infect 2012; 18(9): E314-30.
7. Stawicki SP, Firstenberg MS, Lyaker MR, *et al*. Septic embolism in the intensive care unit. Int J Crit Illn Inj Sci 2013; 3(1): 58-63.
8. Wang HH, Tsai SH, Yu CY, *et al*. The association of haemoglobin A_1C levels with the clinical and CT characteristics of Klebsiella pneumoniae liver abscesses in patients with diabetes mellitus. Eur Radiol. 2014; 24(5): 980-9.
9. Raja CS, Karthick P. Role of alcoholism in liver abscess. Int J Res Med Sci 2017; 2(4): 1313-1319.
10. Chou DW, Wu SL, Chung KM, et al. Septic pulmonary embolism caused by a Klebsiella pneumoniae liver abscess: clinical characteristics, imaging findings, and clinical courses. Clinics (Sao Paulo) 2015; 70(6): 400-7.
11. Jun JB. Klebsiella pneumoniae liver abscess. Infect Chemother 2018; 50(3): 210-218.
11. Jun JB. Klebsiella pneumoniae liver abscess. Infect Chemother 2018; 50(3): 210-218.
12. Parrott AM, Shi J, Aaron J, *et al*. Detection of multiple hypervirulent *Klebsiella pneumoniae* strains in a New York City hospital through screening of virulence genes. Clin Microbiol Infect 2021; 27(4): 583-589.

Diagnosis of Pulmonary Sequestration in Adult Patient Using 3D- Image Vascular Reconstruction: A Case Report and Literature Review

Felisbela Gomes[1], Shih-Lung Cheng[1,2], Cheng-Hung How[3]

We reported the case of a 51-year-old male who had suffered from chronic cough for decades. He was a non-smoker and lived independently in his daily life. He was prescribed antitussive agents for years to treat the chronic cough. This time, he experienced fever and productive cough with purulent sputum, and then visited the outpatient department. A retrocardiac mass-like lesion was noted on chest radiograph. Computed tomography (CT) angiography revealed an aberrant systemic artery from the descending thoracic aorta toward the basal segment of the left lower lung lobe, with increased attenuation of the corresponding territory, and compression of the segmental bronchioles by the engorged vasculature. CT angiography 3D–image vascular reconstruction disclosed an accessory artery rising from the descending thoracic aorta, and then dividing toward the left lower lung lobe. Intra-lobar pulmonary sequestration was diagnosed. Then, video-assisted thoracoscopic left lower lobe lobectomy was performed. The pathology of the specimen was compatible with pulmonary sequestration.

3D–image vascular reconstruction is non-invasive. The image study showed the anomalous feeding artery and the draining vein, which helped reach the diagnosis of pulmonary sequestration. In addition, the image was useful in surgical planning. ***(Thorac Med 2024; 39: 78-83)***

Key words: pulmonary sequestration, 3D-image vascular reconstruction, computed tomography angiography, video-assisted thoracoscopic lobectomy

Introduction

Pulmonary sequestration refers to a non-functioning portion of lung tissue that has no communication with the normal bronchial tree, and receives a blood supply from an anomalous systemic artery, most commonly directly from the thoracic aorta. Pryce DM, in 1946, introduced the term “sequestration” for this condition, which was derived from the Latin verb sequestare, meaning ‘to separate” [1]. Pulmonary sequestration is divided into 2 types: intralobar

[1]Department of Internal Medicine, Far Eastern Memorial Hospital, [2]Department of Chemical Engineering and Materials Science, Yuan-Ze University, [3]Division of Thoracic Surgery, Department of Surgery, Far Eastern Memorial Hospital

Address reprint requests to: Dr. Shih-Lung Cheng, Department of Internal Medicine, Far Eastern Memorial Hospital, Taipei, Taiwan.

and extralobar. Intralobar pulmonary sequestration is located within a normal lung lobe, and does not have its own visceral pleura. Extralobar pulmonary sequestration is located outside the normal lung lobe, and has its own visceral pleura. Lung sequestration is commonly diagnosed in children, but rarely in adults, and comprised 0.15-6.4% of all congenital pulmonary malformations, 60% of which were diagnosed within the first decade of life [2].

The clinical presentations of lung sequestration depend on type, size and location. Most affected patients are asymptomatic. However, if the patients are symptomatic, the most common presentations are respiratory distress and recurrent respiratory infection in early life. Infection is less common with extralobar pulmonary sequestration [3].

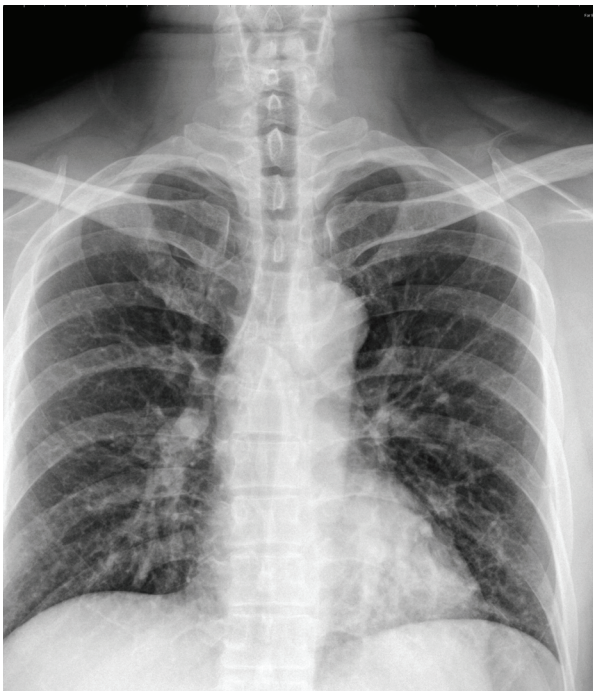

Fig. 1. Chest radiograph revealed abnormal and irregular density at the retrocardiac region, and indicated that a mass lesion should be ruled out.

Case Presentation

A 51-year-old male, a non-smoker, lived at home and was totally independent. He experienced chronic cough for decades and was prescribed antitussive agents for years. Then, beginning on December 1, 2022, he began suffering from productive cough with purulent sputum for 2 weeks. Fever up to 38.2 degrees Celsius was also noted. He visited the outpatient department on December 20, 2022. A retrocardiac mass-like lesion was noted on the chest radiograph (Fig. 1). The patient was concerned about the use of a contrast medium, so low-dose computed tomography (CT) was performed on December 28, 2022. The CT image revealed a lobulated mass lesion, near the thoracic aorta, lying in the left lower lung lobe, and an abnormal cluster of bronchovascular bundles in the lung window.

He was then admitted for further examination on December 29, 2022. Identification of the details of the anatomy with the great vessels was necessary. CT angiography revealed an aberrant systemic artery from the descending thoracic aorta toward the basal segment of the left lower lung lobe with increased attenuation of the corresponding territory, and compression of the segmental bronchioles by the engorged vasculature. Pulmonary sequestration was suspected (Fig. 2). We also arranged CT angiography 3D–image vascular reconstruction to confirm and disclose an accessory artery rising from the descending thoracic aorta, and then dividing toward the left lower lung lobe, favoring the diagnosis of an intralobar sequestration type (Fig. 3AB). Therefore, the patient underwent video-assisted thoracoscopic left lower lobe lobectomy on December 3, 2022. During the surgery, a left lower lung lobe sequestration with a feeding vessel directly from the thoracic

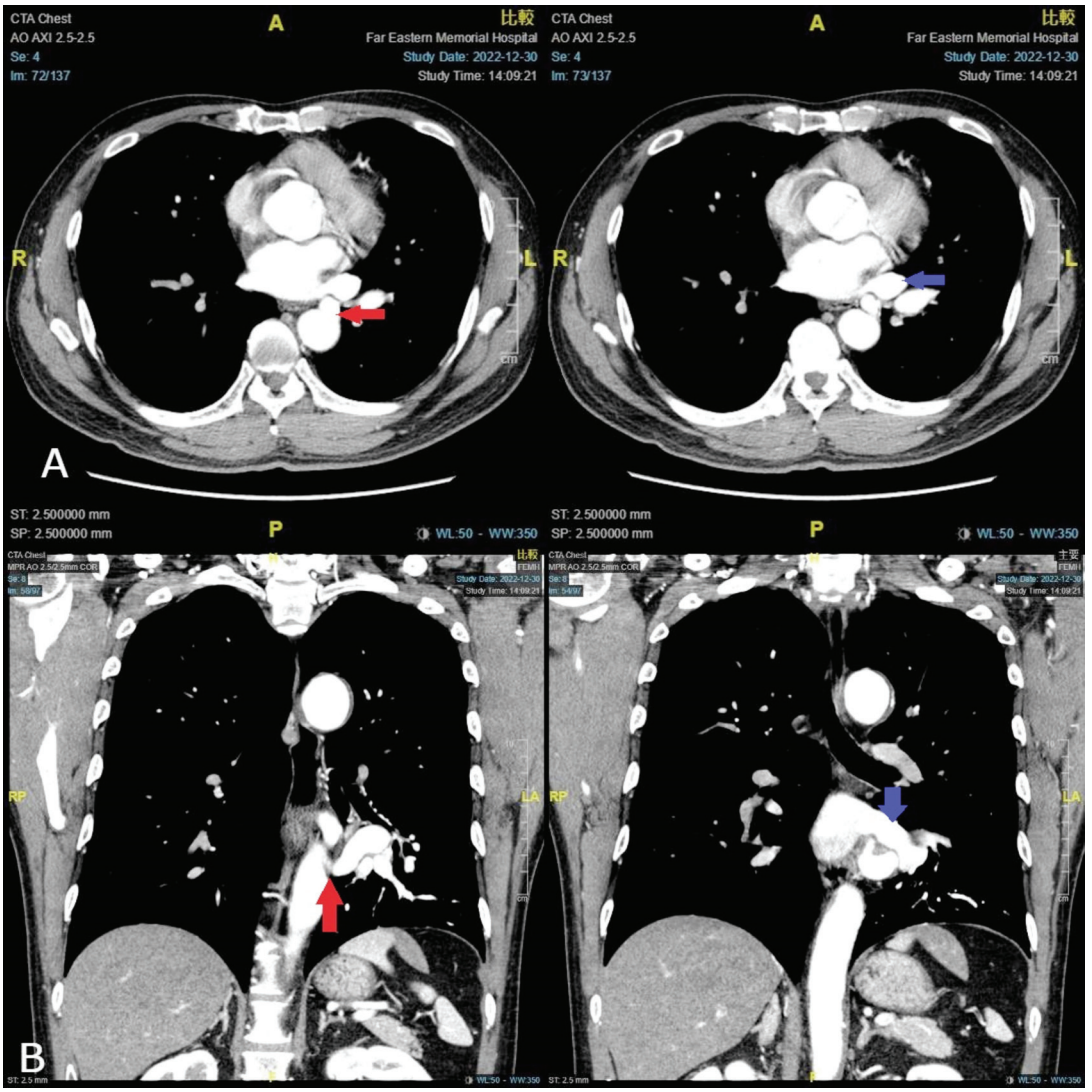

Fig. 2. 2A (sagittal) and 2B (coronal): Computed tomography angiography showed an abnormal artery (red arrow) rising from the thoracic descending aorta, that directly drained back to the left atrium, with a lack of connection to the pulmonary circulation.

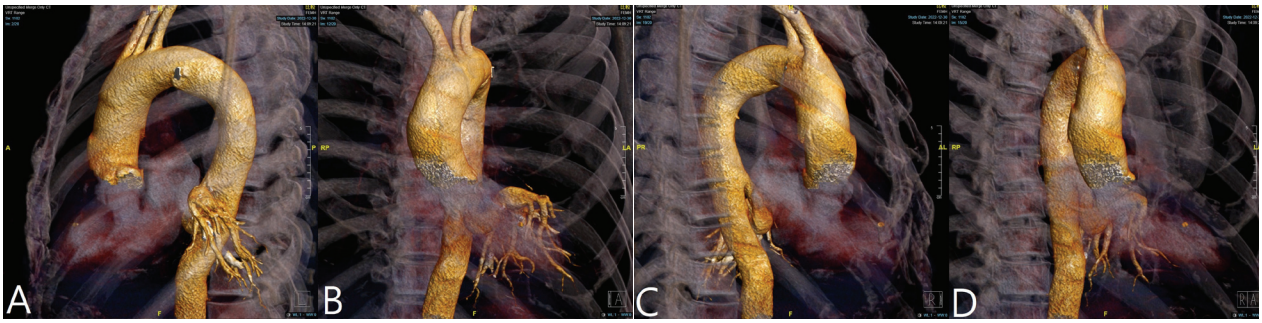

Fig. 3. Computed tomography angiography 3D–image vascular reconstruction showed an accessory artery rising from the descending thoracic aorta and then dividing toward the left lower lung lobe. Is there some description for the A,B,C, and D images?????

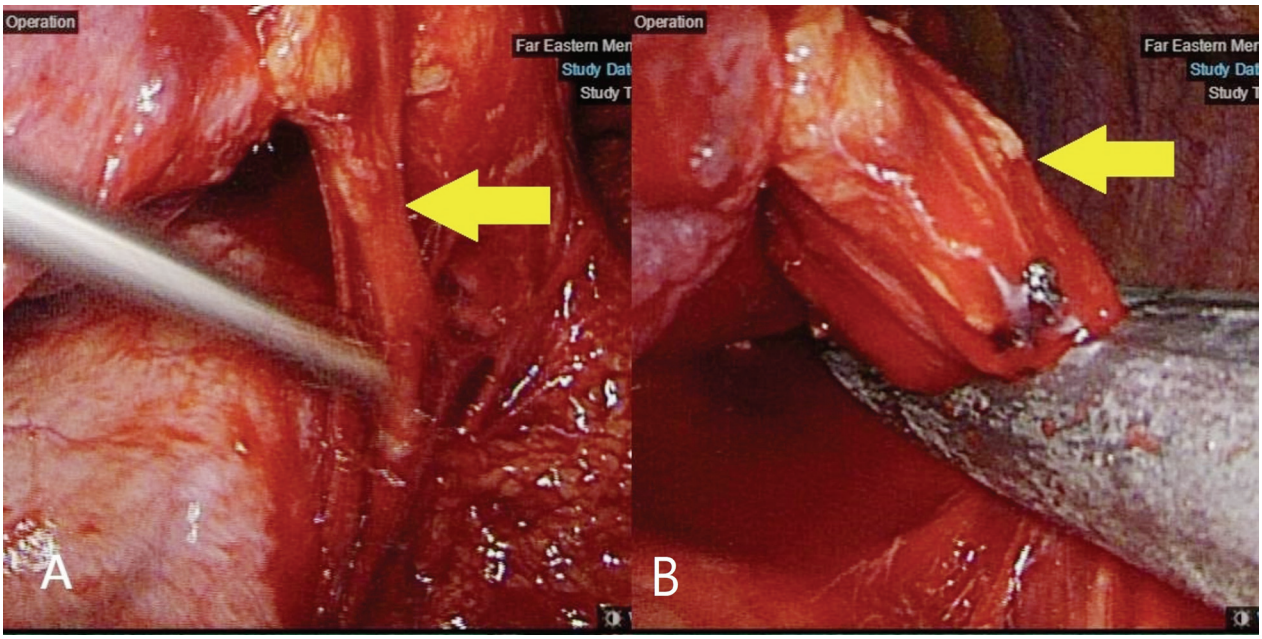

Fig. 4. (A), (B): The feeding artery that came from the aorta was identified and ligated.

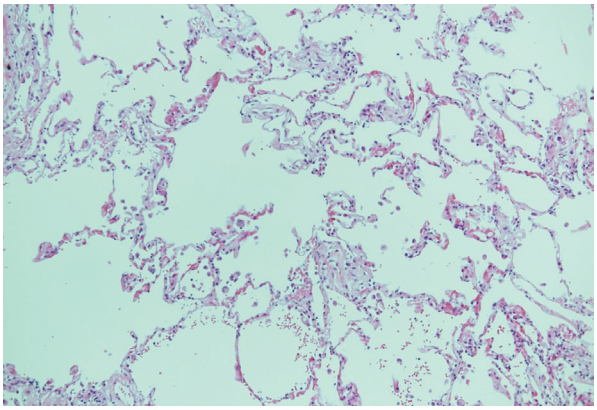

Fig. 5. Pathology showed part of the parenchymal maldevelopment, which was compatible with pulmonary sequestration.

descending aorta, without connection to the bronchial tree, was noted, and resection was performed smoothly (Fig. 4). The pathology of the specimen was shown as a part of parenchymal maldevelopment, which is compatible with pulmonary sequestration (Fig. 5).

A follow-up chest radiograph (Fig. 6) showed post-operation change without significant complications. He recovered smoothly

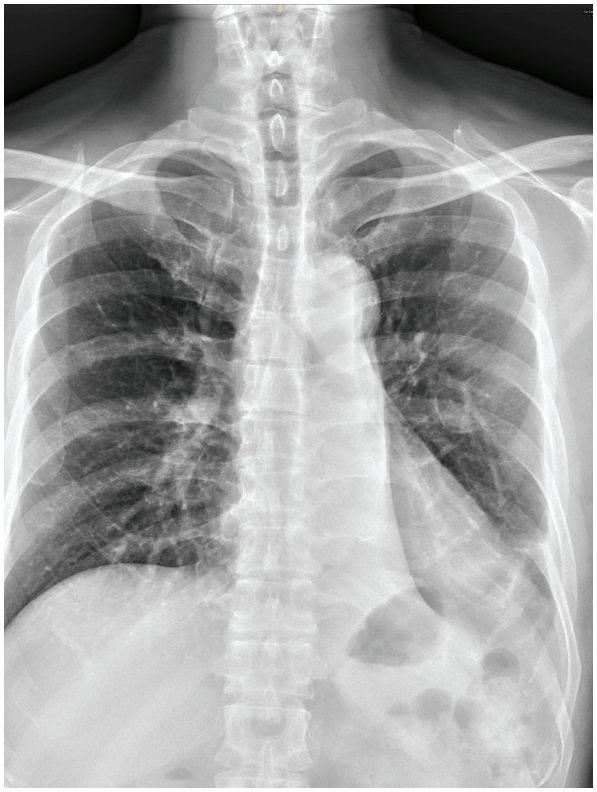

Fig. 6. Follow-up chest radiograph showed post-operation change without significant complications.

after the operation, and was followed up at the outpatient department with resolution of the chronic cough.

Discussion

Pulmonary sequestration is a rare congenital malformation, and is usually diagnosed in pediatric patients [2]. A single retrospective study compiled by van Raemdonck D, *et al*., compared pediatric and adult patients with pulmonary sequestration. The study mentioned that the extralobar type is more commonly asymptomatic. In contrast, the intralobar type may present with recurrent infections. This study also mentioned that there were no significant differences between pediatric patients and adult patients in terms of sex, type of sequestration, pulmonary venous drainage, and associated anomalies. The only recognized significant difference in this study was that adult patients had a higher rate of infections and a higher number of lobectomies, but there were no differences in early and late outcomes between the 2 groups [4]. Even though most patients are asymptomatic or present with mild symptoms only, there are reports that mention major or even fatal sequelae, such as aspergillosis and fatal hemoptysis [5-7].

CT plays an important diagnostic role in pulmonary sequestration, and there is some debate regarding the need for angiography. However, arranging angiography or even a 3D-reconstruction image may provide better identification of the arterial supply, venous drainage and parenchymal changes in a single examination, and thereby provide the thoracic surgeon better pre-operation anatomy information [9-11]. In addition, a 3D-reconstruction image can provide the clearest visualization of the detailed anatomy of the draining veins for pulmonary sequestration. Although axial images of CT angiography are diagnostic for the feeding arteries, 3D images enhance the visualization of small and tortuous arteries and veins. A more detailed view of the feeding arteries and venous drainage is helpful in making preoperative decisions [12, 13]. Even though most of the current evidence focuses on pediatric patients, we consider that adult patients would share similar benefits.

Pulmonary lobectomy is a reasonable treatment of choice for symptomatic pulmonary sequestration [14, 15], but even in asymptomatic patients, surgical resection is still suggested to avoid infection [16]. However, in the largest retrospective case series on adults, there is no strong evidence for the benefits of surgery or conservative treatment in asymptomatic patients [17]. In adult patients, the decision on surgical resection requires weighing various factors, including patient general performance and clinical manifestations [18].

In recent years, endovascular embolization and coiling have developed as another therapeutic choice [19-20]. However, further practical experience and studies may be needed to confirm the benefit of this alternative treatment compared with surgical resection.

Conclusion

In this case report, we described the diagnosis and management of a rare case of pulmonary sequestration in an adult, especially using the 3D-reconstruction image to provide a better view of vascular drainage for pre-operation assessment. The patient underwent surgery without significant complications. The intra-operation findings and gross specimen were all

compatible with the diagnosis.

Owning to the limited number of cases, especially in adult patients, there is a lack of large studies to support the diagnostic and management plan. We reviewed some recent articles that supported a diagnosis dependent on CT angiography and management with surgical resection as reasonable methods. However, there are also reports of successful treatment by endovascular embolization. Further studies should be performed, especially those investigating the benefit of surgical intervention in asymptomatic patients and the benefit of endovascular embolization.

References

1. Pryce DM. Lower accessory pulmonary artery with intralobar sequestration of lung; a report of seven cases. J Pathol Bacteriol 1946 Jul; 58(3): 457-67.
2. Savic B, Bertel FJ, Tholen W, *et al*. Lung sequestration: report of seven cases and review of 540 published cases. Thorax 1979; 34: 96-101.
3. Gezer S, Taştepe I, Sirmali M, *et al*. Pulmonary sequestration: a single-institutional series composed of 27 cases. J Thorac Cardiovasc Surg 2007; 133: 955.
4. Van Raemdonck D, De Boeck K, Devlieger H, *et al*. Pulmonary sequestration: a comparison between pediatric and adult patients. Eur J Cardiothorac Surg 2001; 19: 388.
5. Morikawa H, Tanaka T, Hamaji M, *et al*. A case of aspergillosis associated with intralobar pulmonary sequestration. Asian Cardiovasc Thorac Ann 2011; 19: 66-8.
6. Somja J, De Leval L, Boniver J, *et al*. Intrapulmonary lung sequestration diagnosed in an adult. Rev Med Liege 2011; 66: 7-12.
7. Rubin EM, Garcia H, Horowitz MD, *et al*. Fatal massive hemoptysis secondary to intralobar sequestration. Chest 1994; 106: 954-5.
8. Ikezoe J, Murayama S, Godwin JD, *et al*. Bronchopulmonary sequestration: CT assessment. Radiology 1990; 176(2): 375-9.
9. Yasmin R, Stærk DR, Kalhauge A, *et al*. Role of CT angiography in bilateral pulmonary sequestration: a case report. Acta Radiologica Open 2018; 7(3): 1-5.
10. Kang M, Khandelwal N, Ojili V, *et al*. Multidetector CT angiography in pulmonary sequestration. J Comput Assist Tomogr 2006 Nov-Dec; 30(6): 926-32.
11. Kas J, Fehér C, Heiler Z, *et al*. Treatment of adult intrapulmonary sequestration with video-assisted thoracoscopic lobectomy. Magy Seb 2018, 71(3): 126-133.
12. Long Q, Zha Y, Yang Z. Evaluation of pulmonary sequestration with multidetector computed tomography angiography in a select cohort of patients: a retrospective study, Clinics 2016; 71(7): 392-398.
13. Lee EY, Siegel MJ, Sierra LM, *et al*. Evaluation of angioarchitecture of pulmonary sequestration in pediatric patients using 3D MDCT angiography. AJR 2004; 183: 183–188.
14. Lin TH, Huang WL, Chang CC, *et al*. Uniportal video-assisted thoracoscopic surgery lobectomy and segmentectomy for pulmonary sequestration. J Thorac Dis 2018 Jun; 10(6): 3722-3728.
15. Berna P, Cazes A, Bagan P, *et al*. Intralobar sequestration in adult patients. Interact Cardiovasc Thorac Surg 2011 Jun; 12(6): 970-2.
16. Lee EY, Siegel MJ, Sierra LM, *et al*. Evaluation of angioarchitecture of pulmonary sequestration in pediatric patients using 3D MDCT angiography. AJR 2004; 183: 183-8.
17. Sun X, Xiao Y. Pulmonary sequestration in adult patients: a retrospective study. Eur J Cardiothorac Surg 2015 Aug; 48(2): 279-82.
18. Alsumrain M, Ryu JH. Pulmonary sequestration in adults: a retrospective review of resected and unresected cases. BMC Pulm Med 2018 Jun 05; 18(1): 97.
19. Zener R, Bottoni D, Zaleski A, *et al*. Transarterial embolization of intralobar pulmonary sequestration in a young adult with hemoptysis. J Thorac Dis 2017 Mar; 9(3): E188-E193.
20. Ojha V, Samui PP, Dakshit D. Role of endovascular embolization in improving the quality of life in a patient suffering from complicated intralobar pulmonary sequestration - A case report. Respir Med Case Rep 2015; 16: 24-8.

Disseminated *Mycobacterium kansasii* Infection Presenting as Multiple Osteolytic Lesions and Prominent Mediastinal Lymphadenopathy in an Immunocompetent Woman: A Case Report

Yi-Ting Chen[1], Ya-Ting Chang[2], Chih-Jen Yang[1,3]

Mycobacterium kansasii (*M. kansasii*) is a nontuberculous mycobacterium that causes various infections in humans, including pulmonary disease, lymphadenitis, and skin and soft tissue infections. Disseminated *M. kansasii* infection, although rare, can occur in individuals with weakened immune systems or chronic lung diseases. This case report presents a 65-year-old woman with no immunocompromising conditions who experienced fever, chest pain, dyspnea, and respiratory tract infection symptoms for several weeks. Medical imaging revealed enlarged lymph nodes in the upper mediastinum and subcarinal region. Despite inconclusive results from a biopsy, a positron emission tomography (PET) scan showed increased metabolic activity in multiple lymph nodes and bones. The patient underwent a chest wall tumor excision, which showed no signs of malignancy but eventually led to the identification of *M. kansasii* through tissue culture. The patient responded well to treatment with a combination of rifampin, ethambutol, and clarithromycin, as confirmed by a follow-up chest CT scan showing significant improvement in lymphadenopathy and bony lesions after 3 months. ***(Thorac Med 2024; 39: 84-90)***

Key words: Disseminated *M. kansasii* infection, osteolytic bone destruction, mediastinal lymphadenopathy, immunocompetent patient

Introduction

Nontuberculous mycobacteria (NTM) may have diverse clinical manifestations, such as pulmonary diseases, disseminated disease, superficial lymphadenitis, and skin and soft tissue infection [1-2]. The organism *M. kansasii* is commonly found in various environments, with water and soil being prevalent habitats, and tap water serving as the primary reservoir for this pathogen [3-5]. *M. kansasii* typically manifests as a pulmonary disease that closely resembles

[1]Division of Pulmonary and Critical Care Medicine, Department of Internal Medicine, Kaohsiung Medical University Hospital, Kaohsiung Medical University, Kaohsiung, Taiwan. [2]Division of Infectious Disease, Department of Internal Medicine, Kaohsiung Medical University Hospital, Kaohsiung Medical University, Kaohsiung, Taiwan. [3]School of Post-Baccalaureate Medicine, College of Medicine, Kaohsiung Medical University, Kaohsiung, Taiwan
Address reprint requests to: Dr. Chih-Jen Yang, Department of Internal Medicine Kaohsiung Medical University Hospital, Kaohsiung Medical University No. 100, Tzyou First Road, Kaohsiung City, Taiwan.

tuberculosis [6]. However, disseminated infection is rare, and may arise in individuals with compromised immune systems, especially those with a human immunodeficiency virus (HIV) infection [1].

Here, we report an immunocompetent woman who was infected with *M. kansasii*, and presented with multiple osteolytic destruction and prominent mediastinal lymphadenopathy. This report highlights the challenging diagnostic workup of *M. kansasii* disease and its clinical improvement after appropriate treatment.

Case Report

This 65-year-old female patient presented with a medical history of Alzheimer's disease and no immunocompromised status. The patient initially presented with fever, respiratory tract symptoms, dyspnea, and chest pain, leading to her hospitalization for intravenous antibiotic treatment. A suspicion of right lower lung pneumonia and bilateral pleural effusion prompted the initiation of antibiotics. The acid-fast stains from her sputum revealed no abnormalities, raising further questions about the underlying cause of her symptoms.

Laboratory investigations, including the assessment of tumor markers such as carcinoembryonic antigen (CEA), squamous cell carcinoma antigen (SCC), and tissue polypeptide antigen (TPA), indicated that all levels were within the normal range. However, a chest CT scan painted a different picture, showing enlarged lymph nodes in the upper mediastinum and subcarinal region (Fig. 1A & Fig. 1B), rais-

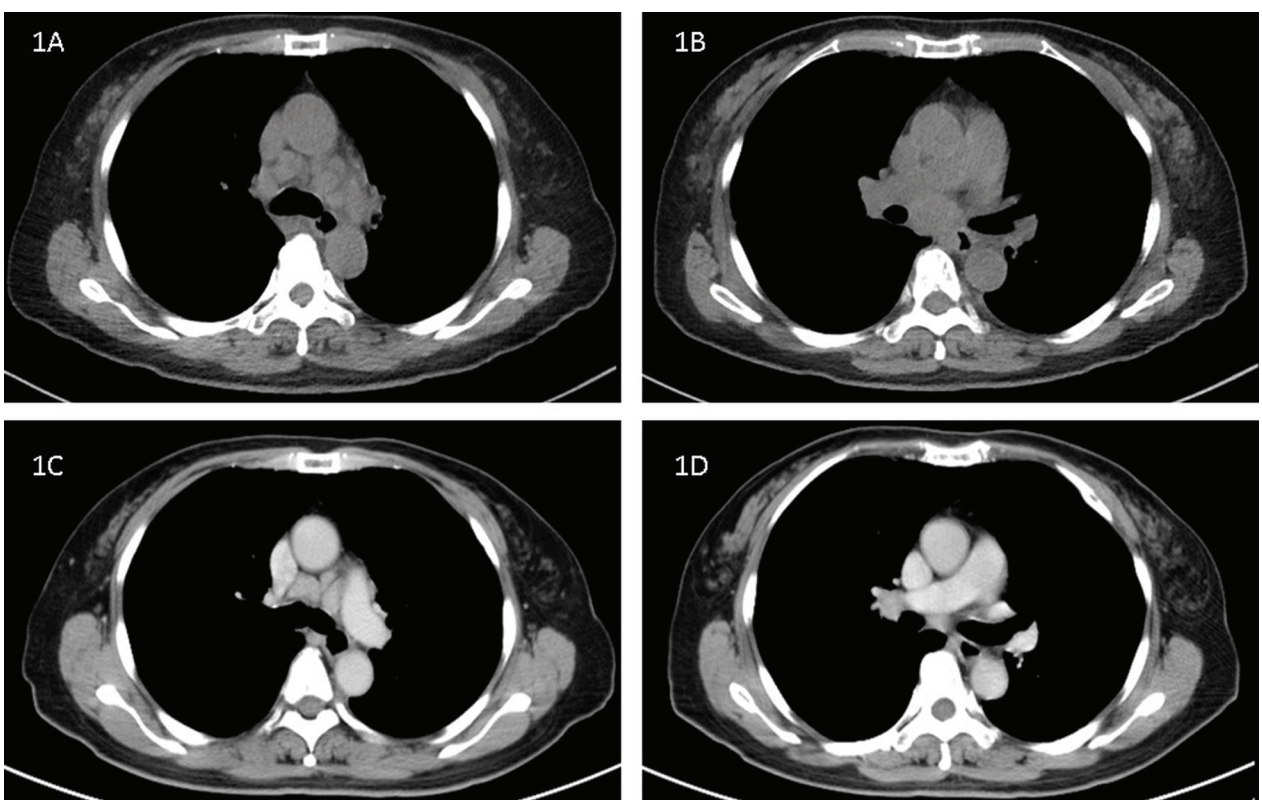

Fig. 1. 1A. & Fig. 1B. Chest CT showed enlargement of the lymphadenopathy at the upper mediastinum and subcarinal region. Fig. 1C & Fig. 1D. Chest CT after 3 months of treatment disclosed a decrease of the size of the lymphadenopathy.

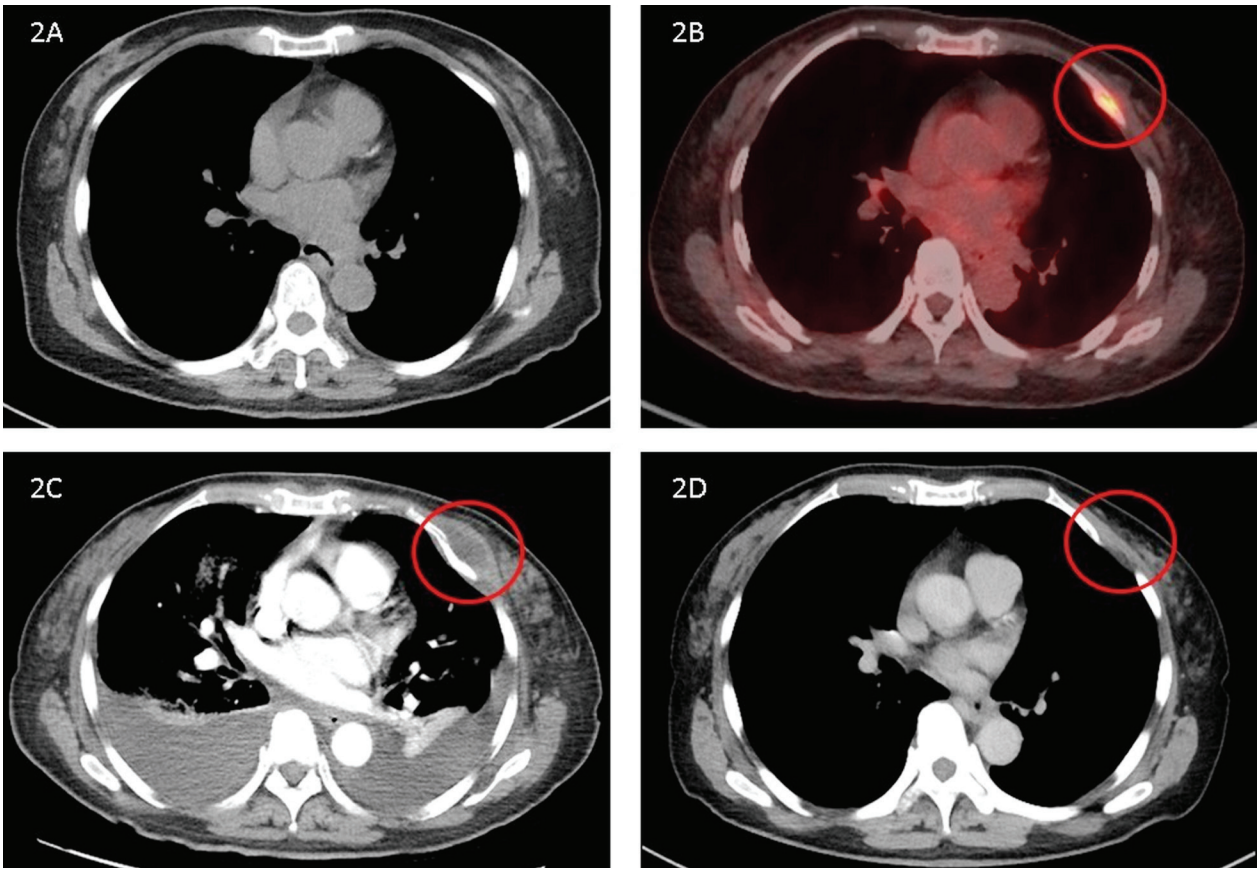

Fig. 2. 2A. Chest CT showed enlargement of the lymphadenopathy at the upper mediastinum before treatment of M. kansasii. Fig. 2B. PET scan revealed bone/ marrow avidity at the left rib cage. Fig. 2C. Chest CT showed progression of the left chest wall tumor and bilateral pleural effusion. Fig. 2D. Chest CT identified improvement in the left chest wall tumor and in the bilateral pleural effusion after 3 months of treatment.

ing concerns about the possibility of lymphoma or a metastatic mass. To further investigate, an endobronchial ultrasound-guided transbronchial needle aspiration (EBUS-TBNA) biopsy was performed. The biopsy results came back negative for malignancy, leaving the etiology of the symptoms still unclear.

Further imaging studies were conducted to explore the extent of the disease. A PET scan conducted to investigate the patient's persistent fever revealed increased uptake in multiple bones and bone marrow, particularly in the pelvis, sacrum/coccyx, sternum, and rib cages. These findings, primarily indicating osteosclerosis (Fig. 2B), raised strong suspicions of bone metastasis. Subsequent bone scans confirmed multiple skeletal lesions, further supporting the possibility of bone metastasis. As the patient's dyspnea progressively worsened, thoracocentesis was performed, yielding transudative effusion without any malignant cells. However, repeated chest CT scans revealed progression of the skeletal osteolytic lesions, including in the ribs, sternum, and spine. Prominent lesions were palpable on physical examination of her thoracic cage. In addition, significant enlargement of lymph nodes was observed bilaterally in the supraclavicular regions, upper mediastinum, precarinal region, and subcarinal region. Bilateral pleural effusion was also evident (Fig.

2C). Blood tests showed elevated levels of C-reactive protein (CRP): 302 mg/L, indicating systemic inflammation, although blood cultures did not yield bacterial growth.

To establish a definitive diagnosis and guide appropriate treatment, a surgeon was consulted for the excision of the chest wall tumor (Fig. 3). However, the excised tissue revealed no evidence of malignancy, further deepening the mystery. Nevertheless, the tissue culture eventually yielded *M. kansasii*, providing an unexpected explanation for the patient's symptoms.

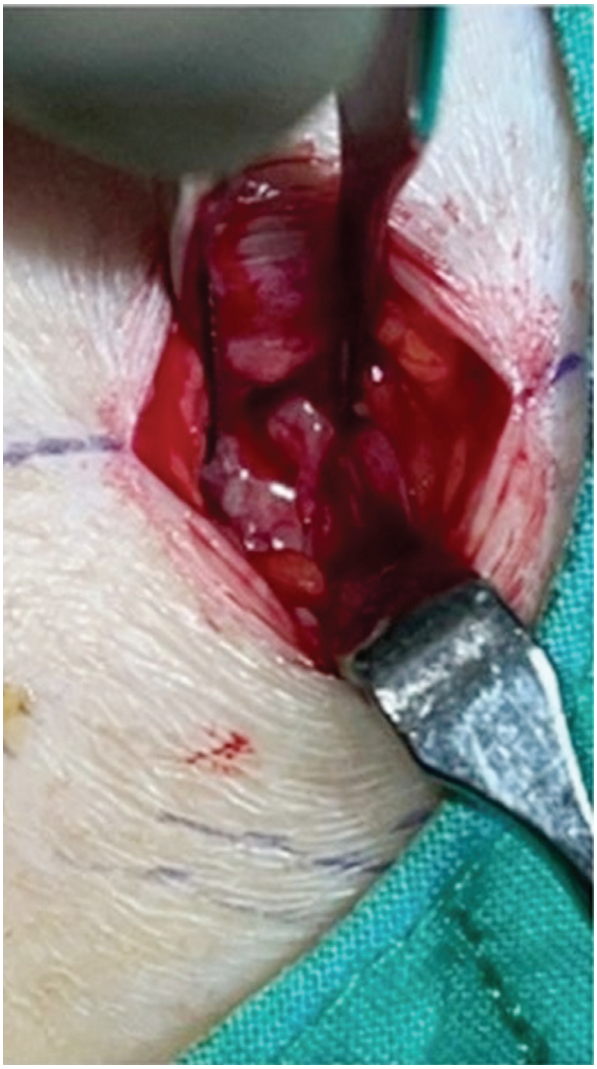

Fig. 3. Chest wall tumor dissection operationally.

Consequently, a treatment regimen consisting of rifampin, ethambutol, and clarithromycin was initiated to combat the disseminated *M. kansasii* infection, following the recommended guidelines.

The patient's progress was closely monitored, and a follow-up chest CT performed 3 months later showed a remarkable reduction in the size of the lymphadenopathy in the upper mediastinum (Fig. 1C & Fig. 1D). Furthermore, the left chest wall tumor and bilateral pleural effusion had completely resolved (Fig. 2D), indicating a positive response to the treatment. The patient's overall condition improved significantly, with restored spirits, a better appetite, and gradual weight gain, highlighting the successful management of the *M. kansasii* infection and its associated complications.

Discussion

We reported an immunocompetent woman who presented multiple osteolytic lesions and lymphadenopathy. *M. kansasii* finally was yielded via culture from the surgical biopsy specimens, and she regained her health after accurate treatment.

An abnormal mass or lymphadenopathy in the mediastinum can be caused by either neoplastic or benign growths. To effectively manage and predict the outcome of these conditions, it is crucial to diagnose them quickly and accurately. This necessitates obtaining sufficient materials for high-quality pathological, genetic, immunological, and other assessments [7]. The introduction of EBUS has revolutionized the diagnostic approach for mediastinal diseases. This minimally invasive procedure allows real-time monitoring of TBNA. It has replaced more invasive biopsies like mediastinoscopy, offer-

ing a simpler, well-tolerated, cost-effective, and safer alternative [8-10].

Disseminated disease caused by NTM infection is rare, but could affect multiple organs, including the lungs, lymph nodes, skin, soft tissues, and bones. Bone involvement may present as osteolytic lesions, and is frequently misdiagnosed as malignancy with metastasis, tuberculosis, or fungal infections, indicating a lack of awareness among clinicians [11].

Disseminated *M. kansasii* infection is very rare, and has occurred mostly in immunocompromised hosts, such as those with an HIV infection, in several case reports [12-19]. Disseminated disease is rare among individuals who are HIV-negative, and typically arises in conjunction with significant immunosuppression [14].

Insufficient research on the clinical and imaging features of NTM-related osteolytic lesions further delays the correct diagnosis and treatment. Typical radiographic and CT findings of NTM-related bone involvement include osteolytic lesions, bone defects, low-density areas, pathological fractures, and periosteal proliferation. Bone scan and PET/CT show increased uptake and metabolic activity in multiple bones. Etiological culture and molecular biology techniques, such as follow-up polymerase chain reaction (PCR) and gene sequencing, are essential for accurate diagnosis and improved clinical outcomes [11].

Combination therapy is generally effective in treating *M. kansasii* infection in patients who are not infected with HIV. For patients with susceptible organisms, sputum clearance usually occurs within 4 months of treatment, and the majority of patients have a low risk of relapse [14]. Also, current guidelines recommend a treatment regimen of rifampicin, ethambutol, and either isoniazid or clarithromycin for 15-18 months for HIV-infected patients with *M. kansasii* infection [15].

The guideline from the American Thoracic Society suggests using a combination of 3 drugs, namely isoniazid, rifampin, and ethambutol, for the treatment of *M. kansasii* infection. The recommended therapy duration is a minimum of 12 months, and should be discontinued only if the culture test shows negativity [2]. In addition to these 3 drugs, moxifloxacin, a fluoroquinolone, has demonstrated promising in vitro activity against *M. kansasii* [16]. For patients who are unable to tolerate isoniazid, a viable alternative could be a combination therapy of rifampin, ethambutol, and clarithromycin, which has proven effective against other NTM [17].

A comprehensive review of the literature analyzed the characteristics of 63 cases of disseminated *M. kansasii* infection in non-HIV infected patients [18]. The mean age of the patients was 45 years, and 79.7% of them were male. Hematological malignancy was found to be the most common underlying disease, but a relatively high percentage of previously healthy individuals (23.8%) also contracted the infection. The infection caused by *M. kansasii* affected various visceral organs, with the lungs, lymph nodes, spleen, liver, and bone marrow being the most involved sites. The prognosis of disseminated *M. kansasii* infection was poor, with a mortality rate of 60.3%. The presence of underlying disease and/or immunosuppression was identified as the best predictor of the outcome of disseminated *M. kansasii* infection [19]. Patients with underlying disease had a higher mortality rate than those without underlying disease (75% and 53.3%, respectively).

It is crucial to report cases of NTM in

the population to better understand the prevalence of these rare strains, which can pose challenges in terms of treatment. Despite the positive response to therapy in the reported patient, it is still important to promptly implement all available diagnostic procedures to facilitate early initiation of appropriate therapy. For this case, co-administered rifampin, ethambutol, and clarithromycin resulted in a good response. Appropriate diagnosis leads to an appropriate treatment.

Conclusion

Disseminated *M. kansasii* infection is an uncommon occurrence in non-HIV patients. It can present with diverse clinical features, such as multiple osteolytic bone destruction or mediastinal lymphadenopathy, which can make diagnosis challenging. Accurately identifying the underlying cause is essential to provide appropriate treatment and achieve a favorable outcome. A combination of diagnostic procedures, including tissue culture, imaging, and biopsy, may be used to establish a diagnosis. Treatment typically involves a combination of antimicrobial agents, including rifampin, ethambutol, and clarithromycin. Early diagnosis and appropriate treatment are crucial, and all diagnostic procedures should be utilized to ensure accurate identification of the underlying cause and the provision of successful treatment.

References

1. Wolinsky E. Nontuberculous mycobacteria and associated diseases. Am Rev Respir Dis 1979; 119[(1): 107-59.
2. Griffith DE, Aksamit T, Brown-Elliott BA, *et al*. An official ATS/IDSA statement: diagnosis, treatment, and prevention of nontuberculous mycobacterial diseases. Am J Respir Crit Care Med 2007; 175(4): 367-416.
3. Bennett JE, Dolin R, Blaser MJ, *et al*. Mandell, Douglas, and Bennett's principles and practice of infectious diseases, 8th edition, Saunders Elsevier; 2015: 2842-8.
4. Jonson MM, Odell JA. Nontuberculous mycobacterial pulmonary infections. J Thorac Dis 2014; 6: 210-20.
5. Chou YH, Hsu MS, Sheng WH, **et al**. Disseminated *Mycobacterium kansasii* infection associated with hemophagocytic syndrome. Int J Infect Dis 2010; 14(3): e262-4.
6. Reich JM, Johnson RE. Mycobacterium avium complex pulmonary disease presenting as an isolated lingular or middle lobe pattern. The Lady Windermere syndrome. Chest 1992; 101(6): 1605-9.
7. Wallace MB, Pascual JM, Raimondo M, *et al*. Minimally invasive endoscopic staging of suspected lung cancer. JAMA 2008; 299: 540-546.
8. Rintoul RC, Skwarski KM, Murchison JT, *et al*. Endobronchial and endoscopic ultrasound-guided real-time fine-needle aspiration for mediastinal staging. Eur Respir J 2005; 25: 416-421.
9. Annema JT, van Meerbeeck JP, Rintoul RC, *et al*. Mediastinoscopy vs endosonography for mediastinal nodal staging of lung cancer: a randomized trial. JAMA 2010; 304: 2245-2252.
10. Navani N, Nankivell M, Lawrence DR, *et al*. Lung cancer diagnosis and staging with endobronchial ultrasound-guided transbronchial needle aspiration compared with conventional approaches: an open-label, pragmatic, randomised controlled trial. Lancet Respir Med 2015; 3: 282-289.
11. Tang M, Huang J, Zeng W, *et al*. Retrospective analysis of 10 cases of disseminated nontuberculous mycobacterial disease with osteolytic lesions. Infect Drug Resist 2021; 14: 4667-4679.
12. Wagner D, Young LS. Nontuberculous mycobacterial infections: a clinical review. Infection 2004; 32(5): 257-70.
13. Bloch KC, Zwerling L, Pletcher MJ, *et al*. Incidence and clinical implications of isolation of *Mycobacterium kansasii*: results of a 5-year, population-based study. Ann Intern Med 1998; 129(9): 698-704.
14. Johnston JC, Chiang L, Elwood K, *et al*. *Mycobacterium kansasii*. Microbiol Spectr 2017; 5(1).

15. Lundgren JD, Gatell JM, Rockstroh JK, *et al*. EACS Guidelines, Version 7. 1. European AIDS Clinical Society (EACS); 2014.
16. Guna R, Muñoz C, Domínguez V, *et al*. In vitro activity of linezolid, clarithromycin and moxifloxacin against clinical isolates of *Mycobacterium kansasii*. J Antimicrob Chemother 2005; 55: 950-3.
17. Wallace RJ Jr, Brown BA, Griffith DE, *et al*. Initial clarithromycin monotherapy for Mycobacterium avium-intracellulare complex lung disease. Am J Respir Crit Care Med 1994; 149: 1335-41.
18. Han SH, Kim KM, Chin BS, *et al*. Disseminated *Mycobacterium kansasii* infection associated with skin lesions: a case report and comprehensive review of the literature. J Korean Med Sci 2010; 25(2): 304-8.
19. Breathnach A, Levell N, Munro C, *et al*. Cutaneous *Mycobacterium kansasii* infection: case report and review. Clin Infect Dis 1995; 20(4): 812-7.

Rapid Progression of Diffuse Parenchymal Lung Disease in a Woman with Dual Positives of Anti-MDA-5 and Anti-RO-52 Amyopathic Dermatomyositis, Resulting in Refractory Hypoxemia and Death Following Surgical Lung Biopsy: A Case Report and Literature Review

Chi-En Chen[1], Chih-Hsin Lee[1], Lung-Fang Chen[2], Yin-Chun Chang[3]

A 55-year-old female presented with Gottron's papule, mechanic's hands, and periungual erythematous change. She was diagnosed with amyopathic dermatomyositis with positive anti-MDA-5 and anti-RO52 antibodies. Despite aggressive immune-modifying therapy and comprehensive antimicrobial treatment, she developed rapidly progressive diffuse parenchymal lung disease following a surgical biopsy that resulted in refractory hypoxemia and death. We performed a literature review and scrutinized the clinical course for possible etiologies of the devastating complications following surgical biopsy in our patient. We found that transbronchial lung cryobiopsy, an emerging novel technique, could be a potential diagnostic alternative to surgical lung biopsy to avoid postoperative morbidities and mortalities in patients with amyopathic dermatomyositis with diffuse parenchymal lung disease. ***(Thorac Med 2024; 39: 91-98)***

Key words: Amyopathic dermatomyositis, anti-MDA-5 antibodies, diffuse parenchymal lung disease, video-assisted thoracoscopic surgical lung biopsy, transbronchial lung cryobiopsy, organizing pneumonia

Introduction

Dermatomyositis (DM), a subtype of idiopathic inflammatory myopathies (IIMs), is characterized by chronic inflammation of the skin and muscles. Systemic dysfunctional inflammation may involve the lung parenchyma and increase the risk of lung cancer. The 5 most recognized types of IIMs are dermatomyositis, immune-mediated necrotizing myopathy, overlap myositis (including anti-synthetase syndrome), sporadic inclusion-body myositis,

[1]Division of Pulmonary Medicine, Department of Internal Medicine, Wan Fang Hospital, Taipei Medical University, [2]Division of Allergy, Immunology and Rheumatology, Department of Internal Medicine, Wan Fang Hospital, Taipei Medical University, [3]Division of Thoracic and Cardiovascular Surgery, Department of Surgery, Wan Fang Hospital, Taipei Medical University
Address reprint requests to: Dr. Yin-Chun Chang, Division of Thoracic and Cardiovascular Surgery, Department of Surgery, Wan Fang Hospital, Taipei Medical University.

and polymyositis [1, 2]. Among the various subtypes of IIMs, patients who are positive for anti-melanoma differentiation-associated gene 5 (MDA-5) antibodies tend to have more skin manifestations and less muscle involvement. Patients without evidence of myositis are recognized as clinically amyopathic dermatomyositis (CADM). These patients are frequently associated with rapidly progressive diffuse parenchymal lung disease (DPLD) and a poor prognosis [1, 3, 4]. Among patients with DM showing lung parenchymal involvement, the mortality rate is distinctively higher in those with CADM (45%) than in patients with other types of DM (6%) [5].

For patients with DM who manifest DPLD irresponsive to immune-modifying therapy (IMT), histopathological study is crucial in multidisciplinary assessment to rule out concomitant secondary processes such as superimposed infections. Although less invasive, transbronchial lung biopsy using conventional forceps is limited by the smaller size and crush artifacts of the specimens, and is usually inadequate in such challenging scenarios [6]. Obtaining an adequate sample of lung tissue may require surgical lung biopsy (SLB) to disclose diagnostic histopathological features. On the other hand, for patients with DPLD, SLB was associated with substantial postoperative complications and mortalities. Patients with a more severe lung disease appear to be at a greater risk for complications with SLB [7]. The in-hospital mortality rates were 1.7% and 16.0% for elective and non-elective procedures, respectively [7-8].

Here, we report the case of a patient with CADM-associated DPLD who experienced unrelenting progression of hypoxemia despite aggressive IMT and comprehensive antimicrobial treatment. She developed fatal hypoxemic respiratory failure following non-intubated video-assisted thoracoscopic surgery (VATS) for SLB. A literature review was performed to evaluate the potential role of transbronchial lung cryobiopsy (TBLC) as a diagnostic alternative for CADM-associated DPLD to prevent the devastating complications of SLB and their associated poor outcomes.

Case Description

Initial presentations and diagnosis

A 55-year-old woman with a 10-year history of urticaria was otherwise healthy until 4 months before her first admission. She suffered from tenderness, swelling, and erythematous change over the bilateral periorbital area for 2 months. She was treated with oral non-steroid anti-inflammatory drugs, antihistamines, and topical corticosteroids at a family medicine outpatient clinic. The symptoms did not improve, and she was referred to a dermatologist. A right lower eyelid skin biopsy revealed perivascular and peri-adnexal infiltration of lymphocytes and plasma cells with prominent mucin deposition at the upper to deep dermis. These findings suggested tumid lupus erythematosus. The dermatologist then liaised with a rheumatologist for a comprehensive evaluation of autoimmune diseases. The rheumatologist reported dry eyes, dry mouth, and bilateral knee joint pain. On physical examination, oral ulcer, bilateral finger's periungual erythematous change, mechanic's hand, and Gottron's papules were noted. The patient denied morning stiffness, malar rashes, myalgia, or proximal muscle weakness.

The initial laboratory investigations revealed mild leukopenia and normocytic anemia. C-reactive protein was equivocal (0.104 mg/

dL) and the erythrocyte sedimentation rate was elevated (77 mm/hour). Anti-dsDNA and anti-SSA/Ro were positive (27.0 IU/ml and 11.0 U/ml, respectively), and anti-SSB/La was negative. In addition, the antinuclear antibody (ANA) test, which is associated with systemic lupus erythematosus (SLE), revealed a negative titer of 1:40. Anti-MDA-5 was positive, and anti-Ro-52 was strongly positive. Creatine kinase, an enzyme in the heart, brain, and skeletal muscles, was normal (64U/L). Other autoimmune autoantibodies data are listed in Table 1.

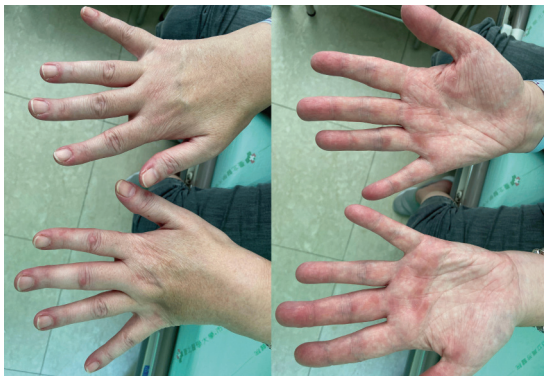

Fig. 1. Physical examination on admission revealed Gottron's papules and mechanics hands.

Associated diffuse parenchymal lung disease with rapid progression

CADM was impressed, and the patient was treated with oral prednisolone and hydroxychloroquine. A pulmonary function test revealed normal spirometry and lung volumes, while the diffusion capacity of the lung for carbon monoxide was moderately impaired (48% of the predicted value). Her skin and joint symptoms persisted despite medications, and she developed shortness of breath 1 month later. She was treated with a high-dose steroid, and azathioprine was added. However, her dyspnea progressed, and pulse oxyhemoglobin desaturation (SpO_2 < 92%) was recorded on the 1-minute sit-to-stand test. She underwent cyclophosphamide 400 mg pulse therapy and a course of rituximab

Table 1. Results of Autoimmune Autoantibody Titers

	Reference range, adult	Initial workup in an outpatient clinic	Follow-up during hospitalization
Anti-ENA screening (ratio)	<0.7~ (Negative) 0.7~1.0 (Equivocal) >1.0~ (Positive)	**1.89 Positive**	—
Anti-nuclear Ab (titer:x)	40X(-)	40X(-)	—
Anti-EJ	Negative	Negative	—
Anti-OJ	Negative	Negative	—
Anti-PL-12	Negative	Negative	—
Anti-RO52	Negative	**Strong Positive**	—
Anti-MDA5	Negative	**Positive**	—
Anti-Mi-2 alpha	Negative	Negative	—
Anti-Mi-2 beta	Negative	Negative	—
Anti-TIF1γ	Negative	Negative	—
Anti-JO-1	Negative	Negative	—
Anti-PL-7	Negative	Negative	—
Anti-PM-Scl75	Negative	Negative	—

Anti-SRP	Negative	Negative	—
Anti-Ku	Negative	Negative	—
Anti-NXP2	Negative	Negative	—
Anti-SAE1	Negative	Negative	—
Anti-PM-Scl100	Negative	Negative	—
IgE (kU/L)	0~200	42.7	—
Anti-dsDNA (IU/mL)	<10~ (Negative) 10~15 (Equivocal) >15~ (Positive)	**27.00 Positive**	**26.00 Positive**
Anti-β2 Glycoprotein IgG (U/mL)	<7~ (Negative) 7~10 (Equivocal) >10~ (Positive)	1.0 Negative	—
RNP (Elia U/mL)	<5~ (Negative) 5~10 (Equivocal) >10~ (Positive)	2.35 Negative	—
Anti-SmD (Elia U/mL)	<7~ (Negative) 7~10 (Equivocal) >10~ (Positive)	1.0 Negative	—
IgG (mg/dL)	700~1600	1450.0	1470
C3 (mg/dL)	90~180	130	132
HBsAg (COI)	<0.9 Negative	0.182 Negative	—
Anti-HCV (COI)	<0.9 Negative	0.035 Negative	—
ESR-1hr (mm/1hr)	0~20	**38**	54
CK (U/L)	30~223	64	147
LDH (U/L)	140~271	157	225
hsCRP (mg/dL)	>0.3~ (High-risk <0.1~ (Low-risk)	0.104	—
LA 1 (second)	-	55.7	—
LA2 (second)	-	49.3	—
LA1/LA2 Ratio	<1.16	1.04	—
Anti-phospholipid IgG	Negative	—	Negative
SS-A/Ro (Elia U/mL)	<7~ (Negative) 7~10 (Equivocal) >10~ (Positive)	—	**11.00 Positive**
SS-B/La (Elia U/mL)	<7~ (Negative) 7~10 (Equivocal) >10~ (Positive)	—	2.53 Negative
Anti-ribosomal-P Ab (Elia U/mL)	<7~ (Negative) 7~10 (Equivocal) >10~ (Positive)	0.80 Negative	—
Anti-cardiolipin IgG (GPLU/mL)	<10~ (Negative) 10~40 (Weak positive) >40~ (Positive)	—	3.6 Negative

therapy (500 mg each on Day 1 and Day 15). The maintenance dose of oral prednisolone was further increased to 30 mg daily. Her respiratory distress progressed gradually, and the chest X-rays showed diffuse reticulonodular infiltrations, which were more prominent at the lower lung fields. Fever developed, and a computed tomography scan of the chest revealed diffusely interlaced patches of ground-glass opacities (Fig. 2). Levofloxacin 750 mg once daily was prescribed empirically to cover atypical pathogens for community-acquired pneumonia. The fever subsided in subsequent days, but the shortness of breath persisted, and she was admitted 1 week later.

Course of hospitalization

Her blood pressure, temperature, pulse rate, and respiratory rate were 111/69 mmHg, 36.0℃, 107 beats per minute, and 21 breaths per minute, respectively. Her SpO_2 was 92% in ambient air. Fine crackles were audible over bilateral lower lungs on auscultation.

Opportunistic pulmonary infection was suspected; levofloxacin 750 mg once daily, sulfamethoxazole/trimethoprim 1600/320 mg every 8 hours, and doxycycline 100 mg twice daily were added. However, the comprehensive microbiology, radiology, and serology studies were non-diagnostic. Corticosteroids (1 mg per kg of body weight) were used to suppress the progressive lung involvement of the dermatomyositis. Azathioprine was discontinued on the 6th day of admission due to abnormal liver function tests. Levofloxacin was stopped on the 7th day due to generalized skin rash and visual delusion. Her dyspnea progressed, and the resting SpO_2 decreased to 88% while the patient breathed ambient air. She became disoriented and agitated.

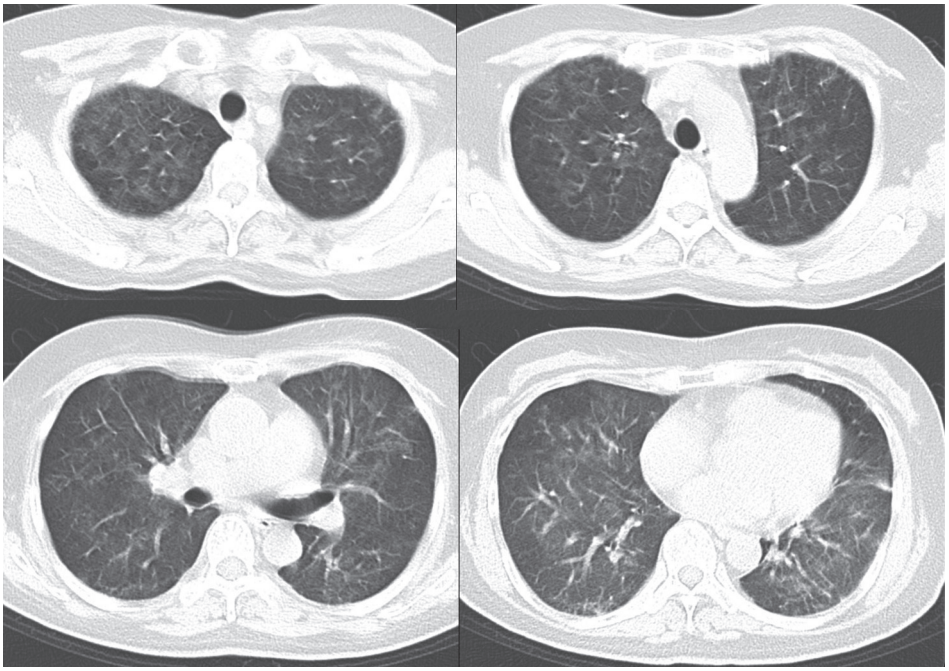

Fig. 2. Chest computed tomography, axial view of the lung window, performed about 1 week before admission, when the patient developed fever and exertional dyspnea, revealed diffusively interlaced patches of ground-glass opacities.

For the rapidly progressing hypoxemic respiratory distress, high-dose intravenous human immunoglobulin therapy (2 g per kg body weight) was started on the 8th day of admission, but her condition continued deteriorating. A pathology survey was advised for the rapid progression of DPLD, despite the potent antimicrobial and anti-inflammatory treatment, and she underwent right upper lobe wedge resection using non-intubated VATS. The operation went smoothly with minimal blood loss (less than 10 ml). She developed hypoxemia in the postoperative recovery room and was intubated and supported with mechanical ventilation using a FiO_2 of 0.35 and a positive end-expiratory pressure (PEEP) of 8 cmH_2O.

Postoperative course

The day after the operation, she passed the spontaneous breathing trial using pressure support at 8 cmH_2O, a FiO_2 of 0.3, and a PEEP of 8 cmH_2O. Five hours after liberation from mechanical ventilation, she developed hypoxemic respiratory failure irresponsive to the attempt of oxygen supplementation with a non-rebreathing oxygen mask. She was re-intubated immediately, and the chest X-ray showed progression of diffuse ground-glass opacities. Acute respiratory distress syndrome ensued, and the PaO_2/FiO_2 ratio was 74.2 when she was supported with a PEEP of 8 cmH_2O. The hypoxemia progressed unrelentingly, despite the attempts to use prone positioning and maximal ventilatory support. Venoarterial extracorporeal membrane oxygenation and continuous venovenous hemofiltration were begun on the 4th postoperative day. Sinus bradycardia (40 beats per minute) and prolongation of the QT interval (corrected QT interval: 550 msec) were noted, and she developed Torsades de pointes. After defibrillation, the electrocardiography turned back to sinus rhythm, and transcutaneous pacing was applied to maintain a heart rate of 60 beats per minute.

The lung biopsy provided a picture of organizing pneumonia favoring immune-mediated interstitial pneumonitis. Massive gastrointestinal bleeding ensued, and the corticosteroids were discontinued. Considering the agonizing complications of the invasive supportive procedures and the poor prognosis of her underlying autoimmune disorder, the healthcare team and her family agreed to withdraw the patient from life-supporting treatment. The patient died of multiple organ failure on the 19th day of hospitalization.

Discussion

Despite the advances in IMT, anti-MDA-5 positive CADM remains a challenging clinical entity due to its association with rapidly progressive DPLD and an exceedingly high mortality rate [4, 9-10]. Patients with dual positives of anti-RO52 and anti-MDA-5 antibodies have an even higher frequency of progressive lung involvement. Xu *et al*., in a cohort with anti-MDA-5 positive CADM, found a lower survival rate for patients with the coexistence of anti-RO52 and anti-MDA-5 antibodies than for those with mild positive anti-MDA-5 antibodies alone [11]. Our patient presented with mechanic's hands and Gottron's papules, which are the pathognomonic clinical signs of DM [12]. With an absence of myalgia or proximal muscle weakness, the clinical diagnosis of CADM was recognized early in the course. The comprehensive serological evaluations showed dual positives for anti-MDA-5 and anti-RO52 autoantibodies. These clinical characteristics alerted the

physicians to the potentially lethal progression of DPLD.

Thus, aggressive IMT, including glucocorticoids, Plaquenil, azathioprine, cyclophosphamide, rituximab, and intravenous human immunoglobulin therapy, was begun following the diagnosis. She experienced progressive hypoxemic respiratory distress, despite the combination of intensive IMT and comprehensive empirical anti-microbial treatment. Due to the suboptimal clinical response and progression of hypoxemia, SLB was performed with the intent of delineating the etiology of refractory DPLD and directing subsequent treatment. However, soon after the VATS for SLB, the patient experienced aggravated hypoxemic respiratory failure, eventually leading to her death.

Although the consequences of acute exacerbations of DPLD, acute respiratory failure, and in-hospital mortality occurred at an incidence of 1.7% in elective cases with CADM-associated DPLD, they were significantly higher in non-elective cases -- up to 16.0% -- as postoperative complications following SLB; therefore, shared decision-making with a thorough evaluation of the risks and benefits of the surgical procedures should be carried out [7-8]. However, such a decision is difficult because the safety profiles, potential diagnostic yields, and risk-benefit balance of SLB are still indeterminate, due to the scarcity of high-quality studies. The acute exacerbations of DPLD following SLB are possibly due to barotrauma and atelectrauma, which aggravate lung injuries during single-lung ventilation [13]. Non-intubated VATS without positive pressure ventilation may have eliminated 1 of the potential triggers of acute exacerbation of DPLD after SLB in a single-center study [14]. Non-intubated VATS was used with our patient, but she still experienced a fatal progression of hypoxemia following the procedure.

In contrast to bronchoscopic lung biopsy using conventional forceps, TBLC is a novel technique that has emerged in recent years, and provides larger and better-preserved lung samples than conventional forceps biopsy. TBLC can be adapted to flexible bronchoscopy platforms in current clinical practice. In a recent study, the risk of pneumothorax and moderate bleeding with TBLC was higher than with traditional bronchoscopic lung biopsy [15]. Physicians familiar with flexible bronchoscopy will likely become proficient in this skill after approximately 70 procedures, and the risk of complications can be reduced following maturation of the physician's experience [16]. Although TBLC cannot be wholly substituted for SLB in all clinical scenarios, the diagnostic yields of TBLC were highly concordant with those of SLB in a multidisciplinary assessment of DPLD [6], and TBLC had lower complication and mortality rates than SLB [17]. With a limited but growing amount of evidence, TBLC was regarded as an acceptable alternative to SLB for making a histopathological diagnosis in patients with DPLD of undetermined type in medical centers with appropriate expertise (conditional recommendation, very low-quality evidence) [18].

Conclusion

CADM with dual positives of anti-MDA-5 and anti-RO-52 autoantibodies is usually accompanied by rapidly progressive DPLD. CADM has excessively high mortality, despite aggressive IMT. For patients with a suboptimal clinical response to maximal IMT and comprehensive anti-microbial treatment, histopathological diagnosis by means of SLB may be

required. Shared decision-making with a thorough evaluation of the risks and benefits of the surgical procedures should be done cautiously. The risk of postoperative morbidities and in-hospital mortality with SLB in this population should not be neglected. In medical centers with adequate experience, TBLC through flexible bronchoscopy could be considered a reasonable diagnostic alternative to SLB.

References

1. Selva-O'Callaghan A, Pinal-Fernandez I, Trallero-Araguas E, *et al*. Classification and management of adult inflammatory myopathies. Lancet Neurol 2018; 17(9): 816-828.
2. Betteridge Z, McHugh N. Myositis-specific autoantibodies: an important tool to support diagnosis of myositis. J Intern Med 2016; 280(1): 8-23.
3. Sontheimer RD. Would a new name hasten the acceptance of amyopathic dermatomyositis (dermatomyositis siné myositis) as a distinctive subset within the idio pathic inflammatory dermatomyopathies spectrum of clinical illness? J Am Acad Dermatol 2002; 46(4): 626-36.
4. Allenbach Y, Uzunhan Y, Toquet S, *et al*. Different phenotypes in dermatomyositis associated with anti-MDA5 antibody: study of 121 cases. Neurology 2020; 95(1): e70-e78.
5. Mukae H, Ishimoto H, Sakamoto N, *et al*. Clinical differences between interstitial lung disease associated with clinically amyopathic dermatomyositis and classic dermatomyositis. Chest 2009; 136(5): 1341-1347.
6. Romagnoli M, Colby TV, Berthet JP, *et al*. Poor concordance between sequential transbronchial lung cryobiopsy and surgical lung biopsy in the diagnosis of diffuse interstitial lung diseases. Am J Respir Crit Care Med 2019; 199(10): 1249-1256.
7. Kreider ME, Hansen-Flaschen J, Ahmad NN, *et al*. Complications of video-assisted thoracoscopic lung biopsy in patients with interstitial lung disease. Ann Thorac Surg 2007; 83(3): 1140-4.
8. Hutchinson JP, Fogarty AW, McKeever TM, *et al*. In-hospital mortality after surgical lung biopsy for interstitial lung disease in the United States. 2000 to 2011. Am J Respir Crit Care Med 2016; 193(10): 1161-7.
9. Ye S, Chen XX, Lu XY, *et al*. Adult clinically amyopathic dermatomyositis with rapid progressive interstitial lung disease: a retrospective cohort study. Clin Rheumatol 2007; 26(10): 1647-54.
10. Nombel A, Fabien N, Coutant F. Dermatomyositis with anti-MDA5 antibodies: bioclinical features, pathogenesis and emerging therapies. Front Immunol 2021; 12: 773352.
11. Xu A, Ye Y, Qiong F, *et al*. Prognostic values of anti-Ro52 antibodies in anti-MDA5-positive clinically amyopathic dermatomyositis associated with interstitial lung disease. Rheumatology 2021; 60(7): 3343-3351.
12. Nagaraju K, Lundberg IE. Inflammatory diseases of muscle and other myopathies, in Polymyositis and Dermatomyositis, 2021, Elsevier: Philadelphia. p. 1548-1551.e6.
13. Kondoh Y, Taniguchi H, Kitaichi M, *et al*. Acute exacerbation of interstitial pneumonia following surgical lung biopsy. Respir Med 2006; 100(10): 1753-9.
14. Jeon CS, Yoon DW, Moon SM, *et al*. Non-intubated video-assisted thoracoscopic lung biopsy for interstitial lung disease: a single-center experience. J Thorac Dis 2018; 10(6): 3262-3268.
15. Sharp C, McCabe M, Adamali H, *et al*. Use of transbronchial cryobiopsy in the diagnosis of interstitial lung disease-a systematic review and cost analysis. QJM 2017; 110(4): 207-214.
16. Almeida LM, Lima B, Mota PC, *et al*. Learning curve for transbronchial lung cryobiopsy in diffuse lung disease. Rev Port Pneumol (2006) 2017 Nov 22; S2173-5115(17)30148-3.
17. Ravaglia C, Bonifazi M, Wells AU, *et al*. Safety and diagnostic yield of transbronchial lung cryobiopsy in diffuse parenchymal lung diseases: a comparative study versus video-assisted thoracoscopic lung biopsy and a systematic review of the literature. Respiration 2016; 91(3): 215-27.
18. Raghu G, Remy-Jardin M, Myers JL, *et al*. Diagnosis of idiopathic pulmonary fibrosis. An official ATS/ERS/JRS/ALAT clinical practice guideline. Am J Respir Crit Care Med 2018; 198(5): e44-e68.

Barotrauma in Patients with COVID-19-Related Severe Pneumonia with Respiratory Failure – Case Series Report From a Medical Center

Mei-Hsueh Chiang[1,*], Pin-Jui Chen[1,*], Chen-Yiu Hung[3], Ching-Tzu Huang[1,3], Hsiu-Feng Hsiao[1,3], Han-Chung Hu[1,2,3]

Coronavirus disease 2019 (COVID-19), caused by severe acute respiratory syndrome coronavirus-2 (SARS-CoV-2), has been recognized as a global pandemic since March 2020. The disease can lead to COVID-19-related pneumonia, and the clinical condition of patients may deteriorate. Respiratory failure could develop, and most patients with severe disease require mechanical ventilator (MV) use. One of the main complications of MV is barotrauma, and an increased incidence of barotrauma was found in COVID-19 patients under ventilator support. Application of a lung protective ventilation strategy is the standard management of COVID-19-associated respiratory failure. We reported 3 patients with COVID-19 pneumonia requiring invasive MV. Using data from electronic medical record systems and ventilator parameters, we discussed the occurrence of barotrauma in COVID-19 patients with respiratory failure and its correlation with MV. ***(Thorac Med 2024; 39: 99-105)***

Key words: COVID-19, hypoxic respiratory failure, mechanical ventilator, barotrauma

Introduction

The ongoing coronavirus disease 2019 (COVID-19) pandemic, caused by severe acute respiratory syndrome coronavirus 2 (SARS-CoV-2), has been a serious public health threat worldwide since March 2020. Most patients with COVID-19 have mild symptoms, while 5-12% develop acute respiratory distress syndrome (ARDS), increasing the average mortality rate to approximately 50% [1-4]. As the disease progresses, patients may develop hypoxic respiratory failure and require invasive mechanical ventilation (MV). One of the major complications of MV is barotrauma, which may increase overall mortality and prolong the inten-

[1]Department of Respiratory Therapy, Chang Gung Memorial Hospital, Taoyuan, Taiwan, [2]Department of Thoracic Medicine, Chang-Gung Memorial Hospital Linkou Branch, Taoyuan, Taiwan, [3]Department of Respiratory Therapy, Chang Gung University, College of Medicine, Taoyuan, Taiwan.
Address reprint requests to: Dr. Han-Chung Hu, Department of Thoracic Medicine, Chang Gung Memorial Hospital. 5, Fu-Shin St., Kwei-Shan, Taoyuan 333, Taiwan.
*These authors contributed equally to this work.

sive care unit (ICU) stay. The incidence of barotrauma among COVID-19 patients in the ICU has been reported to be around 15-32%, even under a protective ventilation strategy [5-6]. Here, we report 3 patients with severe COVD-19 infection who developed barotrauma. We analyze the changes in lung compliance and the parameters displayed on the ventilator as possible mechanisms. This study was approved by the Institutional Review Board of Chang Gung Medical Foundation (No.2112010101).

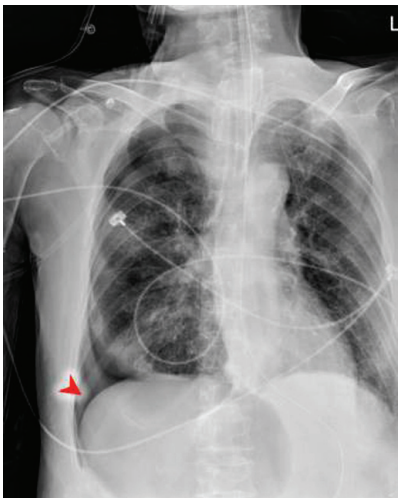

Fig. 1. Patient 1: On day 6 after intubation, right-side pneumothorax.

Case Presentation

Patient 1

This 80-year-old man with underlying coronary heart disease was also a heavy smoker of 2 packs/day for 60 years. He went to our emergency department suffering from fever for 1 day, accompanied with symptoms such as productive cough with white sputum, malaise and drowsiness. On arrival, his oxygen saturation could be maintained above 95% under a nasal cannula set at 5 L/min. His Acute Physiology and Chronic Health Evaluation II (APACHE II) score was 29. The laboratory examination revealed C-reactive protein (CRP) at 105.91 mg/L, procalcitonin at 0.38 ng/ml, interleukin-6 (IL-6) at 42.3 pg/mL, and D-dimer at 450 FEU ng/mL. On day 3 after admission, he was diagnosed with COVID-19 infection via a positive reverse transcription-polymerase chain reaction (RT-PCR) test for SARS-CoV-2 with an initial Ct value of 33.7. On day 8 of admission, he was intubated due to a worsened clinical condition with impending hypoxic respiratory failure. On day 6 under MV, his chest X-ray (CXR) revealed right pneumothorax (Figure 1). During this occurrence of pneumothorax, the ventilator was under a pressure control mode, with settings of peak inspiratory pressure (PIP) of 27 cmH_2O, positive end expiratory pressure (PEEP) of 10 cmH20, tidal volume of 7.0 ml/kg predicted body weight (PBW), and a fraction of inspired oxygen (FiO_2) of 50%. Chest tube insertion was performed and the patient's condition became stable. He was liberated from the ventilator through a spontaneous breathing trial on day 16 after intubation, and successfully shifted to a high-flow nasal cannula (50 L/min, FiO_2 60% and temperature of 34°C). The chest tube was removed 4 days later, after extubation. He was transferred to the general ward on day 38 and was discharged after 63 days of hospitalization.

Patient 2

This was a 75-year-old man with underlying hypertension, diabetes mellitus, pacemaker-treated atrial flutter, and prostate cancer. He was sent to a local hospital initially, due to fever and shortness of breath for 3 days. Suffering from severe hypoxemia, he was intubated for ventilator support. The RT-PCR nasopharyngeal specimen result for SARS-COV-2 (Ct value, 31.29)

was positive. He was later transferred to our hospital for quarantine and intensive care. His APACHE II score was 24. The laboratory examination revealed CRP of 78.75 mg/L, procalcitonin of 0.17 ng/mL, IL-6 of 15.3 pg/mL and D-dimer of 2526 FEU ng/mL. Subcutaneous emphysema was noted 4 days after intubation (Figure 2A). On day 6 after intubation, desaturation and hypotension were detected. CXR showed that the subcutaneous emphysema had extended to the right neck (Figure 2B). He was then placed under a pressure control mode with PEEP of 8 cmH20, tidal volume of 9.1 ml/kg of PBW, and FiO_2 of 35%; PIP was 23 cmH20.

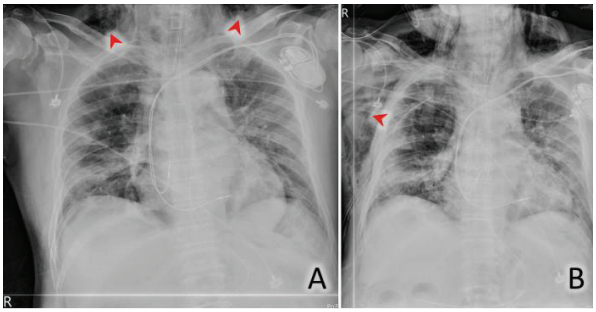

Fig. 2. Patient 2: A. On day 4 after intubation, subcutaneous emphysema. B. On day 6 after intubation, subcutaneous emphysema involved the right neck and thoracic region.

Chest tube insertion was performed immediately, and the patient's condition was quickly stabilized. He was liberated from the ventilator 10 days after intubation, and saturation was 96% under an 8 L/min simple oxygen mask. The chest tube was also removed 1 day after extubation. The patient was de-isolated from the quarantine ICU and transferred to the general ward on day 19. He was discharged after 29 days in the hospital.

Patient 3

This 66-year-old man had underlying hypertension, esophageal cancer and hypo-pharyngeal cancer. He suffered from fever and poor appetite for 1 week, combined with dyspnea. He was transferred to our quarantine ICU after a positive RT-PCR result for SARS-COV-2 with a Ct value of 16.73. His APACHE II score was 28 and CRP was 188.88 mg/L. Worsened shortness of breath occurred 2 days after admission, and oxygen therapy was titrated from a nasal cannula at 3 L/min to a non-rebreathing mask at 15 L/min. Meanwhile, hypotension was noted, thus adequate fluid resuscitation and an inotropic agent were given to maintain hemodynamic stability. He was intubated later due to mixed-type respiratory failure. A lung protective strategy as well as a sedative and neuromuscular blocker were used for his ARDS. Four days after intubation, his CXR revealed right pneumothorax (Figure 3A). His ventilator was pressure-controlled, with PEEP at 10 cmH20 and FiO_2 of 100%. His PIP increased to 39 cmH20 and tidal volume decreased to 4.01 ml/kg of PBW at the moment of pneumothorax. A chest tube was then placed on the right side. Six days after intubation, the CXR showed left pneumothorax (Figure 3B), and another chest tube was placed on the left side. Thirteen days after intubation, the patient experienced profound shock due to severe infection, and then soon died from multiple organ failure.

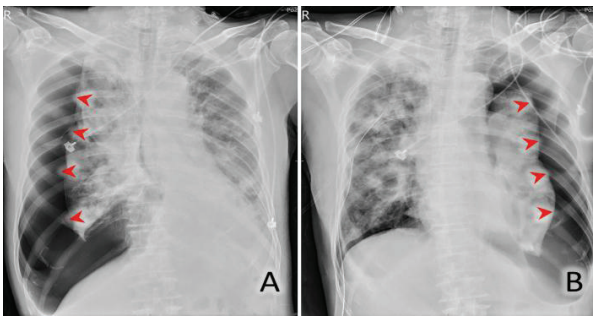

Fig. 3. Patient 3: A. On day 4 after intubation, right pneumothorax. B. On day 6 after intubation, left pneumothorax.

Discussion

Patients with severe COVID-19 infection may develop severe pneumonia with respiratory failure. According to the World Health Organization (WHO) guideline, a lung protective strategy and optimal PEEP are suggested for the management of severe COVID-19 infection [7]. In MV patients, several complications could occur, including oxygen intoxication, ventilator-induced lung injury (VILI), and ventilator-associated pneumonia (VAP). Barotrauma, a form of VILI, frequently occurs in patients under ventilator support; this raised our concern, considering its association with a mortality rate.

In a retrospective study, about 21% of patients of COVID-19-related acute respiratory distress syndrome (CARDS) had an occurrence of barotrauma under MV support [8-9]; however, this complication was also reported in patients with less severe COVID-19 pneumonia or mild ARDS. Several mechanisms for the development of barotrauma in patients infected with COVID-19 have been proposed. One mechanism, suggested by Macklin *et al*., was that when a high pressure gradient was distributed around the alveoli margin and interstitium of the lungs, air from the ruptured alveoli was forced into the mediastinal cavity through bronchovascular sheaths [10]. This was frequently seen in patients with spontaneous emphysema.

A second mechanism for the development of barotrauma was proposed to be related to VILI and patient self-inflicted lung injury (P-SILI). VILI occurs in patients with decreased lung compliance requiring positive pressure ventilation, who are also at risk of over-insufflation. The part of the alveoli with greater compliance may stretch and rupture, leading to barotrauma. On the other hand, the concept of P-SILI was proposed recently. Pleural pressure is negative in the inspiratory phase during spontaneous breathing. In patients with severe lung injury, who may have larger inspiratory efforts, transpulmonary pressure could increase remarkably more than in a patient without spontaneous breathing, while under MV [11]. Then, more inflammatory substances are leaked into the lungs, causing further injury [12].

The third mechanism was reported in a retrospective observational study by Kargirwar *et al*., who classified MV-supported COVID-19 patients who developed barotrauma into 2 groups based on P/F ratios of ≤ 100 and > 100, suggesting that the severity of disease was related to the development of barotrauma [13]. In a review of recent case reports, spontaneous pneumomediastinum and pneumothorax could occur in COVID-19 patients without MV. This may indicate that viral or inflammatory injury could be 1 of the factors accelerating the development of barotrauma. The inflammation of the lung parenchyma that caused the peripheral infiltration seen in the chest radiograph has been found in patients with COVID-19 [14]. When the viral invasion eventually involves the visceral pleura, it probably hastens the onset of air leak in the pleural space [15]. The peculiarities of COVID-19, such as endothelialitis, vasculitis, and vessel thrombosis, are described in the COVID-19 pathophysiology and may lead to diffuse alveolar damage [16-17]. Elevated tumor necrosis factor alfa (TNF-α) and IL-6 are detected in patients infected with COVID-19. Furthermore, COVID-19 pneumonia is featured with multiple organ damage, which is caused by a cytokine storm and thrombo-inflammation. These may contribute to the development of barotrauma [18-19].

In general, higher PIP and PEEP are needed

to ensure adequate oxygenation and ventilation in ARDS patients, and both parameters are prone to barotrauma. However, Gattinoni *et al*. proposed that COVID-19 pneumonia may be divided into 2 types according to lung physiology: L-type and H-type [20]. In the L phenotype, namely atypical ARDS, patients have high compliance, and an absence of recruitable alveoli and a poor response to high PEEP. Compared to the H phenotype, ventilator management using the ARDSnet protocol may have limited benefits for patients with L-type ARDS. In a retrospective study, Kargirwar *et al*. reported patients with COVID-19 pneumonia under a lung protective ventilation protocol (tidal volume 6-8 ml/kg PBW, plateau pressure < 30 cm H_2O and PIP < 40 cm H_2O); 14 patients out of 45 developed pneumothoraxes [13].

In this case series, we reported 3 male patients who were above 65 years old, which placed them at higher risk of developing ARDS if infected with COVID-19 [21]. Their underlying comorbidities, including hypertension, diabetes, malignancy and cardiovascular disease, are also associated with a severity of illness in COVID-19 patients [22]. Their APACHE II scores were 29, 24, and 28, respectively, which reflected a higher severity of disease. Previous reports indicated that patients progressed from symptomatic to moderate or severe ARDS within 2-8 days [21-23]. Chong *et al*. conducted a systematic review and found that the onset of COVID-19-related pneumothorax was 5.4 days after invasive MV initiation [24]. These figures are similar to those in our cases (Table 1).

In the first patient, chronic lung disease should be considered due to his heavy smoking history. Lung disease, such as chronic obstructive pulmonary disease (COPD), is a predisposing factor for developing barotrauma. Also, his laboratory data, including IL-6, CRP and procalcitonin, had higher than normal values, indicating that inflammatory responses were induced. Alveoli injury may be caused by inflammation from a viral infection and then become barotrauma. Barotrauma in the second patient could be attributed to both viral injury and inadequate sedation. We found that our ventilator settings could not strictly maintain a tidal volume of 8 ml/kg of PBW. In that circumstance, administration of sedatives (midazolam) was given. Inadequate sedation may have led to a higher occurrence of P-SILI. Moreover, the CXR of the second patient showed subcutaneous emphysema, which may explained by the Macklin effect. The third patient was maintained under higher ventilator settings due to his decreased lung compliance and severe hypoxemia with hypercapnia. His lung physiology may be classified as an H-phenotype. The differences in tidal volume from post intubation to the onset of pneumothorax in this case was the largest of the 3 cases (Table 1), and his condition deteriorated after contralateral pneumothorax occurred. Continuously high ventilator settings may increase the risk of barotrauma.

The study shows that low lung compliance and high PIP were associated with an increased risk of barotrauma [13]. The third patient in our study had low lung compliance and high PIP, which might have contributed to the greater possibility of pneumothorax. Providing optimal tidal volume and PEEP while maintaining safe plateau pressures (< 30 cmH20) are reasonable measures to prevent hyperinflation and barotrauma. Other clinical conditions and changes should also be closely monitored, especially signs of pneumothorax.

There are several limitations in this case series. First, only 3 cases were included, thus

Table 1. Mechanical Ventilation Records and Outcome of the 3 Patients

Patient	1			2			3		
	Initial	Pre-onset	Onset	Initial	Pre-onset	Onset	Initial	Pre-onset	Onset
P/F ratio	281.5		194.6	217.6	195	228.2	312.7	133.3	115.8
Ventilator parameters									
Mode	Bipap A/C	PCV	PCV	PCV	PCV	PCV	PCV	PCV	PCV
Peak inspiratory pressure (cmH_2O)	22.0	27.0	27.0	28.0	26.0	25.0	35.0	34	39.0
Respiratory rate Set/measured (breath/minute)	16/16	16/16	16/16	20/20	15/17	15/18	20/20	22/22	30/30
Minute ventilation (liter//minute)	6.9	6.9	6.5	11	8.7	8.6	8.4	6.9	7.7
Positive end expiratory pressure, (cmH_2O)	10.0	10.0	10.0	10.0	10.0	10.0	10.0	10.0	10.0
Tidal volume mL/PBW	6.9	6.9	6.6	8.5	7.8	7.3	6.6	6.9	3.7
Compliance, L/cmH_2O	35.8	26.9	25.4	31.0	34.2	31.9	17.5	18.5	8.5
Resistance, cmH_2O/L/sec	14.0	16.0	15.0	17.0	14	22.0	22.1	20.6	30.9
Arterial Blood Gas test									
PH	7.38		7.4		7.42	7.43	7.27	7.32	7.04
$Paco_2$	41.5		49.1		38.7	39.9	47.1	45.1	98.1
Pao_2	282		97		78.1	91.3	281.5	80.0	115.8
Hco_3	24.4		29		24.7	26.3	21.2	22.9	26.4
Ventilator days before barotrauma		6			4			4	
Total ventilator days		15			10			13	
Outcome		Survival			Survival			Expired	

our experiences may not be applied to other cases, and further studies with large sample sizes are needed. Second, because of the high transmission rate of COVID-19 and the concomitant policy of our hospital, CT scan for these patients was not available. Despite these limitations, this report reminds us that possible life-threatening complications could occur in patients with COVID-19 infection in our daily practice.

Conclusion

The reasons for barotrauma in patients with COVID-19 infection are complicated, and may involve more than a single factor. Barotrauma is also found in patients with less severe ARDS or even in those without ARDS. A lung protective strategy with sedative agents for patients with this pulmonary condition is controversial. Barotrauma could still develop under conventional ventilator management. It is crucial to maintain close observation of clinical presentations, arrange necessary examinations for the patients, and focus on the assessment of potential associations which might lead to barotrauma.

References

1. Yang X, Yu Y, Xu J, *et al*. Clinical course and outcomes of critically ill patients with SARS-CoV-2 pneumonia in Wuhan, China: a single-centered, retrospective, observational study. Lancet Respir Med 2020; 8: 475-81.
2. Livingston E, Bucher K. Coronavirus disease 2019 (COVID-19) in Italy. JAMA 2020; 323: 1335.
3. Arentz M, Yim E, Klaff L, *et al*. Characteristics and outcomes of 21 critically ill patients with COVID-19 in Washington State. JAMA 2020; 323: 1612-14.
4. Grasselli G, Pesenti A, Cecconi M. Critical care utilization for the COVID-19 outbreak in Lombardy, Italy: early experience and forecast during an emergency response. JAMA 2020; 323: 1545-6.
5. Diaz R, Heller D. Barotrauma and mechanical ventilation. In: StatPearls [Internet]. Treasure Island (FL): StatPearls Publishing; 2021. PMID: 31424810
6. Gattinoni L, Coppola S, Cressoni M, *et al*. COVID-19 does not lead to a "typical" acute respiratory distress syndrome. Am J Respir Crit Care Med 2020; 201: 1299-300. DOI: 10.1164/rccm.202003-0817LE
7. COVID-19 clinical management: living guidance, 25 January 2021. https://apps.who.int/iris/handle/10665/338882
8. Kahn MR, Watson RL, Thetford JT, *et al*. High incidence of barotrauma in patients with severe coronavirus disease 2019. J Intensive Care Med 2021; 36: 646-54.
9. Belletti A, Palumbo D, Zangrillo A, *et al*. Predictors of pneumothorax/ pneumomediastinum in mechanically ventilated COVID-19 patients. J Cardiothorac Vasc Anesth 2021; 35: 3642-51.
10. Murayama S, Gibo S. Spontaneous pneumomediastinum and Macklin effect: overview and appearance on computed tomography. World J Radiol 2014; 6: 850-4.
11. Carteaux G, Parfait M, Combet M, *et al*. Patient-self inflicted lung injury: a practical review. J Clin Med 2021; 10: 2738.
12. Yoshida T, Uchiyama A, Fujino Y. The role of spontaneous effort during mechanical ventilation: normal lung versus injured lung. J Intensive Care 2015; 3: 18.
13. Kargirwar KV, Rathod D, Kumar V, *et al*. Clinical profile of patients with severe acute respiratory syndrome coronavirus 2 infection developing pulmonary barotrauma on mechanical ventilation. Indian J Crit Care Med 2022; 26: 613-8.
14. Colman J, Zamfir G, Sheehan F, *et al*. Chest radiograph characteristics in COVID-19 infection and their association with survival. Eur J Radiol Open 2021; 8: 100360.
15. Saha BK, Chong WH, Austin A, *et al*. Pleural abnormalities in COVID-19: a narrative review. J Thorac Dis 2021; 13: 4484-99.
16. Konopka KE, Nguyen T, Jentzen JM, *et al*. Diffuse alveolar damage (DAD) resulting from coronavirus disease 2019 infection is morphologically indistinguishable from other causes of DAD. Histopathology 2020; 77(4): 570-8.
17. Ciceri F, Beretta L, Scandroglio AM, *et al*. Microvascular COVID-19 lung vessels obstructive thromboinflammatory syndrome (MicroCLOTS): an atypical acute respiratory distress syndrome working hypothesis. Crit Care Resusc 2020; 22: 95-7.
18. Conti P, Ronconi G, Caraffa A, *et al*. Induction of pro-inflammatory cytokines (IL-1 and IL-6) and lung inflammation by Coronavirus-19 (COVI-19 or SARS-CoV-2): anti-inflammatory strategies. J Biol Regul Homeost Agents 2020; 34: 327-31.
19. Chen L, Xia HF, Shang Y, *et al*. Molecular mechanisms of ventilator-induced lung injury. Chin Med J (Engl) 2018; 131: 1225-31.
20. Gattinoni L, Chiumello D, Rossi S. COVID-19 pneumonia: ARDS or not? Crit Care 2020; 24: 154.
21. Wang D, Hu B, Hu C, *et al*. Clinical characteristics of 138 hospitalized patients with 2019 novel coronavirus-infected pneumonia in Wuhan, China. JAMA 2020; 323: 1061-9.
22. Richardson S, Hirsch JS, Narasimhan M, *et al*. Presenting characteristics, comorbidities, and outcomes among 5700 patients hospitalized with COVID-19 in the New York City area. JAMA 2020; 323: 2052-9.
23. Ezeagu R, Olanipekun T, Santoshi R, *et al*. Pulmonary barotrauma resulting from mechanical ventilation in 2 patients with a diagnosis of COVID-19 pneumonia. Am J Case Rep 2021; 22: e927954.
24. Chong WH, Saha BK, Hu K, *et al*. The incidence, clinical characteristics, and outcomes of pneumothorax in hospitalized COVID-19 patients: a systematic review. Heart Lung 2021; 50(5): 599-608.